Bio-functionalized and Biomimetic Conjugated Polymers for Interfacing Prosthetic Devices with Neural Tissue

by

Laura K. Povlich

A dissertation submitted in partial fulfillment
of the requirements for the degree of
Doctor of Philosophy
(Macromolecular Science and Engineering)
in The University of Michigan
2011

Doctoral Committee:

Professor Jinsang Kim, Co-Chair
Professor David C. Martin, University of Delaware, Co-Chair
Professor Shuichi Takayama
Assistant Professor Joseph M. Corey

To Tatsu, Felicity and Tryp

Acknowledgements

The research presented in this thesis would not be possible without the guidance from my advisers, David C. Martin and Jinsang Kim. I worked with both of them as an undergraduate student and they inspired me to stay in their groups for graduate school. I thank them for their help when I needed assistance and also for allowing me to develop own ideas and projects. I'm grateful to have such caring advisers and I have enjoyed working for them and in their labs. I also thank Joseph M. Corey and Shuichi Takayama for their guidance on my thesis committee. Dr. Corey has been especially helpful with the biological aspect of my thesis and I appreciate our useful conversations and his help with experiments.

My thesis has been a collaborative effort and I must thank the undergraduates, graduate students and post docs who have helped make my research possible. This includes Jae Cheol Cho, Kangwon Lee, Sarah Richardson-Burns, Jeff Hendricks, Charles Shaw, Zachary King, Sarah Spanninga, Jason Le, Jinghang Wu, Bong Sup Shim, Conan Weiland, Fang Fang and Dan Yang. I would especially like to thank Michelle Leach for working with for me for so long to find a cell system that works for our experiments and Kathleen Feldman, Jing Qu and Chin-Chen Kuo for helping me finish some last minute experiments.

I appreciate the financial support for my thesis research from the Army MURI on Bio-Integrating Structural and Neural Prosthetic Materials (W911NF-06-1-0218), NSF

DMR-0802655, NSF CAREER Award DMR 0644864, Rackham Merit Fellowship and Tissue Engineering and Regeneration NIDCR Training grant (T-32). I also appreciate the instrumentation and staff assistance in the W.M. Keck Imaging Facility at the University of Delaware and the Electron Microbeam Analysis Laboratory (EMAL) at the University of Michigan.

I'm grateful to have supportive parents, Terry and Mike Povlich, and friends that have made graduate school a fun experience. Lastly, I'm thankful for the support, honesty and friendship of my boyfriend, Tatsu Osada. Besides proofreading parts of my thesis, Tatsu has also kept me motivated and focused throughout the thesis writing process.

Table of Contents

List of Figures

List of Schemes

List of Tables

List of Appendices

Abstract

Conjugated polymers, such as poly(3,4-ethylenedioxythiophene) (PEDOT) and polypyrrole (PPy), have been developed as effective materials for interfacing prosthetic device electrodes with neural tissue. These polymers, which are semi-conducting, provide an improved interface compared to metal electrodes because of their ionic conductivity, relatively soft modulus, low electrical impedance and ability to incorporate biological molecules. Recent focus has been on the development of conjugated polymers that have biological components in order to improve the biological response upon implantation of these electrodes. In this thesis, carboxylic acid-functionalized 3,4-ethylenedioxythiophene (EDOTacid) monomer was synthesized in order to covalently bind peptides to the surface of conjugated polymer films. EDOTacid was copolymerized with EDOT monomer to form stable, electrically conductive copolymer films referred to as PEDOT-PEDOTacid. The peptide GGGGRGDS was bound to PEDOT-PEDOTacid and was used to increase the adhesion of primary rat motor neurons between 3 to 9 times higher than controls, thus demonstrating that the peptide maintained its biological activity. PEDOT-PEDOTacid films have the potential to bind to a number of neural specific peptides that could control the behavior of neurons and vastly improve the performance of implanted electrodes.

The research in this thesis also investigated the ability of four different monomers – L-3,4-dihydroxyphenylalanine (L-DOPA), 5,6-dimethoxyindole-2-carboxylic acid

(DMICA), 5,6-dihydroxyindole-2-carboxylic acid (DHICA) and 5,6-dihydroxyindole (DHI) – to form electrochemically polymerized conjugated polymer films that mimic the structure of eumelanin, a type of naturally occurring melanin. One of these polymers, poly(5,6-dimethoxyindole-2-carboxylic acid) (PDMICA), was easy to polymerize and had especially interesting electrochromic and nano-structural features. In addition, PDMICA had a relatively high charge capacity (6.5 mC/cm^2) and was not cytotoxic toward cells, making it the best candidate for bio-electrode coatings. Since these films are biomimetic in structure they may produce a less severe immune reaction compared to purely synthetic conjugated polymers. Both PDMICA and PEDOT-PEDOTacid are new materials that could be used in the future to coat prosthetic device electrodes and improve communication between these devices and biological tissue.

CHAPTER 1

Introduction to Conjugated Polymer Biomaterials

1.1 Introduction

The development of conjugated polymers, also referred to as π-conjugated or semi-conducting polymers, has established a new class of materials that can interface electrically active devices with living tissue. These devices include probes for recording from[1,2] or stimulating individual neurons in the central nervous system,[3,4] prosthetic devices that can record from or stimulate peripheral nerves,[5,6] cochlear implants,[7] retinal implants[8] and cardiac pacemakers.[9] Typical device electrodes are made from electrically conductive inorganic materials such as gold, platinum, stainless steel, and iridium oxide. These materials produce flat, hard electrodes that do not integrate well with soft, ionically conducting tissue. In addition, there is an increasing need for smaller electrodes in order to record or stimulate localized areas of tissue for greater device specificity. Reducing the surface area of a metal electrode will result in an increase in electrical impedance and will produce a device with decreased recording and stimulating capabilities. On the other hand, conjugated polymers are a softer class of organic materials that can be synthesized with much higher surface area and drastically reduced impedance compared to metal

electrodes. Also, conjugated polymers can be chemically tailored with specific functional groups and can incorporate biological molecules either through covalent modification or entrapment during polymerization. These biological molecules could help reduce the inflammatory response and scar formation that occur upon implantation of a device in living tissue.[10] Consequently, the development and optimization of conjugated polymers for interfacing devices with biological tissue has been the focus of research groups around the world.[11-16]

Conjugated polymers have π-conjugated backbones that facilitate the movement of electrons or holes when the polymers are reduced or oxidized, resulting in conductivity.[17,18] The types of conjugated polymers used for electrode coatings have monomers with low oxidation potentials and include polypyrrole (PPy), polythiophenes, polyanilines and derivatives of these polymers (Figure 1.1). An especially important derivative of polythiophene is poly(3,4-ethylenedioxythiophene), or PEDOT. This polymer and its derivatives have produced promising bio-electrode materials and will be discussed in depth in this chapter. Many other types of conjugated polymers exist, but they cannot all be easily synthesized as films on electrodes via electrochemical oxidation of the monomer. Electrochemical polymerization is the most common method for preparing conjugated polymer electrode coatings since it produces films grown directly off of an electrode surface. In this synthesis route, a monomer and electrolyte solution are placed in a cell with a working electrode, a counter-electrode and a reference electrode. Upon application of an electric potential or current, the monomer is oxidized and forms radical cations at the electrode surface (Figure 1.1). If conditions are suitable, the radical cations react to form polymer chains that precipitate onto the electrode surface.[19] As-

polymerized polymer chains have charged backbones and thus must incorporate counter-ions from the electrolyte in order to create a neutral, stable film. Doping with counter-ions allows the positive charge or hole to move throughout the conjugated backbone and provides substantial charge capacity to the material. In addition, if the polymer films are oxidized or reduced, mobile anions or cations can move in and out of the film to compensate for changes in backbone charge. Many different types of anions have been used as dopants including small molecules, such as perchlorates, chlorides and sulfonates, polymers with anionic pendant groups and anionic biological molecules.

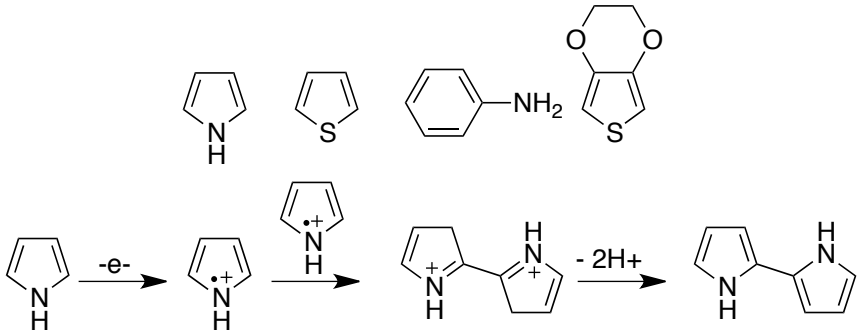

Figure 1.1 Monomer structures for commonly electrochemically polymerized polymers (top): pyrrole, thiophene, aniline and 3,4-ethylenedioxythiophene. Electrochemical dimerization scheme for pyrrole (bottom). The same radical cation process continues until precipitation of the polymer.

In this chapter we introduce the different types of conjugated polymers that have been used to interface devices with tissue. The material properties and biological interactions of the two most common conjugated polymer biomaterials, PPy and PEDOT, are discussed in detail, along with novel derivatives of these polymers. In addition, the benefits of coating neural electrodes with PEDOT and PPy are presented, as well as the present limitations of these materials. To conclude the bio-functionalized and biomimetic conjugated polymers developed in this thesis are introduced and their possible benefits to the field of conjugated polymer biomaterials are discussed.

1.2 Conjugated Polymer Biomaterial Coatings

1.2.1 Polypyrrole (PPy)

The extensive study of electrochemically polymerized polypyrrole (PPy) films began in the 1980's, although there are reports of chemically polymerized PPy as early as 1963.[20-22] Since it was demonstrated that PPy could be easily deposited on metal electrodes,[23] its chemical, electrical, mechanical and structural properties have been studied in detail. These properties, however, are highly dependent on the conditions used during electrochemical polymerization, including the solvent, dopant, pH, current or voltage and temperature.[24,25] Most importantly, it has been shown that the dopant used can affect the morphology of PPy films and, consequently, the electrical impedance of the material.[26,27] Cui *et al*. demonstrated that PPy films doped with small peptide fragments have fuzzy morphologies with high surface area.[28] As a result, the films have impedance magnitudes that are 1-2 orders of magnitude lower than bare gold at a frequency range from 10 -10^4 Hz.

The interactions between PPy and living cells have also been examined, along with any potential toxicity. Williams and Doherty showed that electrochemically-polymerized PPy doped with *p*-toluene sulfonate and washed with methanol is not cytotoxic to L929 mouse fibroblast and neuro2a neuroblastoma cells.[29] Additionally, a small current was applied through the PPy films and the cells continued to proliferate. Other studies using primary neural cells and tissue explants have shown similar results and indicate that unfunctionalized PPy is biopassive *in vitro*, meaning the polymer does not influence cell behavior.[30] However, the ability of PPy to facilitate electrical current has been used to change cellular morphology. Schmidt *et al.* subjected primed PC-12

cells to electrical stimulation on PPy and the cells produced longer neurites and spread out more on the substrate compared to control samples.[31] Although the cells could be electrically stimulated using the bare indium tin oxide (ITO) electrode, the cells did not adhere well to ITO, demonstrating that the cells prefer the rough, organic surface of PPy.

Shimidzu *et al.* established that PPy can be doped with polyanions such as sodium poly(styrene sulfonate) (PSS).[32] These negatively charged polymers become entangled with PPy as electrochemical polymerization occurs and provide additional mechanical integrity to the films. Since the anionic polymer is trapped in the conducting polymer film, the cation, sodium, is the mobile species. PPy has also been polymerized with polyanions that are biologically active such as growth factors,[33] polymers with extracellular matrix protein fragments, peptides,[28] enzymes,[34] heparin[35] and hyaluronic acid.[34,36] Biological molecules can be incorporated with a co-dopant to improve the quality of the conjugated polymer films. In addition, these molecules may be physically trapped by the growing PPy film, rather than simply acting as the dopant. Unlike the passive nature of polypyrrole, the addition of bioactive molecules to electrode films can provide a means for directing cellular behavior. Importantly, it has been shown that biological molecules retain their biological activity after being trapped in conducting polymer. Kim *et al.* demonstrated that nerve growth factor (NGF) can be incorporated in PPy through electrochemical polymerization and the resulting films promote neurite outgrowth in PC-12 cells.[33] Also, the conducting polymer still has low impedance and high charge capacity. Interestingly, it has also been shown that live cells can be trapped in conducting polymer during electrochemical polymerization. Campbell *et al*. incorporated erythrocytes into PPy to create immuno-sensors. The erythrocytes can bind

to specific anti-bodies, which changes the electrical resistance of PPy, thus providing a sensing mechanism.[37]

The main problem with using PPy for biomedical applications is its chemical and electrical instability.[38,39] Since pyrrole is unfunctionalized at both its α and β carbon positions, it has four available reactive sites during electrochemical polymerization. In an oxidative environment α-β' coupling can occur and water or other nucleophilic compounds can react at the β carbon, creating defects in the polymer backbone. This type of reaction can also occur in the polymer during electrical stimulation. Yamato *et al*. compared the electrical stability of PPy and PEDOT, both with PSS counter-ion.[38] After holding the polymers at a constant potential in phosphate buffered saline for 16 hours, the authors found that PPy lost 95% of its original electrochemical activity, whereas PEDOT only lost 11% of its original activity. It was predicted, based on previous literature, that hydroxide ions attack the β-position on the pyrrole repeat unit and break the conjugation of the polymer backbone (Scheme 1.1). PEDOT, on the other hand, does not react with hydroxide ions since it has diethoxy functionalization at the β position. This study and cyclic voltammetry (CV) comparisons by Cui and Martin (Figure 1.2) demonstrated that PEDOT is more suitable than PPy for devices that require long-term implantation and consistent electrical activity.[40]

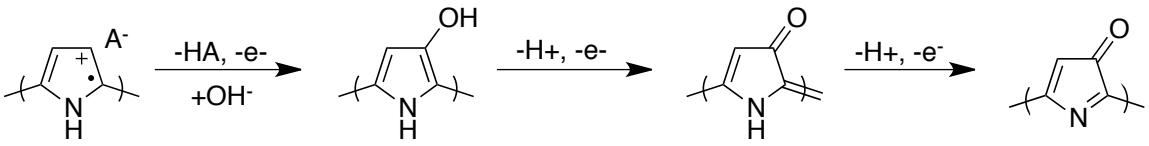

Scheme 1.1 Side reactions during electrochemical stimulation of PPy. Hydroxide ions react at the β position and break the conjugation in the polymer.

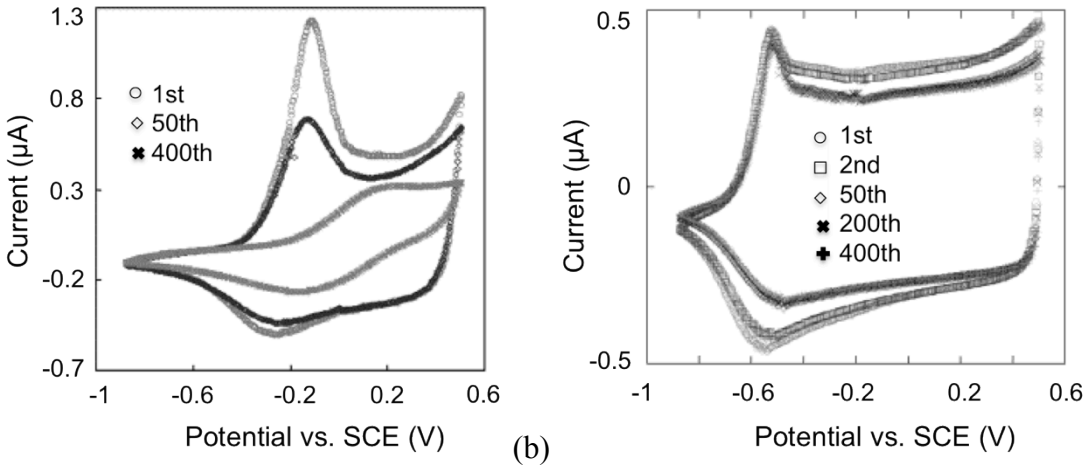

Figure 1.2 Electrochemical stability by cyclic voltammetry of (a) PPy:PSS and (b) PEDOT:PSS with scan rate 0.1V/s. While PPy:PSS loses its charge storage capacity with repeated cycles, PEDOT:PSS maintains a relatively large storage capacity.[40] Reprinted from *Sensors and Actuators B: Chemical*, 89, Cui, X. and Martin D.C. "Electrochemical deposition and characterization of poly(3,4-ethylenedioxythiophene) on neural microelectrode arrays", 92-102, Copyright (2003), with permission from Elsevier.

1.2.2 Poly(3,4-ethylenedioxythiophene) (PEDOT)

The electrochemical polymerization of 3,4-ethylenedioxythiophene (EDOT) was first published in 1992 and the polymer PEDOT quickly became of interest as an electrode coating for its low oxidation potential and high chemical and electrical stability.[41,42] Similar to polypyrrole, it was shown that PEDOT has a high charge capacity and low impedance compared to the electrodes used for deposition. High surface area morphologies and tailored microstructures have been created that lower the impedance even further, making the polymer even more suitable for small bio-electrode coatings.[43-45] Although not necessarily an important property for biological applications, PEDOT films are also electrochromic, changing from dark blue to sky blue as the polymer is oxidized.[46]

In vitro toxicity and biocompatibility experiments have demonstrated that PEDOT, like PPy, is not cytotoxic to cells. Hep-2 human epithelial cells were shown to adhere better to PEDOT doped with perchlorate counter-ion than stainless steel

electrodes and exhibited normal morphology and proliferation.[47] When treated with bovine serum albumin and other cell culture medium proteins the PEDOT samples adsorbed quantities of protein similar to polystyrene cell culture wells and stainless steel. Extracellular matrix protein adsorption allows cells to adhere to substrates *in vitro* but protein adsorption *in vivo* may result in foreign body recognition followed by an inflammatory response. To further examine the cytotoxicity of EDOT and PEDOT and to create hybrid conducting polymer-live cell electrodes, Richardson-Burns *et al*. polymerized EDOT around living SH-SY5Y neuroblastoma cells.[48] EDOT monomer was not significantly toxic to the cells over the time period needed for polymerization and the cells were able to survive the polymerization process. This finding has led to the polymerization of EDOT in tissue and the possibility of *in vivo* polymerization.[49]

Like other electrochemically polymerized conjugated polymers, PEDOT can incorporate anionic polymers and biomolecules as dopants, including peptides,[40] hyaluronic acid (HyA), heparin, fibrinogen,[50] collagen[33] and adenosine 5'-triphosphate (ATP).[51] Asplund *et al*. incorporated HA, heparin and fibrinogen into PEDOT as dopants and investigated the electrical and surface properties of the films.[50] These biomolecules are abundant in the human body and may be more suitable counter-ions for *in vivo* applications when compared to PSS. HA is a glycosaminoglycan found in the extracellular matrix of neural tissue, heparin is a polysaccharide anti-coagulant and fibrinogen is a glycoprotein involved in coagulation and thrombosis. PEDOT:HA and PEDOT:heparin films polymerized in a manner similar to PEDOT:PSS. On the other hand, PEDOT:fibrinogen was difficult to polymerize due to adherence of fibrinogen on the metal electrode surface prior to polymerization. In order to overcome this problem, a

layer of PEDOT was deposited first, followed by PEDOT:fibrinogen. PEDOT:HA and PEDOT:heparin films have impedance and capacitance behavior similar to PEDOT:PSS, but PEDOT:fibrinogen did not produce films with adequate electrical and ionic conductivity. Additionally, it has been shown that PEDOT:heparin and PEDOT:HA films are not cytotoxic to L929 fibroblasts and SH-SY5Y neuroblastoma cells.[52] The incorporation of ATP, a nucleotide involved in multiple cellular functions including neural communication, also has interesting implications.[51] PEDOT:ATP films have a rough morphology, low impedance and promote adhesion of PC-12 cells. In addition, ATP is small enough to be released from conducting polymer films through electrical stimulation, resulting in an ATP delivery system.[53]

1.2.3 PPy and PEDOT Derivatives and Copolymers

Derivatives of PPy and PEDOT have been synthesized to produce conducting polymer films with additional chemical or biological functionality (Figure 1.3). Monomers with charged functional groups such as sulfonatoalkoxy-EDOT (S-EDOT) have been synthesized and can be used as self-dopants during electrochemical polymerization.[54] Another EDOT derivative that has been synthesized incorporates the hydroxymethyl functional group, which improves the solubility of EDOT in water. Additional functionality can also be added through reactions with hydroxy groups. Luo *et al*. used hydroxymethyl-functionalized EDOT (EDOT-OH) to create pendant carboxylic acid (EDOT-COOH), azide (EDOT-N_3) and N-hydroxysuccinimide groups (EDOT-NHS) on the EDOT monomers.[55] The films produced by microemulsion electrochemical polymerization of these monomers are ultra-smooth and have low cytotoxicity. In addition, the carboxylic acid can then be further functionalized with peptides or proteins

through carbodiimide chemistry. Carboxylic acid-functionalized pyrroles have also been synthesized both as a pendant off of the pyrrole nitrogen and as an end-cap off of the α-position on the pyrrole ring.[56,57] RGD peptide-functionalized PPy made from these monomers have been used to increase cellular adhesion in human umbilical vascular endothelial cells compared to regular PPy. Derivatives of PPy based on poly(3,4-alkylenedioxypyrrole)s such as poly(3,4-etheylenedioxypyrrole) (PEDOP) also show potential for bio-electrode coatings. These polymers have better chemical and electrical stability than PPy and also very low oxidation potentials.[58] Many other EDOT derivatives have also been synthesized for non-biological applications and have been reviewed in detail by the Reynolds group.[18,59]

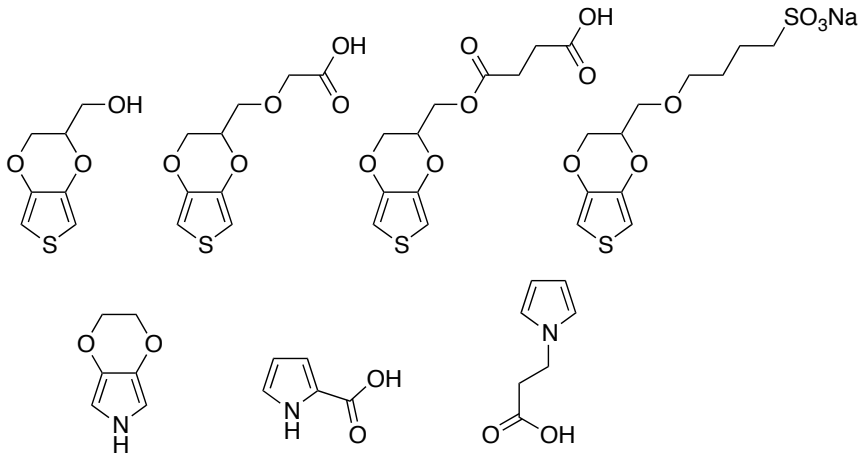

Figure 1.3 Example functionalized monomers for conjugated polymer electrode coatings (from top left): EDOT-OH, C_2-EDOT-COOH, C_4-EDOT-COOH,[55] S-EDOT,[54] EDOP,[58] Py-α-COOH[57] and PyCOOH.[56]

The chemical functionality and material properties of conjugated polymer films can also be tailored through the process of electrochemical copolymerization. Monomers with similar oxidation potentials can be simultaneously polymerized to make random copolymer films. Block copolymer films can be formed by sequential polymerization of monomers. With this method, however, it is unclear whether the second polymer is

covalently bonded to the first polymer or if they form two unbonded layers. Commonly, functionalized monomers are copolymerized with unfunctionalized monomers to create films with optimized functionality and stability. Biotin-functionalized pyrrole has been copolymerized with pyrrole in order to create stable, conducting films that can react with the protein avidin.[60] Biotin-functionalized enzyme or other protein can then bind to another avidin reactive site, thus producing biomolecule immobilized films.[61] Copolymerization is also advantageous in the formation of films with S-EDOT. Since this monomer is charged, the electrochemical polymerization of pure S-EDOT forms water-soluble oligomers.[62] Incorporation of unfunctionalized EDOT increases the hydrophobicity of the polymer and allows precipitation of the copolymer onto an electrode surface. Other copolymers have been formed including PEDOT/PPy,[63] PEDOT/PEDOT-OH,[64] PEDOT/polyindole[65] and PPy/polyindole.[66]

1.3 PPy and PEDOT on Neural Electrodes

Early studies of neural stimulation through conjugated polymers were performed by the Langer group. As mentioned previously, Schmidt *et al.* demonstrated that electrical stimulation of PC-12 neural cells on PPy:PSS results in enhanced neurite outgrowth.[31] This work ignited the applications of electrically conducting polymers towards living tissue interfaces. Soon after, Cui *et al*. reported that PPy:PSS could be selectively coated on a device with multichannel micro-electrodes, often called the 'Michigan Probe', which are designed for single cell neural stimulation and recording. Compared to bare Au, this PPy:PSS coating can reduce the impedance of a micro-electrode site by more than two orders of magnitude. *In vivo* guinea pig tests demonstrated that PPy:PSS coatings improved acute neural recordings dramatically

compared to bare metal electrodes.[67] In order to mimic extracellular matrix, the same group mixed extracellular matrix components such as fibronectin and laminin fragments with the PPy coating.[28] Human neuroblastoma cells showed a greater affinity for these PPy/peptide coatings than Au electrodes *in vitro*. Furthermore, this polymeric electrode coating has shown great potential for *in vivo* and possibly chronic neural communication. The PPy/peptide interface promotes the adhesion of living neural cells, demonstrated by *in vivo* guinea pig implantation and histology experiments. Although inflammatory gliosis still proceeds over time, the PPy/peptide certainly improved recording over a 3 week period by recruiting neural cells to the electrode interface.[39]

In a report by Nyberg *et al*., PEDOT:PSS coated micro-electrodes demonstrated more sensitive and stable recordings of cortical cell neural networks compared to ITO electrodes.[68] In addition, Ludwig *et al*. demonstrated the *in vivo* biocompatibility of PEDOT by implanting PEDOT:perchlorate coated 'Michigan Probes' in the motor cortexes of 8 rats.[69] PEDOT lowered the impedance of the electrodes and increased the signal-to-noise ratio for 6 weeks after implantation. However, after 6 weeks scar formation around the implant created an increase in impedance for both the PEDOT-coated and control neural probes. Formation of a glial scar remains a major limitation for coated and uncoated neural electrode probes. During this process, non-neuronal cells are recruited to the surface of the implant and neural cells are pushed further away, making it difficult to maintain electrical communication (Figure 1.4).[70] Since typical PEDOT and PPy lack the ability to control cell behavior, scar formation is still seen when coated probes are implanted.

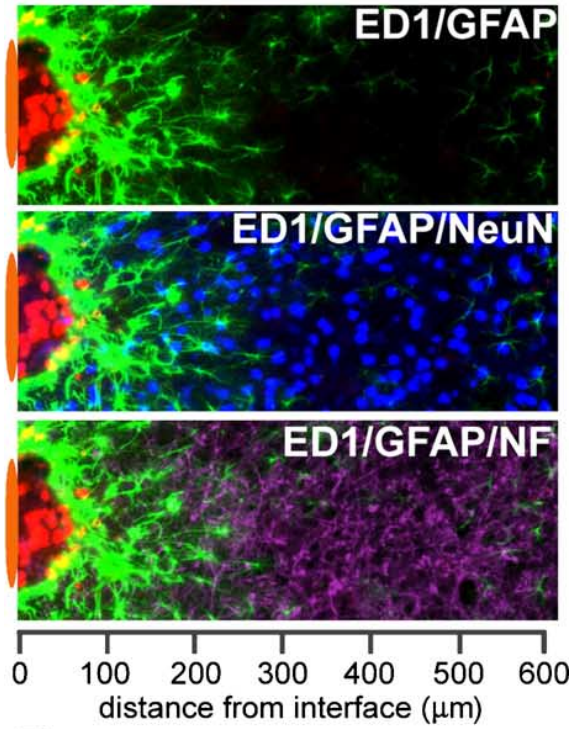

Figure 1.4 Stratification of cellular immunoreactivity using cell-type-specific markers at the microelectrode– brain tissue interface. Representative images collected from two adjacent sections of an animal with a 4-week microelectrode implant illustrate the general appearance of the foreign body response characterized by minimally overlapping inflammatory (ED1) and astrocytic (GFAP) phenotypes adjacent to the implant interface. The area of inflammation and intense astrocyte reactivity contains a reduced number of NeuN+ neuronal bodies and a loss of neurofilament (NF) density. The position of the microelectrode is illustrated by the orange oval (drawn to scale) at the left of each image. Images were captured in grayscale and pseudocolored for illustration.[70] Reprinted from *Experimental Neurology*, 195, Biran, R.; Martin, D.C.; and Tresco, P.A., "Neuronal cell loss accompanies the brain tissue response to chronically implanted silicon microelectrode arrays", 115-126, Copyright (2005), with permission from Elsevier.

1.4 Bio-functionalized and Biomimetic Conjugated Polymers

There are numerous methods for providing conjugated polymers with biological functionality, the most common being entrapment or doping of the polymer with biomolecules during polymerization, as described above for PEDOT and PPy. However, this process may decrease the electrical and mechanical properties of the resulting film. Also, the molecules that can be entrapped typically need to be negatively charged or

require a co-dopant. Therefore, we are interested in exploring covalent modification of conjugated polymers in order to provide functionality that can control cell behavior and attempt to overcome glial scar formation. As discussed earlier, Lee *et al*. have shown that biological molecules can be attached to PPy through the synthesis of PPy variations that have carboxylic acid functionality. In a similar approach, we have developed carboxylic acid-functionalized EDOT (EDOTacid, Figure 1.5a) with the acid positioned directly off of the diethoxy ring.[71] Chapter 2 in this thesis examines the synthesis of EDOTacid and its co-polymerization with EDOT while incorporating both small molecule and polymeric counter-ions. In addition, the physical properties of the copolymer, PEDOT-PEDOTacid, are discussed. Covalent functionalization of PEDOT-PEDOTacid with RGD peptide and its interactions with cells are presented in Chapter 3. We have shown that PEDOT-PEDOTacid-RGD can be used to increase cell adhesion, providing a new tool for neural probe electrodes or any other electrode-tissue interface application.

Another approach we have explored to create more biocompatible conjugated polymer coatings is the formation of polymers that mimic the structures of naturally occurring melanins. These natural conjugated polymers or oligomers are found in pigmented tissues such as hair, skin, eyes, ear and certain parts of the brain.[72] Eumelanin, a specific type of melanin, has been electrochemically polymerized to produce dark brown films with broadband absorption;[73] however, these films have not been investigated as biomaterials. The functions and structures of natural melanins are not completely understood, making it difficult to develop synthetic versions. However, it is important for scientists in the biomaterials field to try to understand if natural or synthetic melanins can provide useful interfaces for between tissues and devices. In this thesis we

present our own attempts at making synthetic melanin films using a variety of monomers (Figure 1.5b-e). Chapter 4 details the polymerization and characterization of poly(5,6-dimethoxyindole-2-carboxylic acid) (PDMICA), a melanin-like film with interesting electrochromic and structural properties. Chapter 5 explores the use of electrochemically polymerized synthetic melanins as biomaterials and explains how PDMICA films have the most potential as bio-electrode coatings. The final chapter in this thesis explores the future potential of our newly developed conjugated polymers and how they can be combined with other chemical, biological and mechanical methods for improving device-tissue interfaces. While the experiments and discussion presented for both PEDOT-PEDOTacid and synthetic melanin films center around electrochemically polymerized coatings for neural electrode applications, both types of materials could also be chemically polymerized and used for a variety of biological and non-biological applications that require electrically or ionically conducting polymeric materials.

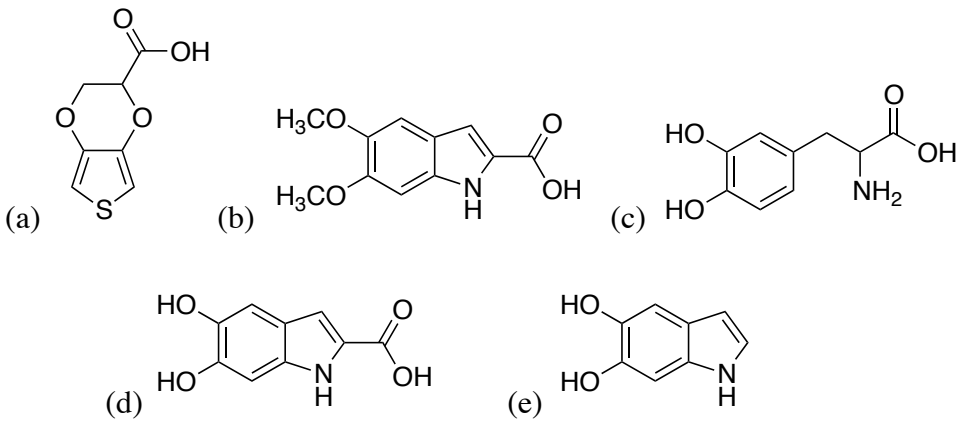

Figure 1.5 Monomer structures used to make electrochemically polymerized films in this thesis: (a) EDOTacid, (b) 5,6-dimethoxyindole-2-carboxylic acid (DMICA), (c) L-3,4-dihydroxyphenylalanine (L-DOPA), (d) 5,6-dihydroxyindole-2-carboxylic acid (DHICA) and (e) 5,6-dihydroxyindole (DHI).

1.5 References

(1) Hoogerwerf, A. C.; Wise, K. D. *IEEE Transactions on Biomedical Engineering* **1994**, *41*, 1136-46.

(2) Nordhausen, C. T.; Maynard, E. M.; Normann, R. A. *Brain Research* **1996**, *726*, 129-40.

(3) Campbell, P. K.; Jones, K. E.; Huber, R. J.; Horch, K. W.; Normann, R. A. *IEEE Transactions on Biomedical Engineering* **1991**, *38*, 758-68.

(4) Tehovnik, E. J. *Journal of Neuroscience Methods* **1996**, *65*, 1-17.

(5) Akin, T.; Najafi, K.; Smoke, R. H.; Bradley, R. M. *IEEE Transactions on Biomedical Engineering* **1994**, *41*, 305-13.

(6) Navarro, X.; Krueger, T. B.; Lago, N.; Micera, S.; Stieglitz, T.; Dario, P. *Journal of the Peripheral Nervous System* **2005**, *10*, 229-58.

(7) Wilson, B. S.; Dorman, M. F. *Hearing Research* **2008**, *242*, 3-21.

(8) Margalit, E.; Maia, M.; Weiland, J. D.; Greenberg, R. J.; Fujii, G. Y.; Torres, G.; Piyathaisere, D. V.; Hearn, T. M. O.; Liu, W.; Lazzi, G.; Dagnelie, G.; Scribner, D. A.; de Juan, E.; Humayun, M. S. *Survey of Ophthalmology* **2002**, *47*, 335-356.

(9) Trohman, R. G.; Kim, M. H.; Pinski, S. L. *Lancet* **2004**, *364*, 1701-19.

(10) Polikov, V. S.; Tresco, P. A; Reichert, W. M. *Journal of Neuroscience Methods* **2005**, *148*, 1-18.

(11) Berggren, M.; Richter-Dahlfors, A. *Advanced Materials* **2007**, *19*, 3201-3213.

(12) Guimard, N.; Gomez, N.; Schmidt, C. *Progress in Polymer Science* **2007**, *32*, 876-921.

(13) Wallace, G. G.; Spinks, G. M. *Chemical Engineering Progress* **2007**, *103*, S18-S24.

(14) Kotov, N. A.; Winter, J. O.; Clements, I. P.; Jan, E.; Timko, B. P.; Campidelli, S.; Pathak, S.; Mazzatenta, A.; Lieber, C. M.; Prato, M.; Bellamkonda, R. V.; Silva, G. A.; Kam, N. W. S.; Patolsky, F.; Ballerini, L. *Advanced Materials* **2009**, *21*, 3970-4004.

(15) Poole-Warren, L.; Lovell, N.; Baek, S.; Green, R. *Expert Review of Medical Devices* **2010**, *7*, 35-49.

(16) Owens, R. M.; Malliaras, G. G. *MRS Bulletin* **2010**, *35*, 449-456.

(17) Chiang, C. K.; Fincher, C. R.; Park, Y. W.; Heeger, A. J.; Shirakawa, H.; Louis, E. J.; Gau, S. C.; MacDiarmid, A. G. *Physical Review Letters* **1977**, *39*, 1098-1101.

(18) Kumar, D.; Sharma, R. C. *European Polymer Journal* **1998**, *34*, 1053-1060.

(19) Sabouraud, G.; Sadki, S.; Brodie, N. *Chemical Society Reviews* **2000**, *29*, 283-293.

(20) McNeill, R.; Weiss, D. E.; Wardlaw, J. H.; Siudak, R. *Australian Journal of Chemistry* **1963**, *16*, 1056-1075.

(21) Asavapiriyanont, S.; Chandler, G. K.; Gunawardena, G. A.; Pletcher, D. *Journal of Electroanalytical Chemistry* **1984**, *117*, 229-244.

(22) Street, G. B.; Lindsey, S. E.; Nazzai, A. I.; Wynne, K. J. *Molecular Crystals and Liquid Crystals* **1985**, *118*, 137-148.

(23) Diaz, A. F.; Kanazawa, K. K.; Gardini, G. P. *Chemical Communications* **1979**, 635-636.

(24) Satoh, M.; Kaneto, K.; Yoshino, K. *Synthetic Metals* **1986**, *14*, 289-296.

(25) Imisides, M. D.; John, R.; Riley, P. J.; Wallace, G. G. *Electroanalysis* **1991**, *3*, 879-889.

(26) Silk, T. *Synthetic Metals* **1998**, *93*, 59-64.

(27) Silk, T. *Synthetic Metals* **1998**, *93*, 65-71.

(28) Cui, X.; Lee, V. A.; Raphael, Y.; Wiler, J. A.; Hetke, J. F.; Anderson, D. J.; Martin, D. C. *Journal of Biomedical Materials Research* **2001**, *56*, 261-72.

(29) Williams, R. L.; Doherty, P. J. *Journal of Materials Science: Materials in Medicine* **1994**, *5*, 429-433.

(30) George, P. M.; Lyckman, A. W.; LaVan, D. A.; Hegde, A.; Leung, Y.; Avasare, R.; Testa, C.; Alexander, P. M.; Langer, R.; Sur, M. *Biomaterials* **2005**, *26*, 3511-3519.

(31) Schmidt, C. E. *Proceedings of the National Academy of Sciences* **1997**, *94*, 8948-8953.

(32) Shimidzu, T.; Ohtani, A.; Iyoda, T.; Honda, K. *Journal of Electroanalytical Chemistry* **1987**, *224*, 123-135.

(33) Kim, D.-H.; Richardson-Burns, S. M; Hendricks, J. L; Sequera, C.; Martin, D. C. *Advanced Functional Materials* **2007**, *17*, 79-86.

(34) Foulds, N. C.; Lowe, C. R. *Faraday Transactions 1* **1986**, *82*, 1259-1264.

(35) Garner, B.; Georgevich, A.; Hodgson, A. J.; Liu, L.; Wallace, G. G. *Journal of Biomedical Materials Research* **1999**, *44*, 121-9.

(36) Collier, J. H.; Camp, J. P.; Hudson, T. W.; Schmidt, C. E. *Journal of Biomedical Materials Research* **2000**, *50*, 574-84.

(37) Campbell, T. E.; Hodgson, A. J.; Wallace, G. G. *Electroanalysis* **1999**, *11*, 215-222.

(38) Yamato, H.; Ohwa, M.; Wernet, W. *Journal of Electroanalytical Chemistry* **1995**, *397*, 163-170.

(39) Cui, X.; Wiler, J.; Dzaman, M.; Altschuler, R. A.; Martin, D. C. *Biomaterials* **2003**, *24*, 777-87.

(40) Cui, X.; Martin, D. C. *Sensors and Actuators B: Chemical* **2003**, *89*, 92-102.

(41) Heywang, G.; Jonas, F. *Advanced Materials* **1992**, *4*, 116-118.

(42) Dietrich, M.; Heinze, J.; Heywang, G.; Jonas, F. *Journal of Electroanalytical Chemistry* **1994**, *369*, 87-92.

(43) Yang, J.; Kim, D. H.; Hendricks, J. L.; Leach, M.; Northey, R.; Martin, D. C. *Acta Biomaterialia* **2005**, *1*, 125-36.

(44) Yang, J.; Lipkin, K.; Martin, D. C. *Journal of Biomaterials Science Polymer Edition* **2007**, *18*, 1075-89.

(45) Yang, J.; Martin, D. C. *Materials Research* **2006**, *21*, 1124-1132.

(46) Pei, Q.; Zuccarello, G.; Ahlskog, M.; Inganas, O. *Polymer* **1994**, *35*, 1347-1351.

(47) del Valle, L. J.; Aradilla, D.; Oliver, R.; Sepulcre, F.; Gamez, A.; Armelin, E.; Aleman, C.; Estrany, F. *European Polymer Journal* **2007**, *43*, 2342-2349.

(48) Richardson-Burns, S. M.; Hendricks, J. L.; Foster, B.; Povlich, L. K.; Kim, D.-H.; Martin, D. C. *Biomaterials* **2007**, *28*, 1539-52.

(49) Richardson-Burns, S. M.; Hendricks, J. L.; Martin, D. C. *Journal of Neural Engineering* **2007**, *4*, L6-L13.

(50) Asplund, M.; von Holst, H.; Inganäs, O. *Biointerphases* **2008**, *3*, 83-93.

(51) Xiao, Y. H.; Li, C. M.; Toh, M.-L.; Xue, R. *Journal of Applied Electrochemistry* **2008**, *38*, 1735-1741.

(52) Asplund, M.; Thaning, E.; Lundberg, J.; Sandberg-Nordqvist, A. C.; Kostyszyn, B.; Inganäs, O.; von Holst, H. *Biomedical Materials* **2009**, *4*, 045009.

(53) Pernaut, J.-M.; Reynolds, J. R. *Journal of Physical Chemistry B* **2000**, *104*, 4080-4090.

(54) Xiao, Y.; Cui, X.; Martin, D. C. *Journal of Electroanalytical Chemistry* **2004**, *573*, 43-48.

(55) Luo, S.-C.; Mohamed Ali, E.; Tansil, N. C.; Yu, H.-H.; Gao, S.; Kantchev, E. A. B.; Ying, J. Y. *Langmuir* **2008**, *24*, 8071-7.

(56) Lee, J.-W.; Serna, F.; Nickels, J.; Schmidt, C. E. *Biomacromolecules* **2006**, *7*, 1692-5.

(57) Lee, J.-W.; Serna, F.; Schmidt, C. E. *Langmuir* **2006**, *22*, 9816-9.

(58) Schottland, P.; Zong, K.; Gaupp, C. L.; Thompson, B. C.; Thomas, C. A.; Giurgiu, I.; Hickman, R.; Abboud, K. A.; Reynolds, J. R. *Macromolecules* **2000**, *33*, 7051-7061.

(59) Groenendaal, L. B.; Jonas, F.; Freitag, D.; Pielartzik, H.; Reynolds, J. R. *Advanced Materials* **2000**, *12*, 481-494.

(60) Torres-Rodriguez, L. M.; Roget, A.; Billon, M.; Bidan, G.; Livache, T. *Chemical Communications* **1998**, *5819*, 1993-1994.

(61) Cosnier, S.; Galland, B.; Gondran, C.; Le Pellec, A. *Electroanalysis* **1998**, *10*, 808-813.

(62) Stéphan, O.; Schottland, P.; Le Gall, P.-Y.; Chevrot, C.; Mariet, C.; Carrier, M. *Journal of Electroanalytical Chemistry* **1998**, *443*, 217-226.

(63) Sonmez, G.; Sarac, A. S. *Synthetic Metals* **2003**, *135-136*, 459-460.

(64) Doherty, W. J.; Wysocki, R. J.; Armstrong, N. R.; Saavedra, S. S. *Macromolecules* **2006**, *39*, 4418-4424.

(65) Xu, J.; Nie, G.; Zhang, S.; Han, X.; Hou, J.; Pu, S. *Journal of Materials Science* **2005**, *40*, 2867-2873.

(66) Wan, F.; Li, L.; Wan, X.; Xue, G. *Journal of Applied Polymer Science* **2002**, *85*, 814-820.

(67) Cui, X.; Hetke, J. F.; Wiler, J. A.; Anderson, D. J.; Martin, D. C. *Sensors and Actuators A: Physical* **2001**, *93*, 8-18.

(68) Nyberg, T.; Shimada, A.; Torimitsu, K. *Journal of Neuroscience Methods* **2007**, *160*, 16-25.

(69) Ludwig, K. A.; Uram, J. D.; Yang, J.; Martin, D. C.; Kipke, D. R. *Journal of Neural Engineering* **2006**, *3*, 59-70.

(70) Biran, R.; Martin, D. C.; Tresco, P. A. *Experimental Neurology* **2005**, *195*, 115-26.

(71) Kim, J.; Cho, J. C.; Povlich, L. K.; Martin, D. C. US Patent 7,708,908 **2010**.

(72) Fedorow, H.; Tribl, F.; Halliday, G.; Gerlach, M.; Riederer, P.; Double, K. L. *Progress in Neurobiology* **2005**, *75*, 109-24.

(73) Subianto, S.; Will, G.; Meredith, P. *Polymer* **2005**, *46*, 11505-11509.

CHAPTER 2

Synthesis and Electrochemical Polymerization of Carboxylic Acid-Functionalized 3,4-Ethylenedioxythiophene (EDOTacid)

2.1 Introduction

Conjugated polymers such as poly(3,4-ethylenedioxythiophene) (PEDOT) and polypyrrole (PPy) have been used to improve the electrical performance of metal electrodes.[1,2] However, these polymers lack functional groups that provide a means for covalent modification and can only be altered by varying the counter-ion used during polymerization. Therefore, there is a need for new functionalized heteroaromatic compounds that can be used to create conjugated polymers with new or improved properties. While a large variety of functional 3,4-ethylenedioxthiophene (EDOT) monomers have already been synthesized, most of these monomers are tailored for electronic or electrochromic devices, rather than biological applications.[3] These include EDOT derivatives with alkyl and aromatic appendages,[4,5] 3,4-ethylenedithiathiophenes,[6] macromolecules that contain EDOTs linked together with other conjugated molecules,[7] and even EDOT moieties that incorporate metal atoms such as cobalt.[8]

Carboxylic acids provide a method for functionalizing monomers with more complex entities such as biological molecules. Specifically, peptide-coupling methods have been well developed to react carboxylic acids with amines, creating amide linkages.[9] Other research groups have developed carboxylic acid functionalized pyrrole and EDOT monomers, shown in Figure 2.1. Functionalized polypyrrole (PPy) has been

shown to successfully couple with peptides to provide bioactive surfaces.[10,11] However, as discussed in Chapter 1, PPy has inferior electrical properties and stability compared to PEDOT[12] and, therefore, there is greater interest in creating functionalized PEDOT. Luo *et al.* synthesized carboxylic acid functionalized EDOTs, C2-EDOT-COOH and C4-EDOT-COOH, and demonstrated that they can be reacted with *N*-hydroxysuccinimide (NHS) to form peptide-reactive monomers and polymers.[13] The carboxylic acid functionalized EDOTs have also been shown to change the conjugated polymers' conductivity profiles in aqueous buffers, demonstrating other possible benefits of using acid-functionalized monomers.[14]

The EDOT-COOH monomers developed by Luo *et al*. have ether and ester linkages to the carboxylic acids. Linkers from the EDOT unit to the carboxylic acids may prove to be useful, but the length and functionality of the linker also add complexity. The ester linkage is especially a problem if the intended application of the polymer is biological because the ester bond could be hydrolyzed over time. Therefore, we have developed and synthesized a 3,4-ethylenedioxythiophene monomer that has the simplest possible carboxylic acid modification off of the ethylenedioxy-ring (EDOTacid, Figure 2.1). The synthesis, polymerization and polymer characterization are discussed in this chapter and Chapter 3 will provide detail about the bio-functionalization of the polymer and its interactions with cells. In addition to providing a means for further modification, it is shown that carboxylic acids can be used to tailor the electrical properties, morphology and hydrophobicity of PEDOT-based conjugated polymers.

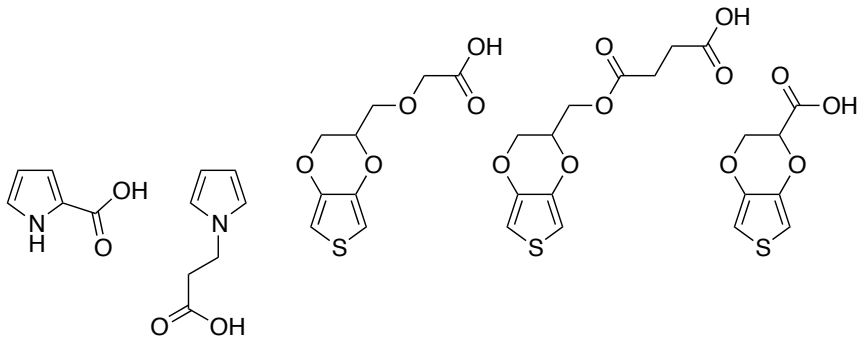

Figure 2.1 Carboxylic acid -functionalized monomers that can be used to synthesize functionalized conjugated polymers (from left to right): Py-α-COOH,[11] PyCOOH,[10] C_2-EDOT-COOH, C_4-EDOT-COOH[13]and the monomer discussed in this chapter, EDOT-COOH or EDOTacid.[15]

2.2 Experimental Procedures

2.2.1 Synthesis of EDOTacid

EDOTacid, which has been patented by our group,[15] was synthesized in a manner similar to EDOT-OH,[16] as shown in Scheme 2.1. Products formed are designated by Arabic numerals. The synthesis steps for the major intermediates and final product are outlined below.

Diethyl 3,4-dihydroxythiophene-2,5-dicarboxylate (4) Thiodiglycolic acid (1, 25 g, 0.17 mol) was refluxed with sulfuric acid (10 ml) in ethanol (250 ml) overnight. The solution was cooled, diluted with water (150 ml), and the product was extracted into diethyl ether three times. The organic layer was then washed three times with Na_2CO_3/H_2O, dried with $MgSO_4$ and the solvent was removed to produce diethyl thioglycolate (2) (27.06 g, 79% yield). Diethyl thioglycolate (27.06 g, 0.13 mol) was then dissolved in a small amount of ethanol and added dropwise with diethyl oxalate (50 g, 0.34 mol) to sodium ethoxide (250 ml, 0.58 mol) at 0 °C. After complete addition the solution was refluxed for 1 hour to form diethyl 3,4-dihydroxythiophene-2,5-

dicarboxylate disodium salt (3). After filtration, (3) was acidified using hydrochloric acid, and the precipitate was filtered and washed with water. The product (4) was dried and recrystallized in methanol to produce a yield of 80 % (27.02 g). ^{1}H NMR (400 MHz, d_6-DMSO) δ ppm (*J* Hz): 1.214 (t, 6 H, $J_{1,2}$ 7.2 Hz, H^1), 4.205 (q, 4 H, $J_{2,1}$ 7.2 Hz, H^2), 10.305 (br s, 2 H, H^3).

5,7-bis(ethoxycarbonyl)-2,3-dihydrothieno[3,4-*b*][1,4]dioxine-2-carboxylic acid (6) Intermediate (4) (8.75g, 0.034 mol) was added to boiling ethanol (200 ml) followed by epibromohydrin (3.75 ml, 0.045 mol) and K_2CO_3 (0.94 g in 50 ml water). After 1 hour, more epibromohydrin (6.5 ml, 0.079 mol) and K_2CO_3 (0.5 g) were added and the solution was refluxed for 72 hours. The product was diluted with acidified water (150 ml, 5 % HCl) and extracted two times with chloroform. The organic layer was then washed with 5 % aqueous KCl, dried with $MgSO_4$, and the solvent was evaporated. The product, diethyl 2-(hydroxymethyl)-2,3dihydrothieno[3,4-b] [1,4]dioxin-5,7-dicarboxylate (5) was purified by precipitating multiple times in diethyl ether. The by-product, diethyl 3-hydroxy-3,4-dihydro-2*H*-thieno[3,4-*b*][1,4]dioxepine-6,8-dicarboxylate, was also present with (5) but this compound could not react in the next step so it was not separated from (5). Oxidation of the hydroxyl group on (5) was achieved by adding a catalytic amount of pyridinium chlorochromate (2 mol% of (5), 0.18 g, 0.8 mmol) and (5) (8.54 g, mixture with by-product) to a solution of periodic acid (15 g, 0.066 mol) in acetonitrile (240 ml) at 0 °C.[17] The periodic acid was stirred vigorously in acetonitrile for 15 minutes before cooling and after adding all of the reactants the solution was stirred for 3 hours as it warmed to room temperature. After the reaction, the solution was diluted with ethyl acetate (300 ml), washed with a 1:1 solution of brine:water, and the product was

extracted into a solution of sodium bicarbonate and water. The aqueous layer was then acidified with HCl and the product was extracted into ethyl acetate. The organic layer was then dried with $MgSO_4$ and the solvent was removed. The product (6) was recrystallized in xylenes resulting in a 26 % yield from compound (4) to compound (6). ^{1}H NMR (400 MHz, d_6-DMSO) δ ppm (*J* Hz): 1.203 (t, 3 H, $J_{1,2}$ 7.2 Hz, H^1), 1.215(t, 3 H, $J_{3,4}$ 7.2 Hz, H^3), 4.158-4.278 (m, 4 H, H^2, H^4), 5.281 (t, 1 H, $J_{5,6}$ 2.8 Hz, H^5), 4.599 (dd, 1 H, $J_{6,5}$ 2.8 Hz, $J_{6,6'}$ 12.0 Hz, H^6), 4.382 (dd, 1 H, $J_{6',5}$ 2.8 Hz, $J_{6',6}$ 12.0 Hz, $H^{6'}$).

2,3-dihydrothieno[3,4-*b*][1,4]dioxine-2,5,7-tricarboxylic acid (7) Compound (6) (2.8g) was refluxed with KOH (3g, 0.05 mol) in water (100 ml) for 2 hours. After the reaction, the solution was cooled with an ice bath and acidified with HCl. The product was recovered as a white precipitate after stirring in acidified water for 3 hours (~100% yield, 2.36 g, 8.6 mmol). ^{1}H NMR (400 MHz, d_6-DMSO) δ ppm (*J* Hz): 4.942 (t, 1 H, $J_{1,2}$ 2.8 Hz, H^1), 4.428 (dd, 1 H, $J_{2,1}$ 2.8 Hz, $J_{2,2'}$ 11.8 Hz, H^2), 4.319 (dd, 1 H, $J_{2',1}$ 2.8 Hz, $J_{2',2}$ 11.8 Hz, $H^{2'}$).

2,3-dihydrothieno[3,4-b][1,4]dioxin-2-carboxylic acid (EDOTacid, 8) Compound (7) (0.2 g, 0.73 mmol) was decarboxylated by refluxing with copper chromite catalyst (0.021 g, 0.068 mmol) in freshly distilled quinolone (10 ml) at 160 – 170 °C for 2 hours. The solution was diluted with ethyl acetate and filtered to remove catalyst. The product was then washed with 5 % HCl three times, NaCl/water twice and extracted into 2 % KOH. The aqueous layer was then acidified with HCl and the product was extracted into ethyl acetate, dried with $MgSO_4$ and the solvent was removed. To remove residual catalyst, the product was purified further by dissolving in it diethyl ether, filtering off any precipitate and removing the solvent to produce 2,3-dihydrothieno[3,4-b][1,4]dioxin-2-

carboxylic acid *i.e.* carboxylic acid EDOT or EDOTacid (8) (0.1 g, 0.54 mmol, 74 % yield). This reaction scheme resulted in a total yield from compound 1 to compound 8 of 12%. ^{1}H NMR (300 MHz, d_6-DMSO) δ ppm (*J* Hz): 4.972 (t, 1 H, $J_{1,2}$ 3.0 Hz, H^1), 4.367 (dd, 1 H, $J_{2,1}$ 3.0 Hz, $J_{2,2'}$ 12.0 Hz, H^2), 4.220 (dd, 1 H, $J_{2',1}$ 3.0 Hz, $J_{2',2}$ 12.0 Hz, $H^{2'}$), 6.581 (d, 1 H, $J_{3,4}$ 3.6 Hz, H^3), 6.627 (d, 1 H, $J_{4,3}$ 3.6 Hz, H^4).

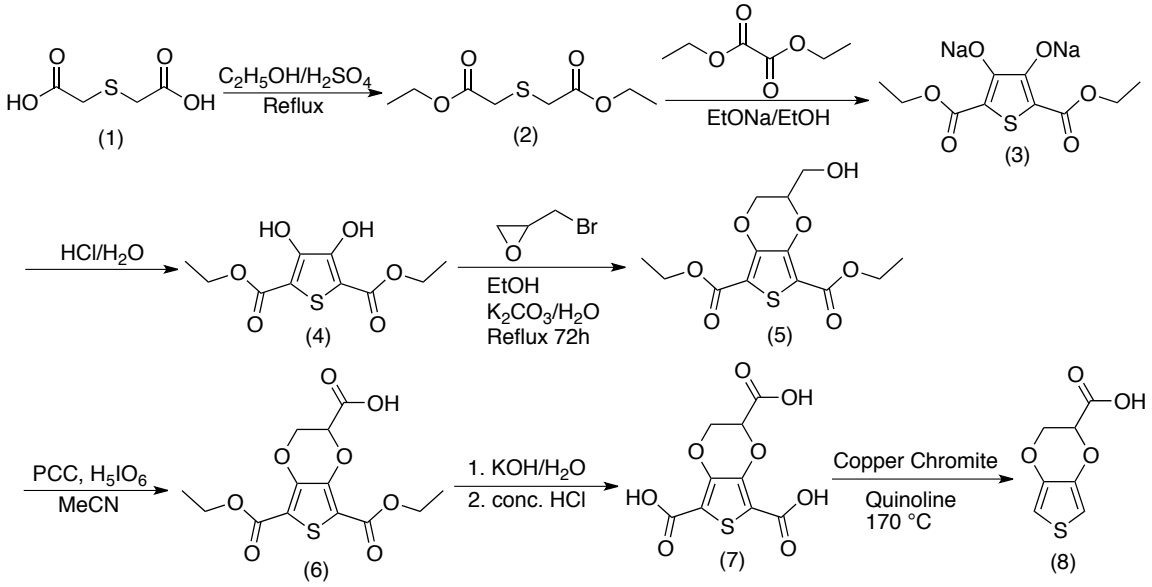

Scheme 2.1 Synthesis of EDOTacid

2.2.2 Electrochemical Polymerization

EDOTacid was electrochemically homo-polymerized or co-polymerized with EDOT in a 2-electrode cell using an Autolab PGstat12 Potentiostat/Galvanostat (EcoChemie) with a platinum wire counter electrode. The possible polymerization methods are shown in Scheme 2.2. The working electrodes used were either sputtered gold-palladium barbell-shaped electrodes (6 mm diameter) on biaxially oriented polyethylene terephthalate (PET, 3M) or evaporated gold electrodes on silicon wafers (Platypus Technologies). The films were electrochemically polymerized in water with 0.05 M lithium perchlorate ($LiClO_4$, Acros Organics) or poly(sodium 4-styrenesulfonate) (PSS, MW ~70,000 g/mol,

Aldrich) counter-ions and total monomer concentrations of 0.01 M. All films were polymerized galvanostatically with a current density between 0.1 – 0.2 mA/cm^2 for 10 minutes and were rinsed with deionized water after polymerization.

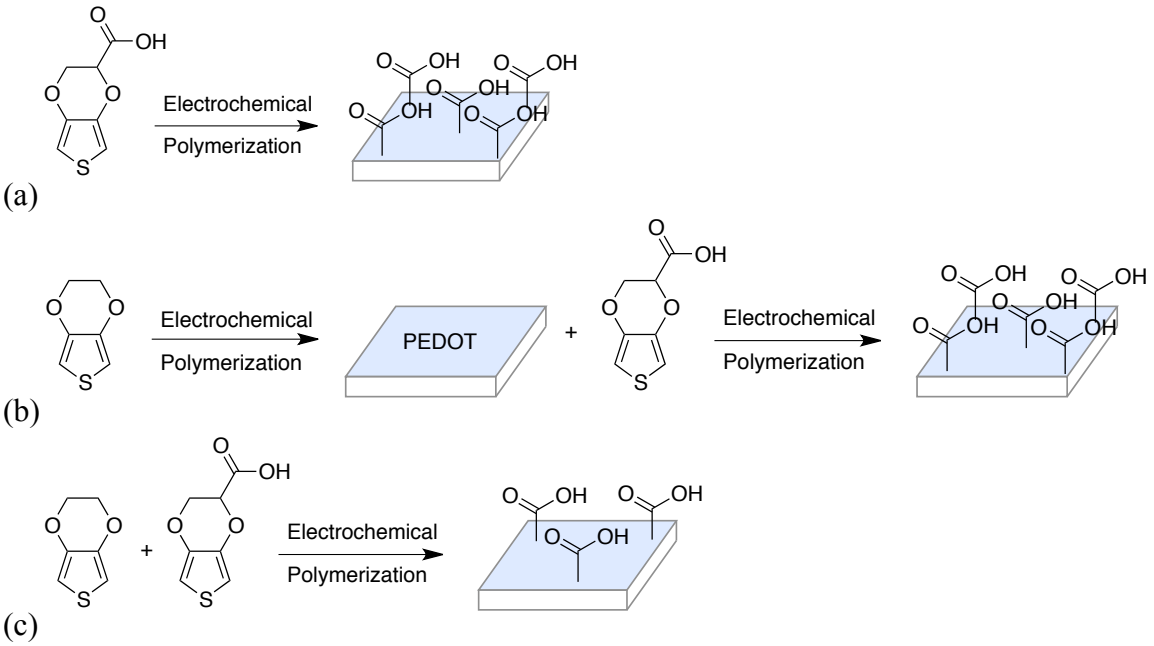

Scheme 2.2 Electrochemical copolymerization methods for forming carboxylic acid functionalized films: (a) homopolymerization of EDOTacid, (b) bilayer polymerization forming PEDOT and then PEDOTacid on top and (c) copolymerization of EDOT and EDOTacid in the same solution. The most stable films were made using method (c).

2.2.3 General Characterization

The chemicals structures for each step of the EDOTacid synthesis were analyzed with ^{1}H nuclear magnetic resonance (NMR) spectroscopy using Varian Inova 400 and Varian Inova 500 NMR spectrometers. The structure of EDOTacid was also confirmed using electron impact (EI) mass spectrometry (Micromass AutoSpec Ultima Magnetic sector mass spectrometer) and Fourier transform infrared spectroscopy (FTIR, Perkin Elmer Spectrum 100 FTIR Spectrometer) in attenuated total reflectance (ATR) mode.

Chemical analysis of electrochemically polymerized films was performed using two different X-ray photoelectron spectroscopy (XPS) systems along with the Perkin

Elmer FTIR Spectrometer described above in ATR mode. The initial XPS was a Kratos Axis Ultra DLD X-ray photoelectron spectrometer with a monochromatic aluminum X-ray source (Al Kα = 1486.6 eV) at a take-off angle of 45° and chamber pressure between 1 x 10^{-8} – 1 x 10^{-9} Torr. Survey pass energy was 160 eV and characteristic region pass energy was 20 eV. The second system used was a PHI 5600 X-ray photoelectron spectrometer with a monochromatic aluminum X-ray source. A take-off angle of 45° was used and the base chamber pressure was < 2 x10^{-9} Torr. The pass energy for the survey spectra and characteristic region spectra were 187.85 eV and 58.7 eV, respectively. All spectra were referenced to the C-C/C-H peak at 285.0 eV.

To analyze the electrical activity of the conjugated polymer films cyclic voltammetry (CV) was performed using the same Autolab potentiostat/galvanostat described above with a platinum counter electrode, a saturated calomel reference electrode and phosphate buffered saline electrolyte (PBS, Hyclone Media). Cycling was performed between -0.6 V and +0.9 V with a scan rate of 0.12 V/s. Morphological studies were conducted using a JEOL JSM-7400F field emission scanning electron microscope at 3kV operating voltage. The films were sputter-coated with gold-palladium for 40-60 seconds in order to provide a more conductive surface. Finally, contact angle measurements were performed to examine the hydrophobicity of the films. After creating a consistently level surface, 1 μl of deionized water was pipetted onto the surface of the substrates and images were captured using a Canon S5 IS camera attached to a tripod. Contact angles were measured using ImageJ software (NIH) with a Drop Shape Analysis plug-in and DropSnake method.[18]

2.3 Results and Discussion

As shown by the NMR spectra in Figure 2.2 EDOTacid was successfully synthesized using the route in Scheme 2.1. The ^{1}H NMR peaks matched with the predicted peaks in terms of position, integration and J-coupling and few impurities were present. Additionally, the FTIR spectrum of EDOTacid (Figure 2.3) demonstrated the presence of a carboxylic acid functional group and EI mass spectrometry results confirmed the predicted molecular weight of 186.0 g/mol (Appendix A along with NMR peak and J-coupling assignments). While the synthesis of the target molecule was successful, it was not highly scalable. Specifically, it was difficult to scale-up the final step of the route larger than hundreds of milligrams, thus a limited quantity of product was produced each time the molecule was synthesized.

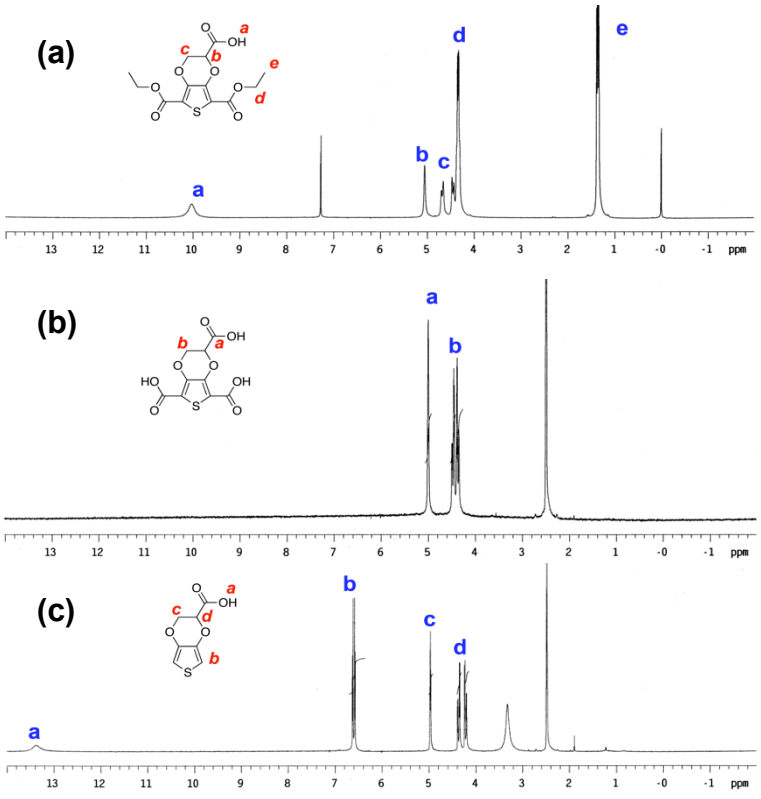

Figure 2.2 NMR spectra for compounds 6 (a), 7 (b) and 8 (c), the final product EDOTacid.

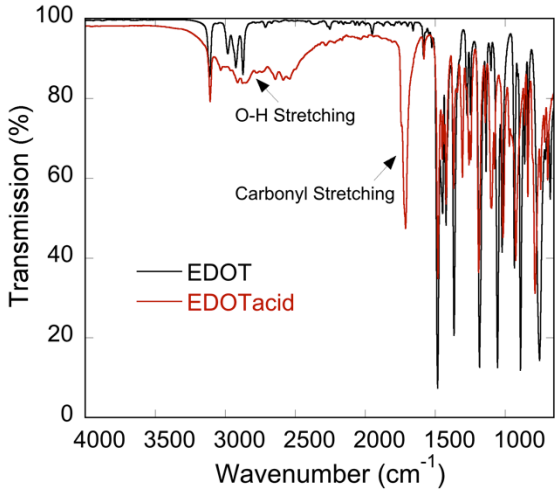

Figure 2.3 FTIR spectra for EDOT and EDOTacid demonstrating the presence of the carboxylic acid on EDOTacid.

Since the synthetic route for EDOTacid proved to be relatively long and difficult to scale-up, other synthetic schemes were investigated. An example alternative route is shown in Scheme 2.3. This route was unsuccessful because the diol product from the second step did not react with the dimethoxythiophene, most likely because the diol underwent a self-condensation reaction instead. In addition, we also attempted to make EDOT-aldehyde through oxidation of bromine-functionalized EDOT (EDOT-Br). This reaction also failed because the necessary conditions for oxidation of EDOT-Br also resulted in polymerization through the thiophene ring. Therefore, the synthesis route shown in Scheme 2.1 seems to be the best method for producing a simple, functionalized monomer with peptide coupling capabilities.

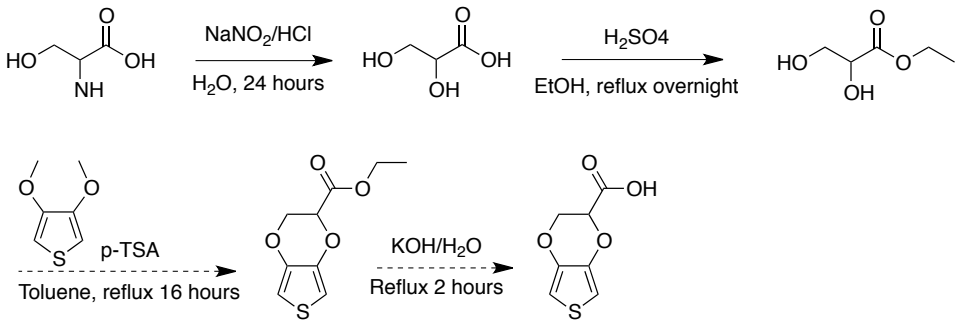

Scheme 2.3 Alternative EDOTacid synthesis route. The third step was unsuccessful, possibly due to self-condensation of the diol.

Scheme 2.2 demonstrates the attempted electrochemical polymerizations schemes for films that contained EDOTacid repeat groups. The first method, Scheme 2.2a, is homo-polymerization of EDOTacid to produce PEDOTacid films in which every repeat unit has a carboxylic acid group. It was possible to electrochemically polymerize this type of film in water with $LiClO_4$ counter-ion, as shown by the XPS data in Figure 2.4. However, PEDOTacid homopolymer films were mechanically and chemically unstable. The films fell apart from minor forces, such as rinsing with water, and due to the high concentration of carboxylic acids, the films dissolved or formed suspensions in high pH buffers. As discussed in Chapter 3, this was a problem when trying to use the carboxylic acids to functionalize the films with peptides. The second method for polymerization of PEDOTacid films first required the polymerization of a PEDOT base layer. EDOTacid was then electrochemically polymerized on top of the layer of PEDOT. It was initially predicted that the growing PEDOTacid would covalently attached to a pre-formed layer of PEDOT. However, it was shown again through treatment with high pH buffers that the PEDOTacid was not covalently bound since it dissolved or suspended in a manner similar to PEDOTacid homopolymer, leaving behind the layer of PEDOT.

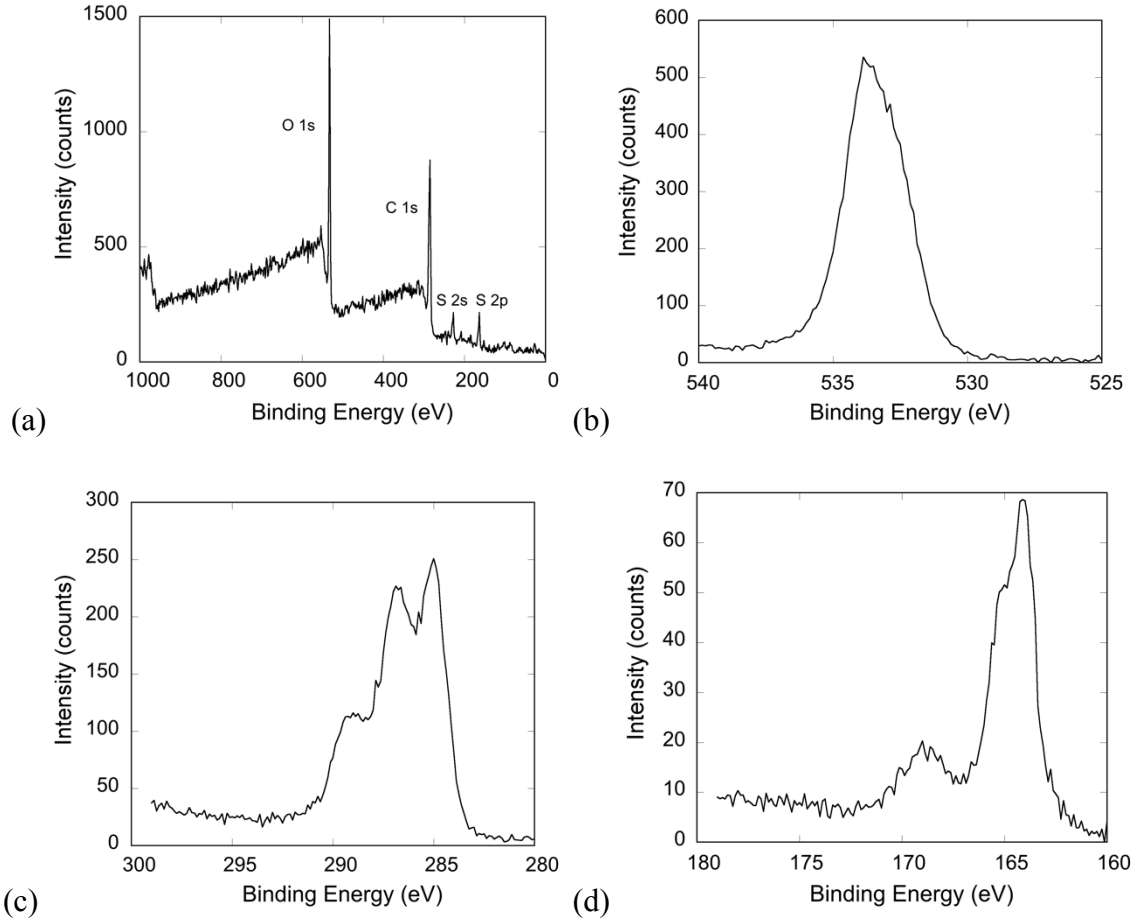

Figure 2.4 XPS (a) survey, (b) O 1s, (c) C 1s and (d) S 2p spectra for PEDOTacid homopolymer films. In the C 1s spectra, the peak at 290 eV represents C=O for the carboxylic acid. This peak was largest in the PEDOTacid homopolymer sample since every repeat unit had a carboxylic acid.

The polymerization scheme that produced the most stable carboxylic acid-functionalized films is shown in Scheme 2.2c. This route involved the co-polymerization of EDOT and EDOTacid and was performed at a 1:1 ratio of the two monomers (0.01 M total concentration). The XPS data in Figure 2.5 demonstrates that PEDOTacid was present in the films, as indicated by the C=O peak around 290 eV. Additionally, the data indicates that EDOT and EDOTacid were incorporated evenly into the copolymer. Six copolymer films were electrochemically polymerized for 10 minutes from the same monomer solution. XPS was performed on the first and sixth sample and Figure 2.5

demonstrates that the two samples were almost chemically identical. Therefore, as the films grew, one monomer was not rapidly consumed before the other and the film composition remained close to the monomer feed ratio of 1:1.

As shown in Figure 2.6, the copolymer films were polymerized evenly and had a dark green-blue color, which is slightly greener in color compared to PEDOT polymerized with the same conditions. In addition, the film thicknesses were approximated to be between 500 nm – 1 μm thick based on previously published results[1] along with the current densities (0.1 – 0.2 mA/cm^2) and total time of polymerization. The films were relatively thin compared to typical conjugated polymer films that are usually on the order of 1 – 10 μm. This was due to the lower current density (0.1 – 0.2 mA/cm^2 compared to 0.5 mA/cm^2), which was necessary for the chosen electrode configuration. PEDOT-PEDOTacid films copolymerized in the manner described above were used for the experiments discussed in the rest of this chapter as well as Chapter 3.

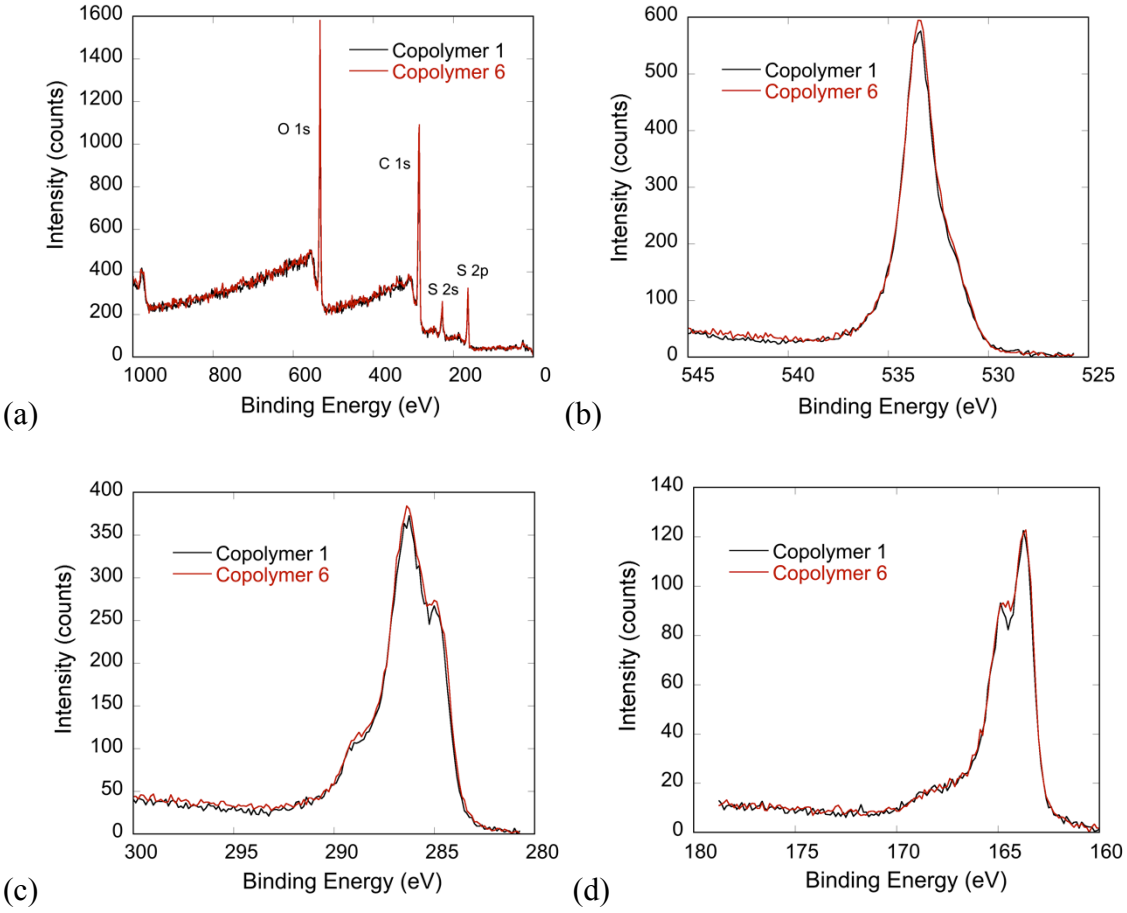

Figure 2.5 XPS (a) Survey, (b) O 1s, (c) C 1s and (d) S 2p spectra for PEDOT-PEDOTacid copolymer films made out of the same solution (1st sample and 6th sample out of six 10 minute depositions). The spectra are very similar, suggesting that both monomers were evenly incorporated into the films.

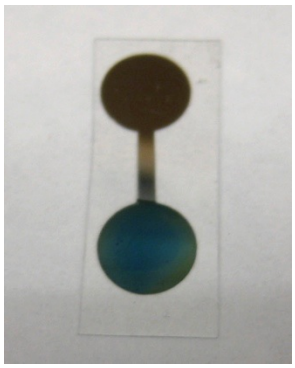

Figure 2.6 PEDOT-PEDOTacid film electrochemically copolymerized from a 1:1 EDOT:EDOTacid monomer solution for 10 minutes at 0.1 mA/cm^2. Diameter of the electrode is 6 mm.

To ensure that the carboxylic acid functional group was intact in the PEDOT-PEDOTacid copolymer films, FTIR was also performed. As shown in Figure 2.7, there were multiple peaks in the IR region for carbonyl stretching peaks and there was a shallow, broad peak in the hydroxyl stretching region. This indicated that there were carboxylic acids in the film and that they had multiple hydrogen-bonded states or that some of them were present as carboxylates rather than carboxylic acids. The FTIR spectrum also demonstrated broad absorption from 4000 to 2000 cm^{-1}. This absorption partially masked O-H stretching and C-H stretching peaks in the same region and is typically seen for conjugated polymers that are in an oxidized state. Broad absorption in a high wavenumber region indicated that the polymer was in a polaron-bipolaron form with delocalized free electron states.[19]

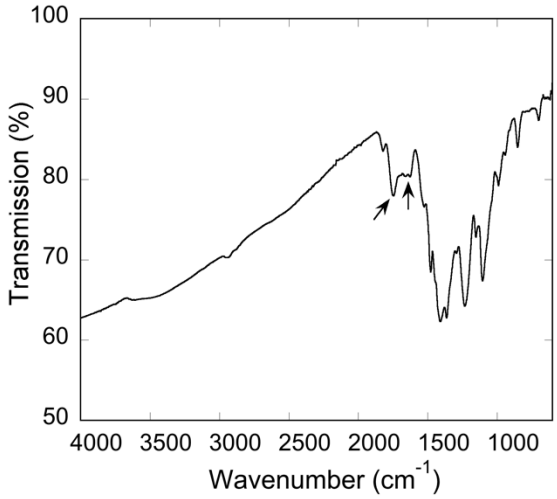

Figure 2.7 FTIR of PEDOT-PEDOTacid copolymer indicating carbonyl stretching peaks around 1750 cm^{-1} and 1650 cm^{-1}. Broad absorption from 4000 cm^{-1} to 2000 cm^{-1} demonstrates that the polymer was in an oxidized, conductive state. The absorption partially masks the other peaks in this range, but a broad peak can be seen around 3500 cm^{-1}, representing the hydroxyl stretching peak on the carboxylic acid.

After studying the chemical composition of PEDOT-PEDOTacid films, we were interested in examining the electrical properties of the films and how they compared to

PEDOT. PEDOT-PEDOTacid copolymers and PEDOT homopolymers were electrochemically polymerized with both $LiClO_4$ and PSS counter-ions and subjected to cyclic voltammetry (CV) for 10 cycles. Figure 2.8 demonstrates that PEDOT-PEDOTacid films with $LiClO_4$ and PSS were electrically responsive and had significant charge capacities, as indicated by the area within the curves. However, PEDOT-PEDOTacid $LiClO_4$ had decreased charge capacity (6.5 mC/cm^2) and relative instability compared to PEDOT $LiClO_4$ (10.4 mC/cm^2). On the other hand, PEDOT-PEDOTacid PSS films had only slightly diminished charge capacity (9.6 mC/cm^2) compared to PEDOT PSS (10.4 mC/cm^2). All of these charge capacities were higher than that of the gold-palladium substrates (3.2 mC/cm^2) and were comparable to published results for PEDOT (16.7 mC/cm^2) and PPy (5.0 mC/cm^2) coated on microelectrodes.[20] However, the charge capacities were much lower than PEDOT that has been tailored to have a high surface area, such as PEDOT grown in surfactant (26.7 mC/cm^2) or PEDOT nanotubes (392 mC/cm^2).[20,21] Besides differences in effective surface area, the PEDOT-PEDOTacid and PEDOT films in this chapter were polymerized with lower deposition charge density (64 mC/cm^2 compared to 430 mC/cm^2 or higher), thus resulting in thinner films and lower charge capacities than the previously published materials. Also, the PEDOT nanotube films reported by Abidian *et al*. grew past the actual electrode area, thus making the calculated charge capacity per area larger than the actual value.

As shown later in this chapter, PEDOT-PEDOTacid films were more hydrophilic than PEDOT films and, therefore, could be more susceptible to swelling in water. Swelling during electrochemical polymerization in water could have affected the electrical properties of the final polymer film by disrupting the connectivity between

multiple polymer chains or by distorting the conformation within individual chains. PEDOT-PEDOTacid PSS films may not have swelled as a significantly as PEDOT-PEDOTacid $LiClO_4$ because PSS is a polymer counter-ion and may have restricted expansion of the conjugated polymer film. The morphologies of PEDOT-PEDOTacid copolymer films were studied with scanning electron microscopy to examine the validity of this swelling hypothesis. At low magnification, the PEDOT-PEDOTacid $LiClO_4$ films had wrinkles or folds that were less that 1 μm wide but 10's of μms long, which indicated that the films were swelling (Figure 2.9). Similar wrinkled morphologies have been seen in other acid-functionalized polythiophene films (unpublished data). However, this type of feature was not seen in PEDOT-PEDOTacid PSS films, indicating that they were less prone to swelling. At higher magnification, copolymer films with both types of counter-ions had relatively rough morphologies that were similar in appearance to the morphologies of PEDOT films (Figure 2.10). Rough features on films made with $LiClO_4$ ranged from spherical objects around 500 nm in diameter to bump-like structures that were as small as 20 nm. Films made with PSS had rough features that were more consistent in size with dimensions around 100 nm. Rough morphologies result in a high overall surface area that can produce low electrical resistance or impedance. The impedances of the films were not thoroughly investigated because they were polymerized on large electrodes that already had relatively low impedances. However, it is predicted that these films would have had dramatically lower impedances compared to metals if they were deposited on microelectrodes, such as those on neural probes.

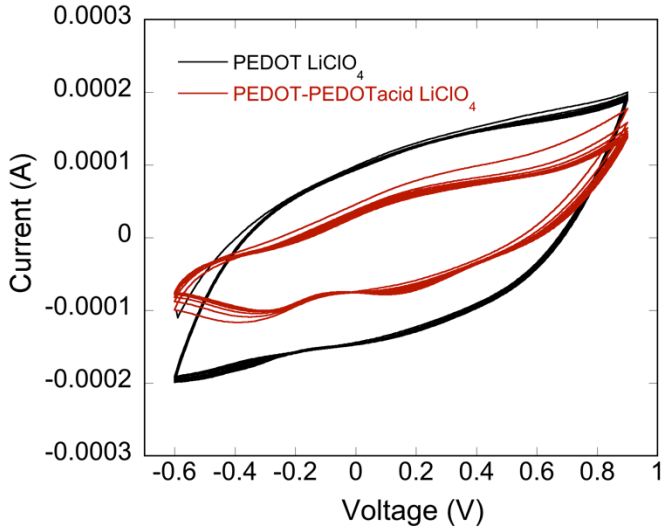

(a)

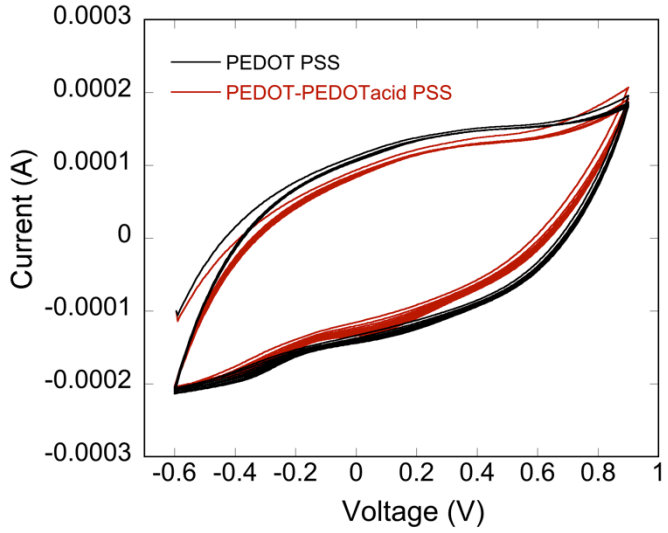

(b)

Figure 2.8 Cyclic voltammetry comparing PEDOT and PEDOT-PEDOTacid films with both (a) $LiClO_4$ and (b) PSS counter-ion.

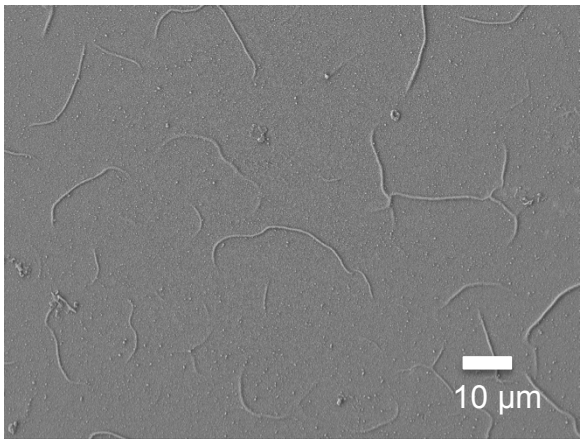

Figure 2.9 SEM image of PEDOT-PEDOTacid LiClO4 film showing wrinkles that formed during electrochemical polymerization, possibly due to swelling of the film.

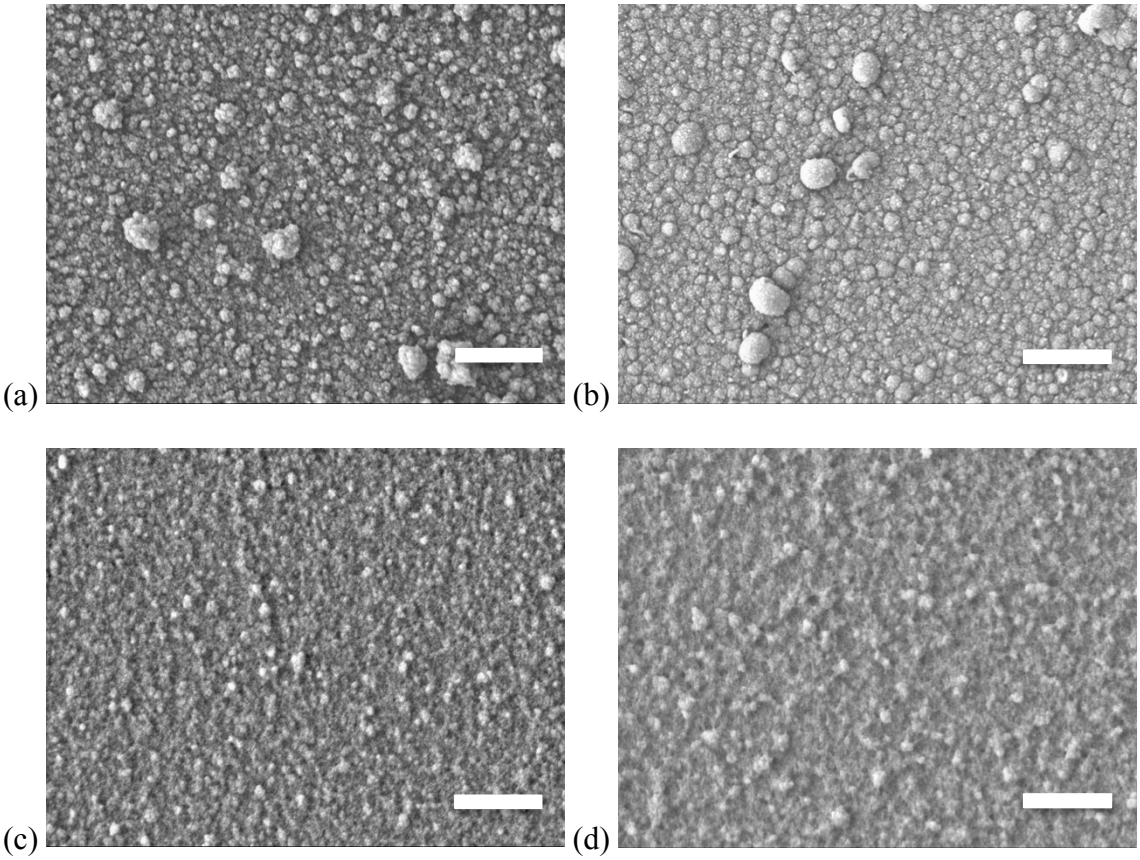

Figure 2.10 SEM images of (a) PEDOT-PEDOTacid $LiClO_4$, (b) PEDOT $LiClO_4$, (c) PEDOT-PEDOTacid PSS and (d) PEDOT PSS demonstrating rough morphologies. Scale bar represents 1 µm.

In order to understand the difference in hydrophobicity between PEDOT and PEDOT-PEDOTacid films and how the hydrophobicity could be altered, the contact angles were measured (Table 2.1). In Figure 2.11 it can be seen clearly that PEDOT-PEDOTacid $LiClO_4$ films were more hydrophilic than PEDOT $LiClO_4$ films. In addition, the hydrophobicity was altered by the counter-ion used; PEDOT-PEDOTacid PSS was slightly more hydrophilic than the same conjugated polymer with $LiClO_4$. Also, electrically oxidizing or reducing the films altered the contact angle. Reducing a conjugated polymer neutralizes the backbone and expels counter-ions while oxidizing makes the backbone more positively charged and recruits more counter-ions to the surface. Finally, changing the amount of PEDOTacid in copolymer films should also vary the hydrophobicity, resulting in a highly tailorable system. It should be noted, however, that copolymer films would become increasingly unstable as more PEDOTacid is added to the composition, as seen by the instability of PEDOTacid homopolymer films. Interestingly, carboxylic acid-functionalized PEDOTs synthesized by Luo *et al*. did not have as low of contact angles as the PEDOT-PEDOTacid reported here. Films made from ester-linked and ether-linked PEDOTacids had contact angles of 44.6° and 40.2°, respectively.[13] There may be a number of reasons for the higher contact angle, the most likely being that the alkyl portion of the linkers increased the hydrophobicity of the films. Also, these films were polymerized in an aqueous microemulsion that resulted in ultrasmooth surfaces, which are quite different from the rough surfaces of the PEDOT-PEDOTacid films discussed in this thesis.

(a) 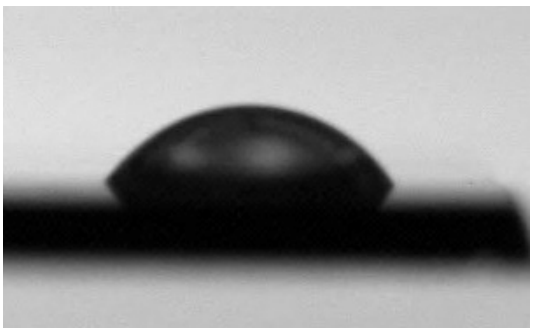 (b) 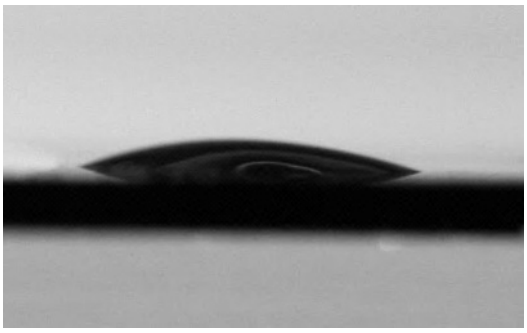

Figure 2.11 Images of (a) PEDOT LiClO4 and (b) PEDOT-PEDOTacid LiClO4 used to measure to contact angles of the films and demonstrating an increase in hydrophilicity for films containing PEDOTacid.

Table 2.1 List of contact angles along with standard deviations for metal and conjugated polymer substrates

Sample	θ_c (°)	Std. Dev. (°)
Gold electrode	89.3	9.8
PEDOT LiClO4 (reduced)	50.1	3.9
PEDOT LiClO4 (oxidized)	42.5	2.5
PEDOT-PEDOTacid LiClO4 (oxidized)	21.2	1.8
PEDOT-PEDOTacid LiClO4 (reduced)	18.1	2.0
PEDOT-PEDOTacid PSS (oxidized)	15.5	3.7

A comparison between PEDOT and PEDOT-PEDOTacid copolymer films is important when considering the application desired for the conjugated polymers. As shown in the CV data, PEDOT films are more stable than copolymer films and have better electrical performance. However, the functionality in PEDOT-PEDOTacid films may outweigh the loss in electrical activity. The carboxylic acid could be used for a variety of purposes. For non-biological applications, PEDOT-PEDOTacid films could be used for devices that require increased ion transport that can be facilitated by both the conjugated polymer backbone and the carboxylic acid. Simply having a more hydrophilic surface could be beneficial for non-biological and biological applications. For instance,

the extremely hydrophilic polymer poly(ethylene glycol) (PEG) is used to prevent the adsorption of proteins to surfaces, which can reduce the immune systems response to a foreign material.[22,23] Important to this work, the carboxylic acid can also be used to functionalize the conjugated polymer with biological molecules. For example, molecules that attract neurons could be attached to conjugated polymers on neural probes to increase the signal strength while communicating with these neurons. The type of molecule attached can be varied based on the area of the body the polymer will be implanted and this concept will be discussed in detail in the next chapter.

A general benefit of PEDOTacid is that the monomer, EDOTacid, has increased solubility in water compared to EDOT, which has a solubility limit around 2.1 g/L or 0.015 M.[16] In addition, EDOT solutions near this concentration must be stirred for at least 4 hours to dissolve the monomer. Since EDOTacid has a carboxylic acid it was easily dissolved in water at 0.01 M. Rather than stirring for hours, EDOTacid solutions only needed to be sonicated briefly to disrupt hydrogen bonding between carboxylic acids. Concentrations up 0.04 M were achieved using this method, as seen by eye, although there was a red-shift in the UV-Vis spectrum, possibly indicating aggregation. Higher concentrations may be possible with longer sonication times or the addition of heat. The benefit of increased water solubility does not translate to carboxylic acid-functionalized EDOTs that have been synthesized by other groups (Figure 2.1). These molecules have alkyl ester and alkyl ether linkers to the acid group that decrease their water solubility, possibly even lower than regular EDOT. Also, as stated previously, the lack of extra functional groups on EDOTacid may make the structure more chemically stable when placed in a biological environment compared to ester or ether linked acid groups.

2.4 Summary and Future Outlook

EDOTacid, a simple carboxylic acid-functionalized EDOT derivative, was successfully synthesized and electrochemically copolymerized with EDOT to produce PEDOT-PEDOTacid conjugated polymer films that were blue-green in color and had relatively rough morphologies. Although the increased hydrophilicity of these copolymers reduced their stability compared to PEDOT, the films were still electrically active and could be used as electrode coatings similar to PEDOT. The carboxylic acid functionality in PEDOT-PEDOTacid provides a means for changing the properties of electrodes and also for attaching other molecules.

Since EDOTacid has a relatively complex synthesis route, alternative molecules are currently being explored that have carboxylic acid functionality but are easier to synthesize. These molecules are part of a group of 3,4-propylenedioxythiophene (ProDOT) derivatives that can be synthesized easily using thiolene chemistry. The resulting monomers have alkyl thioether linkages to the desired functional groups. This added complexity gives the functional groups greater freedom of motion, which could be beneficial for performing surface reactions, but it also affects the solubility and polymerization parameters of the monomers. It will be interesting to see how these new monomers and the resulting poly(ProDOT)-based conjugated polymer films compare to EDOTacid and PEDOT-PEDOTacid films.

2.5 References

(1) Yang, J.; Martin, D. C. *Materials Research* **2006**, *21*, 1124-1132.

(2) Cui, X.; Hetke, J. F.; Wiler, J. A.; Anderson, D. J.; Martin, D. C. *Sensors and Actuators A: Physical* **2001**, *93*, 8-18.

(3) Groenendaal, L. B.; Jonas, F.; Freitag, D.; Pielartzik, H.; Reynolds, J. R. *Advanced Materials* **2000**, *12*, 481-494.

(4) Heywang, G.; Jonas, F. *Advanced Materials* **1992**, *4*, 116-118.

(5) Kumar, A.; Welsh, D. M.; Morvant, M. C.; Piroux, F.; Abboud, K. A.; Reynolds, J. R. *Chemistry of Materials* **1998**, *10*, 896-902.

(6) Wang, C.; Schindler, J. L.; Kannewurf, C. R.; Kanatzidis, M. G. *Chemistry of Materials* **1995**, *7*, 58-68.

(7) Sapp, S. A.; Sotzing, G. A.; Reynolds, J. R. *Chemistry of Materials* **1998**, *10*, 2101-2108.

(8) Kingsborough, R. P.; Swager, T. M. *Advanced Materials* **1998**, *10*, 1100-1104.

(9) Hermanson, G. T. *Bioconjugate Techniques*; 2nd ed.; Elsevier: New York, 2008.

(10) Lee, J.-W.; Serna, F.; Nickels, J.; Schmidt, C. E. *Biomacromolecules* **2006**, *7*, 1692-5.

(11) Lee, J.-W.; Serna, F.; Schmidt, C. E. *Langmuir* **2006**, *22*, 9816-9.

(12) Yamato, H.; Ohwa, M.; Wernet, W. *Journal of Electroanalytical Chemistry* **1995**, *397*, 163-170.

(13) Luo, S.-C.; Mohamed Ali, E.; Tansil, N. C.; Yu, H.-H.; Gao, S.; Kantchev, E. a B.; Ying, J. Y. *Langmuir* **2008**, *24*, 8071-7.

(14) Ali, E. M.; Kantchev, E. A. B.; Yu, H.; Ying, J. Y. *Macromolecules* **2007**, *40*, 6025-6027.

(15) Kim, J.; Cho, J. C.; Povlich, L. K.; Martin, D. C. US Patent 7,708,908 **2010**.

(16) Stéphan, O.; Schottland, P.; Le Gall, P.-Y.; Chevrot, C.; Mariet, C.; Carrier, M. *Journal of Electroanalytical Chemistry* **1998**, *443*, 217-226.

(17) Hunsen, M. *Synthesis* **2005**, 2487-2490.

(18) Stalder, A. F.; Kulik, G.; Sage, D.; Barbieri, L.; Hoffmann, P. *Colloids and Surfaces A: Physicochemical and Engineering Aspects* **2006**, *286*, 92-103.

(19) *Conducting Polymers, A New Era in Electrochemistry*; Inzelt, G., Ed.; Springer: Berlin, 2008; Vol. 29.

(20) Yang, J.; Kim, D. H.; Hendricks, J. L.; Leach, M.; Northey, R.; Martin, D. C. *Acta Biomaterialia* **2005**, *1*, 125-36.

(21) Abidian, M. R.; Kim, D.-H.; Martin, D. C. *Advanced Materials* **2006**, *18*, 405-409.

(22) Zhang, M.; Desai, T.; Ferrari, M. *Biomaterials* **1998**, *19*, 953-60.

(23) Alcantar, N. A.; Aydil, E. S.; Israelachvili, J. N. *Journal of Biomedical Materials Research* **2000**, *51*, 343-51.

CHAPTER 3

Bio-functionalization and Bioactivity of Carboxylic Acid-functionalized Poly(3,4-ethylenedioxythiophene) (PEDOTacid)

3.1 Introduction

Functionalization of materials with biological molecules is vital for tissue engineering and long-term implantation of devices. In these applications it is often necessary to control the position, differentiation and chemical signaling of cells in order to produce a successful outcome. Previous research has demonstrated the use of peptides and proteins for directing cell behavior on a variety of materials.[1,2,3] This type of functionalization may be especially important for stable implantation of chronic neural probes. To work optimally, neural electrodes should be able to record or stimulate neurons in the brain indefinitely. However, when studied in animals, an inflammatory reaction occurs upon implantation of these devices and an insulating glial scar forms around the probes within four weeks.[4] Therefore, options need to be explored to functionalize neural probes with biological molecules that can either minimize scar formation or retain neurons close to the electrode surface.

Conjugated polymers can be polymerized on neural probe electrodes and also have been developed with carboxylic acid functionality. Carboxylic acids can react with peptides to form amide bonds and therefore, can be used to create bio-functionalized conjugated polymers. Lee *et al*. demonstrated the ability of carboxylic acid functionalized polypyrroles to covalently bind with arginine-glycine-aspartic acid (RGD) peptides, a

fragment found in the extracellular matrix protein fibronectin.[5,6] RGD-functionalized films increased the adhesion of endothelial cells compared to regular polypyrrole films. A similarly designed copolymer made from 3,4-ethylenedioxythiophene (EDOT) and carboxylic acid-functionalized 3,4-ethylenedioxythiophene (EDOTacid) was discussed in Chapter 2. This conjugated polymer, called PEDOT-PEDOTacid, has the simplest possible carboxylic acid functionality (-COOH directly off of the EDOT monomer) and could be used to functionalize polymer films with peptides or proteins.

In this chapter, the functionalization of PEDOT-PEDOTacid with RGD peptide is presented. Although RGD is not necessarily the best choice of peptide to exclusively attract neurons *in vivo*, it is the most commonly used peptide for bio-functionalization of materials.[7] RGD is a cell-binding domain found on the extracellular matrix protein fibronectin and has been shown to increase the adhesion of many different types of cells through integrin binding.[8] Most commonly fibroblasts are used to demonstrate the attachment of cells to RGD through the formation of focal adhesions and actin stress fibers during the spreading process, as shown in Figure 3.1.[9] RGD peptide fragments have also been used to increase the adhesion of neural stems cells on phospholipid substrates (Figure 3.2)[10] and dorsal root ganglion (DRG) neurons have been aligned on strips of fibronectin.[11] The aim of the experiments in this chapter is to show that we can functionalize PEDOT-PEDOTacid with RGD and that the peptide remains biologically active at the end of the process. At the end of the chapter we will discuss alternative peptides or biomolecules that may direct the behavior of neurons more effectively.

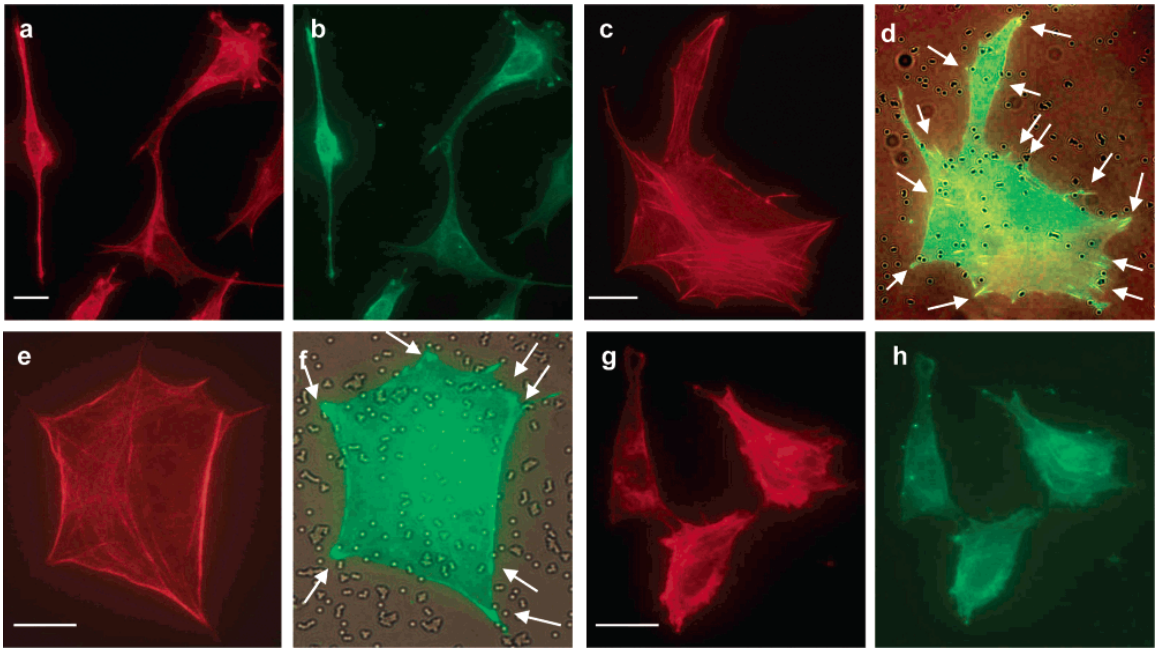

Figure 3.1 Fluorescent micrographs showing actin stress fibers (red) and vinculin (green) staining of attached NR6 cells (mouse fibroblasts) on colloidal array surfaces with different RGD surface coverage: (a, b) 0%; (c-f) 5-10%; (g and h) 95%.[9] Reprinted from *Langmuir*, 20, Zheng, H.; Berg, M.C.; Rubner, M.F. and Hammond, P.T., "Controlling cell attachment selectively onto biological polymer-colloid templates using polymer-on-polymer stamping", 7215-22, Copyright (2004) American Chemical Society.

The peptide used to functionalize PEDOT-PEDOTacid includes a glycine linker before the RGD fragment (Figure 3.3). This spacer provides length and flexibility and enables cell integrins to reach the entire functional peptide segment. In previous literature a minimum distance of 1.1 nm was necessary to promote cell attachment, which corresponds to about 3 glycine units (0.35 nm per glycine).[12] In some reports a spacer was not necessary for cell attachment, however, this may be a result of the surfaces investigated, which were flat and hard.[13,14] It seems likely that a linker would be necessary for cell attachment on polymeric substrates that have soft, rough surfaces. For example, a four-glycine spacer was used for myoblast integrin binding to RGD-modified alginate hydrogels.[15] Other forms of RGD could also be used including those with PEG linkers rather than glycine and cyclic versions of the peptide.[7]

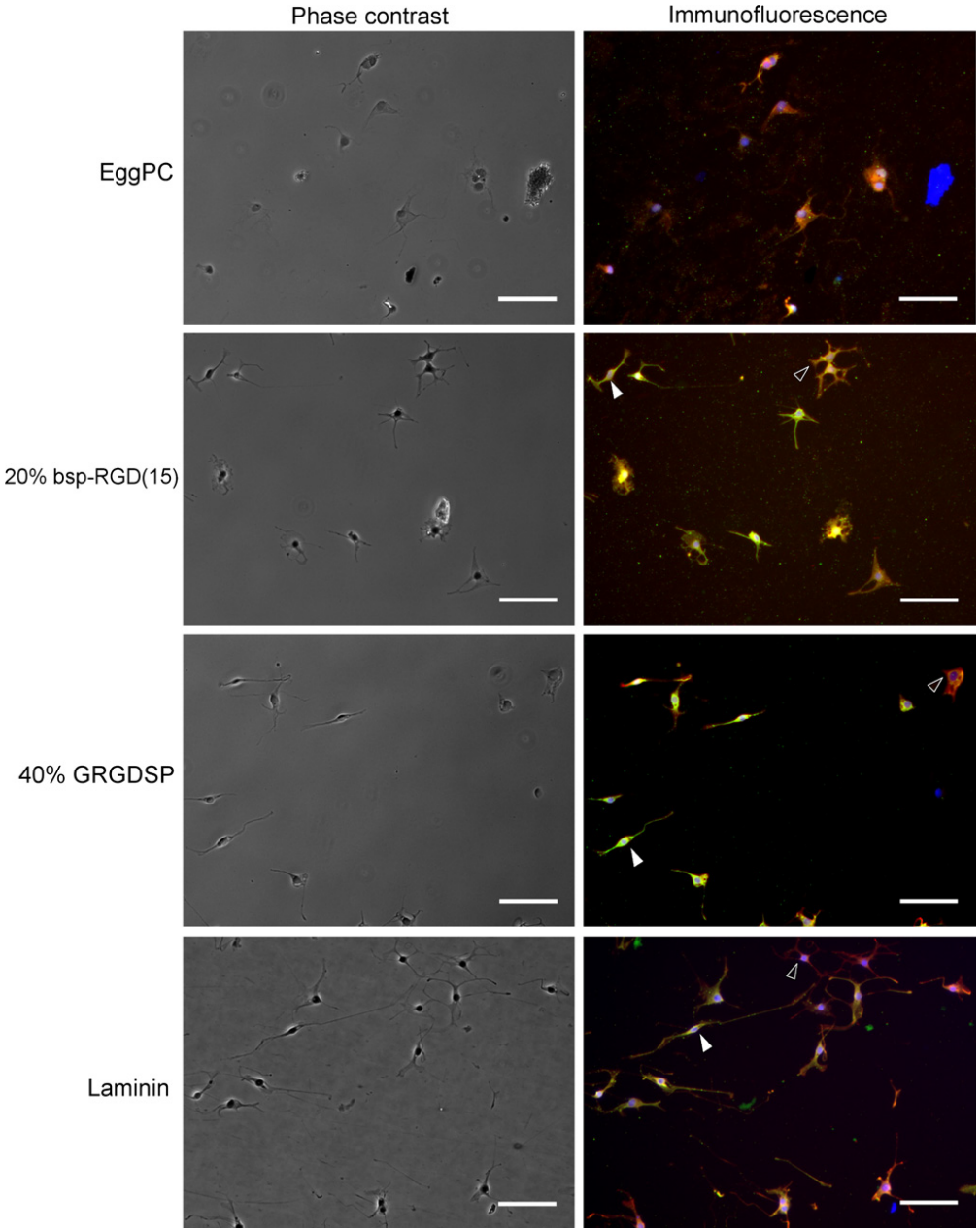

Figure 3.2 Phase contrast and immunofluorescence images of neural stems cells (NSCs) after incubation in mixed differentiating conditions (0.75% FBS and 1 mM forskolin) for 5 days on unmodified phospholipid (EggPC, negative control), RGD substrates and laminin (positive control). β-tubulin III expression is shown in green, GFAP in red, and nuclear DAPI staining in blue. NSCs differentiated into an admixture of neuronal cells with high b-tubulin III expression (filled arrowheads) and astrocytes with high GFAP expression (empty arrowheads). Scale bar: 100 mm.[10] Reprinted from *Biomaterials*, 31, Ananthanarayanan, B.; Little, L.; Schaffer, D.V.; Healy, K.E. and Tirrell, M., "Neural stem cell adhesion and proliferation on phospholipid bilayers functionalized with RGD peptides", 8706-15, Copyright (2010), with permission from Elsevier.

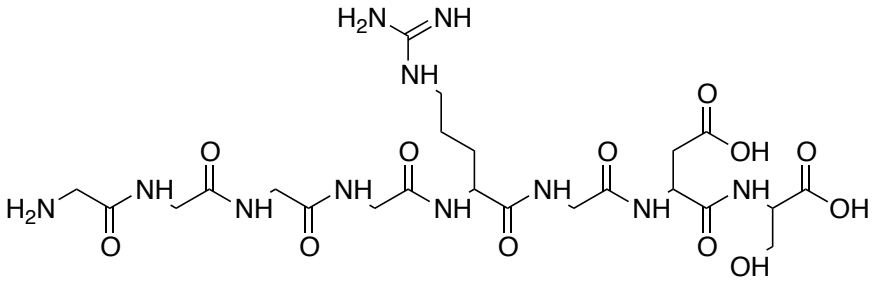

Figure 3.3 Structure of the peptide used for bio-functionalization of EDOTacid: GGGGRGDS.

3.2 Experimental Procedures

3.2.1 Electrochemical Polymerization

EDOTacid was synthesized as described in Chapter 2 and electrochemically co-polymerized with EDOT (1:1 ratio) in a 2-electrode cell using an Autolab PGstat12 Potentiostat/Galvanostat (EcoChemie) with a platinum wire counter electrode. The working electrodes used were either sputtered gold-palladium barbell-shaped electrodes (6 mm diameter) on biaxially oriented polyethylene terephthalate (PET, 3M) or evaporated gold electrodes on silicon wafers (Platypus Technologies). The films were electrochemically polymerized in water with 0.05 M lithium perchlorate ($LiClO_4$, Acros Organics) counter-ion and total monomer concentrations of 0.01 M. All films were polymerized galvanostatically using a current density between 0.1 – 0.2 mA/cm^2 for 10 minutes, which produced films that were approximately 500 nm -1 μm thick. After polymerization the films were rinsed with deionized water to remove excess counter-ions.

3.2.2 Peptide Coupling

PEDOT-PEDOTacid films were coupled with GGGGRGDS or GGGGRGES peptide (Peptide International) as shown in Scheme 3.1. Various carboxylic acid

activation treatments were explored. Successful activation and coupling was achieved using *O*-(7-Azabenzotriazol-1-yl)-*N,N,N′,N′*-tetramethyluronium hexafluorophosphate (HATU, Aldrich, 3.33 mg) and N,N-diisopropylethylamine (DIPEA, Acros Organics, 4.5 µl) in N,N-dimethylformamide (DMF, Aldrich, 1 ml). After activation for 1 hour the films were treated with peptide (2 mg) in 1 ml of 1:1 DMF and dimethylsulfoxide (DMSO, Acros Organics) with 1 µl DIPEA for 16-24 hours. To remove unbound peptide and unreacted HATU, the films were washed with 0.1% sodium dodecyl sulfate (SDS, Acros Organics), pH 9 phosphate buffered saline (PBS, Fisher BioReagents) and finally deionized water.

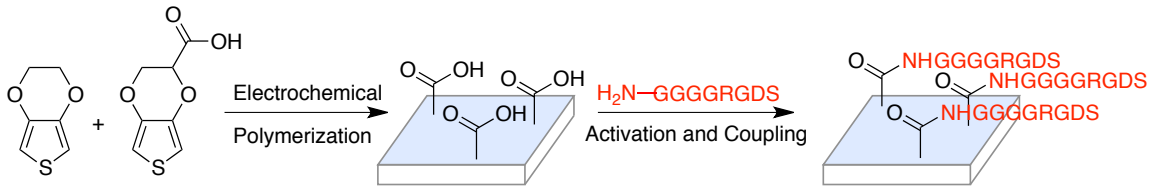

Scheme 3.1 Bio-functionalization of PEDOT-PEDOTacid copolymer film with RGD peptide.

3.2.3 General Characterization

Peptide coupling was verified using two different X-ray photoelectron spectroscopy (XPS) systems along with Fourier transform infrared spectroscopy (FTIR, Perkin Elmer Spectrum 100 FTIR Spectrometer) in attenuated total reflectance (ATR) mode. The initial XPS was a Kratos Axis Ultra DLD X-ray photoelectron spectrometer with a monochromatic aluminum X-ray source (Al Kα = 1486.6 eV) at a take-off angle of 45° and chamber pressure between 1 x 10^{-8} – 1 x 10^{-9} Torr. Survey pass energy was 160 eV and characteristic region pass energy was 20 eV. The second system used was a PHI 5600 X-ray photoelectron spectrometer with a monochromatic aluminum X-ray

source. A take-off angle of 45° was used and the base chamber pressure was $< 2 \times 10^{-9}$ Torr. The pass energy for the survey spectra and characteristic region spectra were 187.85 eV and 58.7 eV, respectively. All spectra were referenced to the C-C/C-H peak at 285.0 eV.

To analyze the electrical activity of the conjugated polymer films cyclic voltammetry (CV) was performed using the same Autolab potentiostat/galvanostat described above with a platinum counter electrode, a saturated calomel reference electrode and phosphate buffered saline electrolyte (PBS, Fisher BioReagents). Cycling was performed between -0.6 V and +0.9 V with a scan rate of 0.12 V/s.

3.2.4 Cell Culture

Primary motor neurons were extracted from the spinal cords of stage E15 rat embryos. Dissection of the cells is described in Appendix B. Cells were seeded on the substrates at a density of 5,000 cells per electrode circle (~20,000 cells/cm^2) in Neurobasal medium with motor neuron additives (albumin, apo-transferrin, biotin, D-galactose, progesterone, putrescine, selenium, β-estradiol, hydrocortisone, catalase, superoxide dismutase, B-27 supplement, L-glutamine and penicillin-streptomycin-neomycin antibiotic). The media was kept serum-free throughout the experiments. Initially, the cells were only seeded on the substrates and after 1 hour the entire well was filled with media. The cells were allowed to incubate for 26 hours. The media was then removed and the cells were fixed with 4% formaldehyde. After the formaldehyde was removed, the samples were washed with PBS (3X) and incubated with block/perm solution (1.25% bovine serum albumin in 1X PBS, 0.05% Triton X-100 and 2.0% normal goat serum) for 30 minutes. The cells were then treated overnight with Tuj1 (neuron-

specific class III beta-tubulin) primary anti-body and stained with FITC-conjugated secondary anti-body the following day. The samples were mounted in Prolong Gold +DAPI (Invitrogen) mounting media and imaged using an EVOS-fl digital inverted fluorescence microscope (Advanced Microscopy Group).

3.3 Results and Discussion

Multiple methods were considered for creating RGD-coupled PEDOT-PEDOTacid films. Initially, we attempted to covalently bind the EDOTacid monomer to RGD peptides bound to polystyrene beads to create EDOT-RGD. While the reaction with peptide was successful, as shown by the matrix-assisted laser desorption/ionization (MALDI) spectrum in Appendix A, the EDOTacid coupled peptide was difficult to separate from unreacted peptide with the equipment we had available. In addition, having peptide attached to the EDOT monomer may have made it more difficult to polymerize, due to the bulkiness of the peptide. Surface reaction of PEDOT-PEDOTacid films with RGD peptides was attempted next using either 1-[3-(dimethylamino)propyl]-3-ethylcarbodiimide methiodide (EDC methiodide) or *N*-(3-dimethylaminopropyl)-*N*′-ethylcarbodiimide hydrochloride (EDC) and *N*-hydroxysulfosuccinimide sodium (sulfo-NHS). These coupling reagents, however, did not react PEDOT-PEDOTacid with peptide. Figure 3.4 shows that films treated with only EDC methiodide had the same nitrogen content as films treated with EDC methiodide and then peptide. It is possible that EDC reacted with the carboxylic acid on PEDOTacid and then rearranged to form unreactive N-acylurea before further reaction could occur.[16]

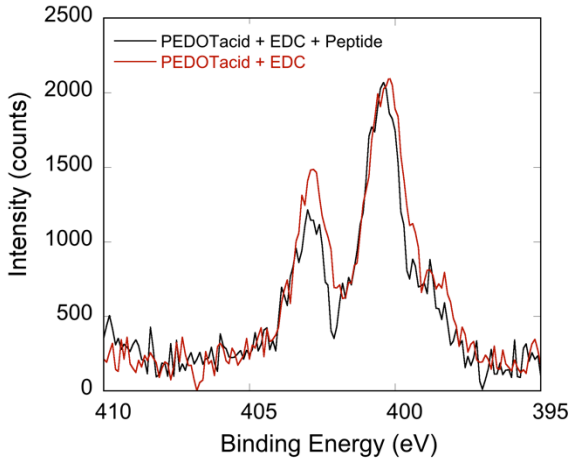

Figure 3.4 N 1s XPS from PEDOT-PEDOTacid films treated with EDC methiodide + peptide or just EDC methiodide, demonstrating the lack of reactivity of the activator with peptide.

Successful peptide coupling was accomplished using HATU and DIPEA in DMF, as shown in the N 1s XPS and FTIR in Figures 3.5 and 3.6, respectively. HATU is known as a stable carboxylic acid activator and is also well known for reacting with sterically hindered carboxylic acids, like the secondary –COOH in EDOTacid. The mechanism for this reaction is shown in Scheme 3.2. Previous literature has demonstrated that this reaction happens very quickly, reaching 60% completion within 2 minutes and 94% completion in 75 minutes.[17] The N 1s XPS spectra for PEDOT-PEDOTacid-RGD or RGE films consistently had a higher nitrogen signal than PEDOT-PEDOTacid-HATU, demonstrating that there was peptide at the surface. In addition, we treated regular PEDOT films with peptide to see if there was a significant amount of non-covalent binding to the conjugated polymer. As shown in Figure 3.5, there was some nitrogen signal for these samples, even after extensive washing with surfactant (SDS) and cyclic voltammetry. This indicates that there were strong non-covalent interactions between PEDOT and the peptide fragments. Although it was difficult to remove all non-covalently bound peptide, the PEDOT-PEDOTacid-RGD or RGE N 1s XPS signal was still larger

than the PEDOT RGD or RGE signal, possibly because covalent binding of peptide to the surface allowed more of the peptide to remain on the surface after washing.

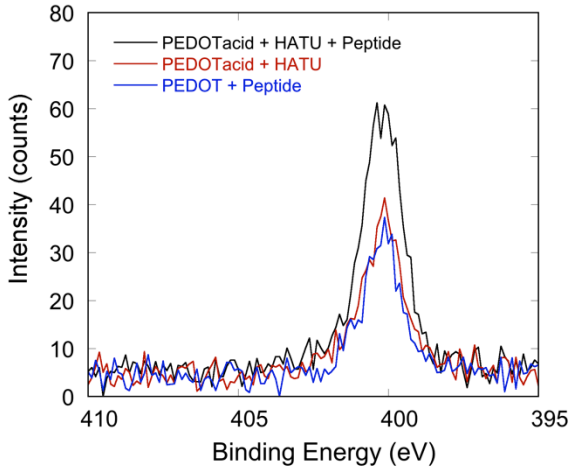

Figure 3.5 N 1S XPS from PEDOT-PEDOTacid films treated HATU + peptide, PEDOT-PEDOTacid treated with only HATU and PEDOT treated with peptide, demonstrating the increase in nitrogen content for fully treated films

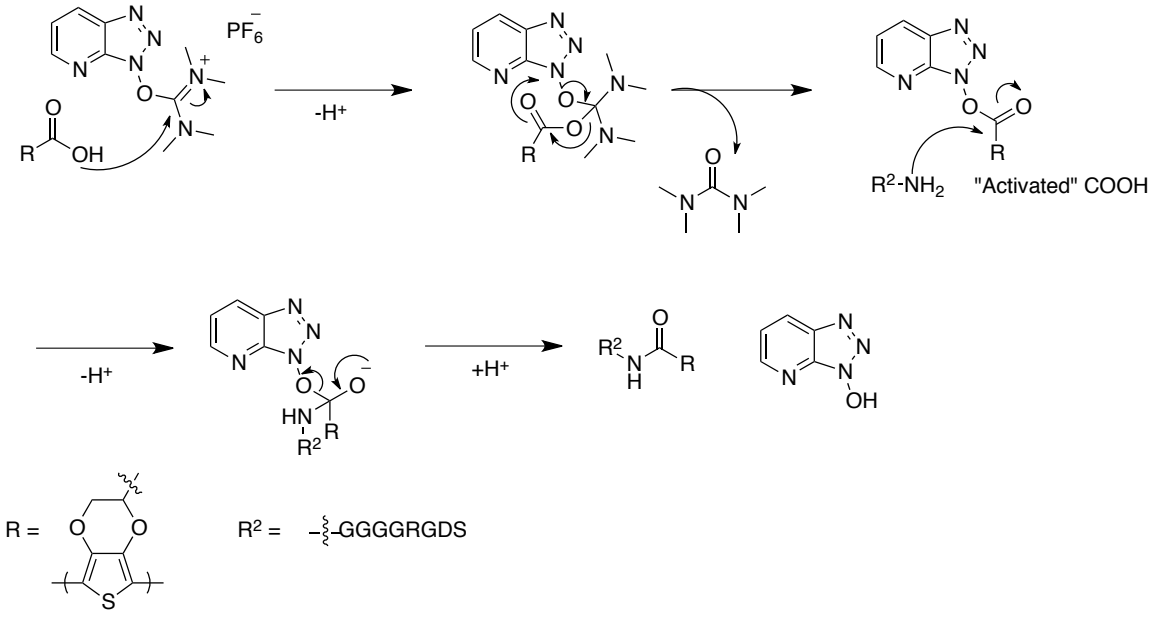

Scheme 3.2 Reaction mechanism of the activator HATU with PEDOT-PEDOTacid and RGD peptide to form PEDOT-PEDOTacid-RGD. A tertiary amine base such as DIPEA is necessary to drive the reaction.

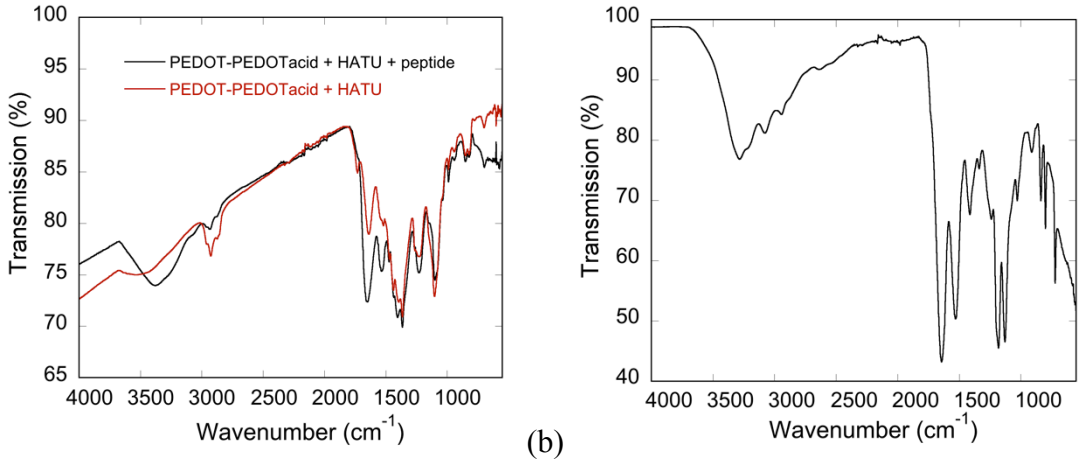

Figure 3.6 FTIR spectra for (a) PEDOT-PEDOTacid treated with HATU and RGD peptide and PEDOT-PEDOTacid treated with only HATU and (b) GGGGRGDS peptide. Peaks around 3400 cm^{-1}, 1660 cm^{-1} and 1540 cm^{-1} indicate the presence of peptide on the films treated with HATU and RGD.

For cell experiments involving peptide-coupled biomaterials, it is important to ensure that the concentration of peptide at the surface is high enough to influence cellular behavior. For instance, Massia *et al*. have shown that concentrations as small as 1-10 fmol/cm^2 were required for fibroblast attachment and spreading on RGD-modified glass substrates.[13] This low concentration, however, may not be applicable to polymers, which are much softer than glass. The lower stiffness of polymers may make it more difficult for cells to firmly attach, thus requiring a higher surface density of RGD. Polymer surfaces have been reported with covalently linked RGD concentrations ranging from pico to nanomoles per cm^2. In addition, variations in surface concentration have been linked to different cellular behavior. Lower concentrations of RGD provide cells with greater mobility whereas high surface concentrations increase cell attachment and proliferation.[18]

To approximate the RGD surface density on PEDOT-PEDOTacid-RGD we used the atomic concentration ratios of nitrogen and sulfur from the N 1s and S 2p XPS. Since

nitrogen was only present in the RGD peptide and sulfur was only present in the PEDOT-PEDOTacid film, we could easily calculate the ratio of peptide to PEDOT-PEDOTacid repeat units, which comes out to approximately 1 RGD peptide for every 10 repeat units of PEDOT-PEDOTacid. Assuming a 1:1 ratio of PEDOTacid to PEDOT repeat units, the peptides reacted with about 20% of the available carboxylic acid units. By using an estimated copolymer density of 1 g/cm^3 and a depth of XPS penetration between 1 - 10 nm, the approximate range for the surface density of RGD or RGE peptide was calculated as 60 – 600 $pmol/cm^2$. This estimated RGD surface density was within the range of published values for RGD biomaterials, as shown by the examples in Table 3.1. The variation in reported concentrations is quite dramatic – femto to nanomoles per cm^2 – and PEDOT-PEDOTacid-RGD surface densities were well above the reported minimum necessary concentrations for cell attachment and spreading.

Table 3.1 RGD surface densities for various synthetic biomaterials that have been used to increase cell adhesion

Peptide-Coupled Surface	**RGD Surface Density (per cm^2)**
Glass[13]	1-10 fmol
PEG Hydrogels[19]	0.1 – 1 pmol
PEG-PAA[20]	12 – 110 pmol
PET[21]	60 – 240 pmol
PEDOT- PEDOTacid	60 – 600 pmol (est. range)
PEG-PAA[22]	475 pmol
Glass[14]	10 nmol

The electrical activity of PEDOT-PEDOTacid-RGD was investigated using cyclic voltammetry, as shown in Figure 3.7. Peptide treated copolymer films had reduced but significant charge capacity (5.7 mC/cm^2) even after harsh chemical treatment with HATU and DIPEA (a reducing agent) in organic solvent and the attachment of peptide. PEDOT

samples that were similarly treated with peptide actually had increased charged capacity (11.8 mC/cm^2) compared to untreated PEDOT (10.4 mC/cm^2), indicating that the covalent attachment of HATU followed by peptide may have a more significant negative impact on the electrical properties than the presence of the chemicals in solution. The results demonstrate that these peptide-coupled conjugated polymer films could be used as electrode coatings where they are required to communicate with cells through recording or stimulating capabilities. Also, it may be possible to increase the charge capacity by attaching a smaller amount of peptide to the surface since the quantity attached to films in these experiments was relatively high.

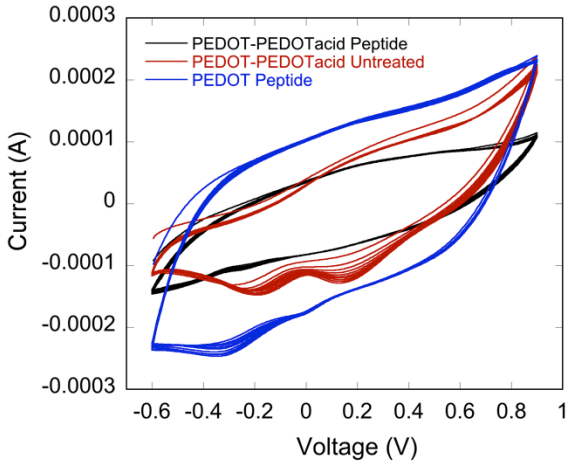

Figure 3.7 Cyclic voltammetry demonstrating the reduced yet significant charge capacity for PEDOT-PEDOTacid films treated with HATU/DIPEA and RGD peptide.

Various cell types and culture conditions were explored to find a system that adequately demonstrates the bioactivity of PEDOT-PEDOTacid-RGD. Initially, we investigated the response of NIH-3T3 mouse fibroblasts (ATCC) on functionalized and unfunctionalized conjugated polymer substrates. It is well known that fibroblasts attach well to RGD peptides; however, NIH-3T3 fibroblasts are an immortalized cell line and adhere well to many surfaces, even without serum. Figure 3.8 demonstrates the adhesion

and spreading of NIH-3T3 fibroblasts without serum on fibronectin, PEDOT-PEDOTacid-RGD, PEDOT-PEDOTacid-RGE and unmodified PEDOT-PEDOTacid for 1 hour. It was difficult to distinguish between the samples since the cells adhered well to all of the surfaces from time points of 1 – 5 hours, thus making it difficult to demonstrate increased adhesion on PEDOT-PEDOTacid-RGD.

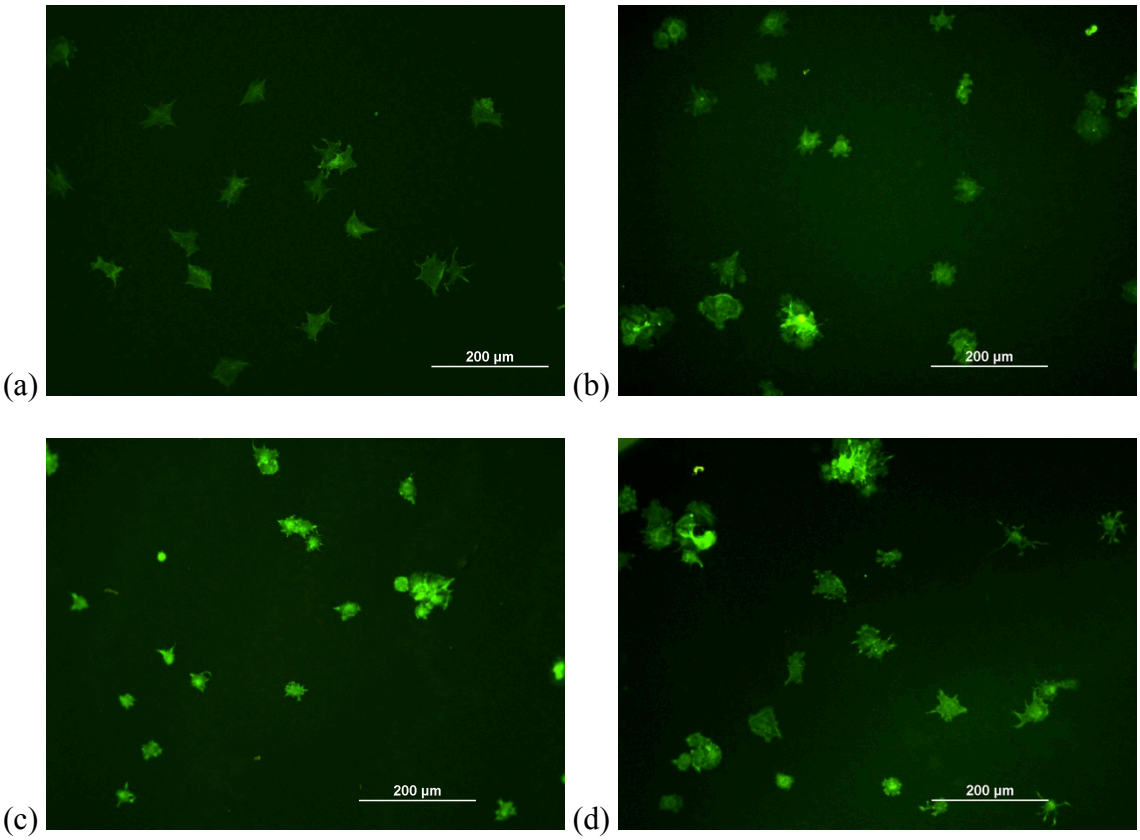

Figure 3.8 NIH-3T3 fibroblasts seeded without serum on (a) fibronectin on glass, (b) PEDOT-PEDOTacid, (c) PEDOT-PEDOTacid-RGE and (d) PEDOT-PEDOTacid-RGD. The cells, stained with phalloidin, show a lack of selectivity for fibronectin or RGD surfaces.

Since immortalized cells did not show the selectivity necessary to demonstrate increased adhesion on PEDOT-PEDOTacid-RGD surfaces, primary cells were investigated. While primary fibroblasts may show the greatest selectivity for RGD peptides, we had easier access to primary rat motor neurons. Primary neurons have

shown an affinity for fibronectin surfaces[11] and are closer to the type of cells that would interact with conjugated polymer coated neural probes *in vivo*. To see if these cells had selectivity for RGD, primary motor neurons were extracted from rat embryos and seeded without serum for 26 hours on PEDOT-PEDOTacid-RGD and negative controls PEDOT-PEDOTacid-RGE, PEDOT-PEDOTacid, PEDOT with non-covalently bound RGD, and PEDOT. After fixation the cells were counted and the developmental stages of the cells were examined. These stages include completely round neurons (stage 0), neurons with short processes (stage 1), neurons with short axons (stage 2) and neurons with axons that are longer than the cell body (stage 3).

The results for the number of cells and the developmental stages of the cells are shown in Figure 3.9. While there were not many total cells on any of the substrates, it is seen in Figure 3.9a that there were more than 3 times more cells on PEDOT-PEDOTacid-RGD than on PEDOT-PEDOTacid-RGE, PEDOT RGD and PEDOT and over 9 times more cells than on PEDOT-PEDOTacid. The lack of cells on GGGGRGES demonstrates that the cells bound specifically to the RGD domain and did not adhere as well to general peptide surfaces. In addition, there were 7 times more cells in stage 3 on PEDOT-PEDOTacid-RGD than PEDOT RGD, 14 times more than PEDOT and there were no cells in stage 3 on the rest of the samples, demonstrating the ability of the cells on PEDOT-PEDOTacid-RGD to become more highly developed. Interestingly, PEDOT-PEDOTacid films had very few cells attached and no cells in stage 3. This may have occurred because carboxylates on the surface produced an overall increase in negative charge, which could have had a repulsive interaction with the negatively charged phospholipid cell membrane. Neural cells are normally strongly attracted to positively

charged surfaces, such as poly-L-lysine, so it follows that they would also be repulsed by negatively charged surfaces.[23] It is also important to note that non-covalently bound PEDOT RGD samples did not have as many cells or as well developed cells as PEDOT-PEDOTacid-RGD. This may have happened because there was less RGD on the surface, (the samples were washed with surfactant) or because the cells that bound to the RGD actually pulled it off of the surface.

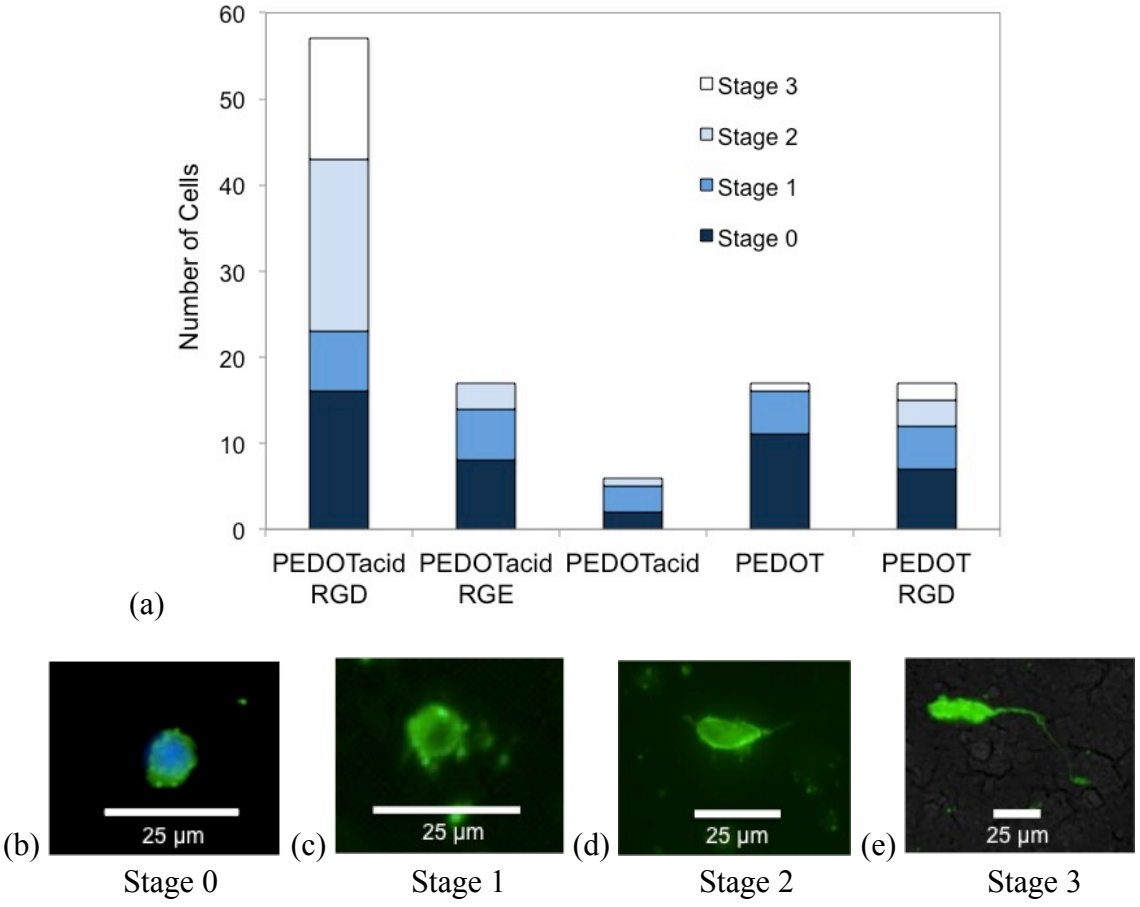

Figure 3.9 (a) Number of primary motor neurons on conjugated polymer samples. Each column represents 2 samples of the same type and the cells are in various stages of development (0 – 3) as depicted in (b – e). More cells attach to PEDOT-PEDOTacid-RGD and these samples also have a greater number of highly developed cells (stage 3).

As stated previously, Lee *et al.* covalently bound RGD to carboxylic acid-modified polypyrroles (PPy), another conjugated polymer.[5,6] It is difficult to directly

compare functionalized PEDOT-PEDOTacid with this material because its bioactivity was tested with a different cell type (human umbilical vascular endothelial cells) and the amount of RGD on the surface was not quantified. Both RGD-functionalized PEDOT-PEDOTacid and PPy had more cells attached compared to unfunctionalized polymer, although the PPy samples were only tested up to 3 hours. The electrical activity of carboxylic acid-PPy either remained similar to PPy, as was the case of end-capped modified PPy, or was better than PPy, as was the case of N-modified PPy, as indicated by conductivity measurements. However, conductivity of the films after RGD-modification was not reported. PEDOT-PEDOTacid and PEDOT-PEDOTacid-RGD films had decreased charge capacities compared to PEDOT and therefore, seemed to be more negatively affected by functionalization. Qualitatively, both functionalized PPy and PEDOT could be used to increase the adhesion of cells or to induce a different biological response through the use of other peptides.

3.4 Summary and Future Outlook

PEDOT-PEDOTacid was functionalized with GGGGRGDS peptide at a high surface density and the resulting biomaterial remained electrically conductive and bioactive, as indicated by the increased adhesion of primary motor neurons. While this is an important proof of principle for peptide-conjugated PEDOT-PEDOTacid films, other peptides or biomolecules could also be attached that exclusively influence neuron behavior. For example, laminin, a glycoprotein found in basement membranes, contains the peptide fragment isoleucine-lysine-valine-alanine-valine (IKVAV) that promotes cell attachment and neurite growth.[24] This peptide has been used by other groups to control the adhesion of PC12 cells and the direction of neurite growth[25] and to preferentially

differentiate neural progenitor cells into neurons rather than astrocytes.[26] Another biomolecule that could be attached to PEDOT-PEDOTacid is L1, a transmembrane protein and neural cell recognition molecule. Azemi *et al*. attached L1 to silicon wafers coated with oxide, which mimicked silicon dioxide neural probe shafts, and coated the unmodified areas with poly(ethylene glycol) (PEG).[27] L1-PEG surfaces promoted longer neurite growth than laminin-PEG surfaces. Also, L1-PEG inhibited the attachment of astrocytes whereas laminin-PEG had more astrocytes attached than any other samples tested. Thus, L1 is an attractive molecule for the recruitment of neurons in neural probe applications and could be attached to PEDOT-PEDOTacid films to make neuron-specific conjugated polymer electrodes.

3.5 References

(1) Alsberg, E.; Anderson, K. W.; Albeiruti, A.; Rowley, J. A.; Mooney, D. J. *Proceedings of the National Academy of Sciences of the United States of America* **2002**, *99*, 12025-30.

(2) Holmes, T. C. *Trends in Biotechnology* **2002**, *20*, 16-21.

(3) Shekaran, A.; García, A. J. *Journal of Biomedical Materials Research. Part A* **2011**, *96*, 261-72.

(4) Biran, R.; Martin, D. C.; Tresco, P. A. *Experimental Neurology* **2005**, *195*, 115-26.

(5) Lee, J.-W.; Serna, F.; Nickels, J.; Schmidt, C. E. *Biomacromolecules* **2006**, *7*, 1692-5.

(6) Lee, J.-W.; Serna, F.; Schmidt, C. E. *Langmuir* **2006**, *22*, 9816-9.

(7) Hersel, U.; Dahmen, C.; Kessler, H. *Biomaterials* **2003**, *24*, 4385-4415.

(8) Pierschbacher, M. D.; Hayman, E. G.; Ruoslahti, E. *Journal of Cellular Biochemistry* **1985**, *28*, 115-26.

(9) Zheng, H.; Berg, M. C.; Rubner, M. F.; Hammond, P. T. *Langmuir* **2004**, *20*, 7215-22.

(10) Ananthanarayanan, B.; Little, L.; Schaffer, D. V.; Healy, K. E.; Tirrell, M. *Biomaterials* **2010**, *31*, 8706-8715.

(11) Zhang, Z.; Yoo, R.; Wells, M.; Beebe, T. P.; Biran, R.; Tresco, P. *Biomaterials* **2005**, *26*, 47-61.

(12) Beer, J. H.; Springer, K. T.; Coller, B. S. *Blood* **1992**, *79*, 117-28.

(13) Massia, S. P.; Hubbell, J. A. *Journal of Cell Biology* **1991**, *114*, 1089-100.

(14) Olbrich, K. C.; Andersen, T. T.; Blumenstock, F. A.; Bizios, R. *Biomaterials* **1996**, *17*, 759-64.

(15) Rowley, J. A.; Mooney, D. J. *Journal of Biomedical Materials Research* **2001**, *60*, 217-223.

(16) Nakajima, N.; Ikada, Y. *Bioconjugate Chemistry* **1995**, *6*, 123-30.

(17) Albericio, F.; Bofill, J. M.; El-Faham, A.; Kates, S. A. *Journal of Organic Chemistry* **1998**, *63*, 9678-9683.

(18) Sagnella, S. *Biomaterials* **2004**, *25*, 1249-1259.

(19) Hern, D. L.; Hubbell, J. A. *Journal of Biomedical Materials Research* **1998**, *39*, 266-76.

(20) Drumheller, P. D.; Hubbell, J. A. *Analytical Biochemistry* **1994**, *222*, 380-388.

(21) Chollet, C.; Chanseau, C.; Remy, M.; Guignandon, A.; Bareille, R.; Labrugère, C.; Bordenave, L.; Durrieu, M.-C. *Biomaterials* **2009**, *30*, 711-20.

(22) Drumheller, P. D.; Elbert, D. L.; Hubbell, J. A. *Biotechnology and Bioengineering* **1994**, *43*, 772-780.

(23) Stenger, D. A.; Pike, C. J.; Hickman, J. J.; Cotman, C. W. *Brain Research* **1993**, *630*, 136-147.

(24) Tashiro, K.; Sephel, G. C.; Weeks, B.; Sasaki, M.; Martin, G. R.; Kleinman, H. K.; Yamada, Y. *Journal of Biological Chemistry* **1989**, *264*, 16174-82.

(25) Patel, N.; Padera, R.; Sanders, G. H.; Cannizzaro, S. M.; Davies, M. C.; Langer, R.; Roberts, C. J.; Tendler, S. J.; Williams, P. M.; Shakesheff, K. M. *FASEB Journal* **1998**, *12*, 1447-54.

(26) Silva, G. A.; Czeisler, C.; Niece, K. L.; Beniash, E.; Harrington, D. A.; Kessler, J. A.; Stupp, S. I. *Science* **2004**, *303*, 1352-5.

(27) Azemi, E.; Stauffer, W. R.; Gostock, M. S.; Lagenaur, C. F.; Cui, X. T. *Acta Biomaterialia* **2008**, *4*, 1208-17.

CHAPTER 4

Electrochemical Polymerization and Characterization of the Synthetic Melanin Poly(5,6-Dimethoxyindole-2-carboxylic acid) (PDMICA)

4.1 Introduction

Melanins are conjugated polymers found in the skin, hair, eyes, ears and brain. In humans and other animals, the two main types of melanin are eumelanin, which consists mostly of dihydroxyindole repeat units, and pheomelanin, which consists of benzothiazine repeat units.[1] The structure-function relationships inherent to these polymers are not entirely clear, especially in the ear and brain, where the melanin is not exposed to sunlight.[2-4] Therefore, it is of interest to study both natural and synthetic versions of melanin in order to understand their biological functions and also to try to utilize them as biomaterials. Most synthetic versions of melanin have been chemically or electrochemically polymerized from the monomers L-3,4-dihydroxyphenylalanine (L-DOPA)[5-8] or tyrosine.[9-12] These polymerizations produce dark brown, amorphous, insoluble polymers or oligomers that contain many different chemical species and thus have broad-band UV-visible absorption.[13] d'Ischia *et al.* recently reviewed current

advances in synthetic melanin preparation, characterization and possible device utilitzation.[14] We are interested in producing novel synthetic melanin derivatives that have well-defined structures and can be used to investigate the optical, electronic and biological properties of melanin.

Electrochromic conjugated polymers have been developed and studied over the past 15 years for various display and "smart" optical applications.[15] By changing the chemical structure of the main chain or pendant groups, researchers have been able to adjust the band gap of these conjugated polymers and therefore have control over the colors displayed.[16] In addition, the stability, switching time and optical contrast of many polymers have been optimized.[15,17,18] Most of these electrochromic polymers are derivatives of polythiophene, polypyrrole and polyaniline. Although some simple polyindoles have been studied for their electrochromic properties,[19,20] polyindoles that have side-groups similar to melanin have not been investigated.

In our attempts to synthesize melanin-like polymers we electrochemically polymerized the monomer 5,6-dimethoxyindole-2-carboxylic acid (structurally similar to the melanin repeat-unit 5,6-dihydroxyindole-2-carboxylic acid, Figure 4.1). The resulting poly(5,6-dimethoxyindole-2-carboxylic acid) (PDMICA) was green, displayed electrochromic activity and had a significant degree of crystallinity. The electrochemical, spectroscopic and structural characterization of the electrochemically polymerized films are presented in this chapter.

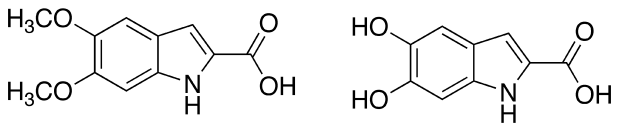

Figure 4.1 The monomer used in this study, 5,6-dimethoxyindole-2-carboxylic acid (DMICA) (left) and one of the components of melanin, 5,6-dihydroxyindole-2-carboxylic acid (DHICA) (right).

4.2 Experimental Procedures

4.2.1 Electrochemical Polymerization

5,6-dimethoxyindole-2-carboxylic acid (DMICA, Alfa Aesar, 0.02 M) was electrochemically polymerized onto ITO-coated glass (Delta Technologies, Ltd) in a 2-electrode cell using an Autolab PGstat12 Potentiostat/Galvanostat (EcoChemie) with a platinum wire counter electrode. The films were electrochemically polymerized in acetone with tetrabutylammonium perchlorate (TBAP, 0.05 M) counter-ion, unless otherwise stated. Other counter-ions were found to be suitable including lithium perchlorate ($LiClO_4$, SigmaAldrich), tetrabutylammonium hexafluorophosphate (TBAPF6, Fluka) and the ionic liquid 1-butyl-3-methylimidazolium tetrafluoroborate (Aldrich), which serves as the solvent and the counter-ion. These other counter-ions also produced electrochromic PDMICA. All films were polymerized galvanostatically using a current density between 0.1 – 0.2 mA/cm^2 for 10 minutes and rinsed with acetone after polymerization.

4.2.2 Electrochromic Characterization

The polymer films were subjected to cyclic voltammetry (CV) using the same Autolab potentiostat/galvanostat with a platinum counter electrode, a saturated calomel reference electrode and phosphate buffered saline electrolyte (PBS, Hyclone Media). Cycling was performed between -1 V and +1 V with a scan rate of 0.01 V/s. UV-Vis

spectrometry was performed on the PDMICA films between 200 to 800 nm using a Cary 50 UV-Vis Spectrometer (Agilent). The absorption was determined before CV and immediately after subjecting the films to different stages of the voltage cycle.

4.2.3 Chemical and Structural Characterization

Chemical analysis was performed on PDMICA films using a PHI 5600 X-ray photoelectron spectrometer with a monochromatic aluminum X-ray source (Al Kα = 1486.6 eV) and a hemispherical electron energy analyzer. The pass energy for the survey spectra and characteristic region spectra were 187.85 eV and 58.7 eV, respectively. A take-off angle of 45° was used and the base chamber pressure was < 2 $x10^{-9}$ Torr. Additional XPS was performed on the DMICA monomer using a Kratos Axis Ultra DLD X-ray photoelectron spectrometer with a monochromatic aluminum X-ray source and chamber pressure between 1 x 10^{-8} – 1 x 10^{-9} Torr. Survey pass energy was 160 eV and characteristic region pass energy was 20 eV. All spectra were referenced to the C-C/C-H peak at 285.0 eV. FTIR was also performed to analyze functional groups using a Perkin Elmer Spectrum 100 FTIR Spectrometer in attenuated total reflectance (ATR) mode.

Thin-film X-ray diffraction (XRD) experiments were conducted using a Bruker D8 Discover diffractometer equipped with a HI-STAR 2D detector. A copper, fixed-tube, 2.2 kW generator was operated at 40 kV, 40 mA for all experiments. A point-focus beam formed by a 500 μm monocapillary collimator was used and the instrument was calibrated using a NIST1976 flat plate XRD standard. Data was collected with an incident beam angle of 5º and the detector at an angle of 15º with a camera length of approximately 15 cm. Molecular modeling of the potential crystal structures was performed using Materials Studio 4.4 (Accelrys) software.

Morphological studies were conducted using a JEOL JSM-7400F field emission scanning electron microscope at 3kV operating voltage. The PDMICA films were sputter-coated for with gold-palladium for 40 seconds in order to provide a more conductive surface.

4.3 Results and Discussion

Electrochemical polymerization of 5,6-dimethoxyindole-2-carboxylic acid produced green PDMICA films that had distinct color changes during CV, shown in Figure 4.2. At negative voltages the polymer was transparent, around zero volts the polymer was green and above 0.5 volts the polymer turned purple. The color changes and corresponding CV peaks were reversible for approximately 3 cycles. After this point the PDMICA film came off the ITO electrode (in the case of perchlorate and hexafluorophosphate counter-ions) or remained intact but lost its electrochromic activity while cycling continued (in the case of ionic liquid counter-ion).

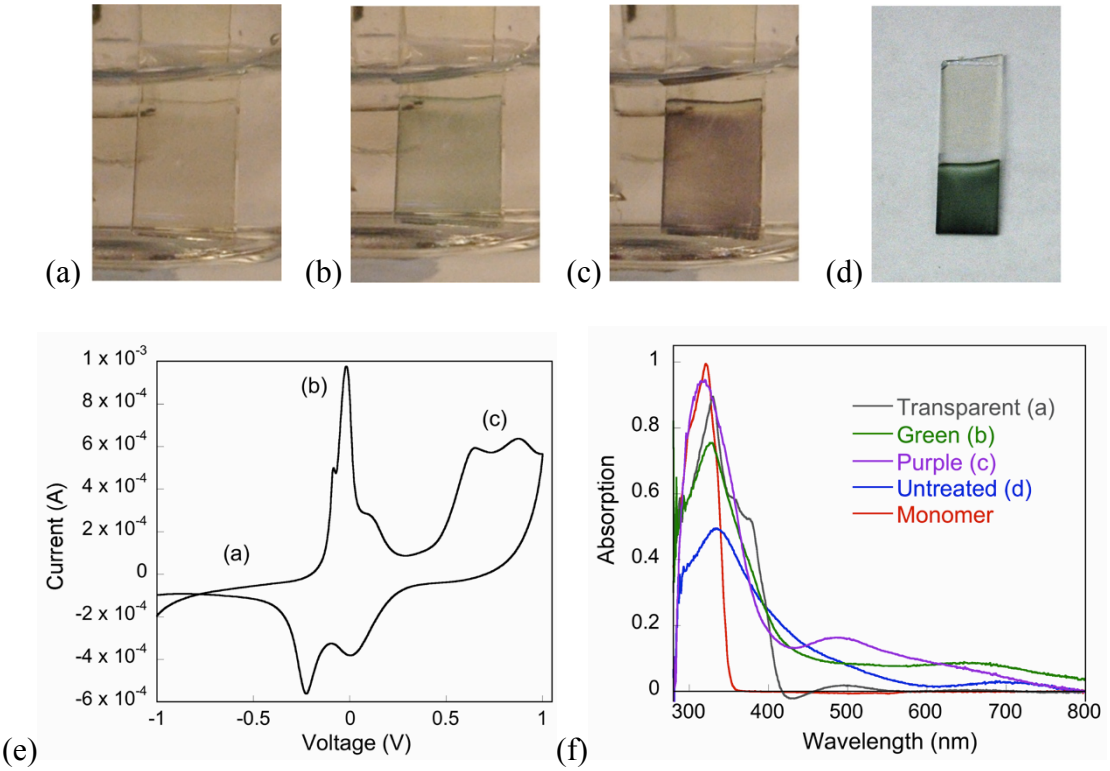

Figure 4.2 Electrochromic PDMICA: the films were transparent when subjected to negative voltages (a), green near zero volts (b) and purple above 0.5 volts (c). The as-polymerized films were also green (d). The cyclic voltammetry curve (e) shows the voltage range for each color. UV-Vis absorption spectra (f) demonstrated different energy absorptions depending on the state of the PDMICA.

Scheme 4.1 demonstrates reversible electronic changes that are possible during CV and can result in color change. As the potential increases PDMICA was oxidized (p-doping) and may have formed radical cation and dication states. These charged states are lower in energy than the neutral form and should have higher wavelength absorption.[15] To investigate the optical changes further we measured the absorptive properties of the PDMICA films (Figure 4.2f). While the monomer did not have any absorption above 360 nm the resulting films had longer wavelength absorption, confirming the formation of extended conjugation by electrochemical polymerization. The transparent films had very little absorption above 420 nm and, besides a peak near

the monomer absorption at 330 nm, there were two smaller shoulders around 350 and 380 nm. As the film did not have significant absorption in the visible wavelength region the film looked transparent. The green films had a broader peak around 330 nm and a small, broad peak around 670 nm. This new peak could be explained by radical cation formation since this peak was lower in energy than any of the peaks seen in the transparent polymer. The highly oxidized or purple form of the polymer had broad absorption peaks around 320 nm and 500 nm. The 500 nm peak was higher in energy than the 670 nm peak seen in the green films and cannot be explained by dication formation. Since the films lost their electrochromic activity after 3 cycles, it is likely that this form resulted from an irreversible chemical reaction. If a dication state was also present, the absorption may have been higher in wavelength than the measured range. Therefore, we can speculate that the chemical structure of the polymer changed irreversibly in the purple form. In addition, the cycling irreversibility may be resolved by cycling in a controlled atmosphere that is free of oxygen and water.

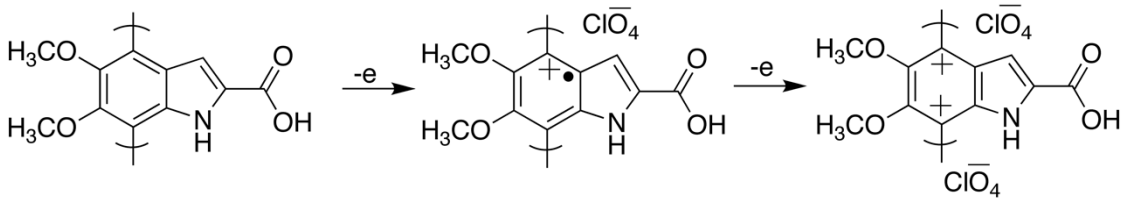

Scheme 4.1 Transition of the PDMICA from a neutral species to oxidized states (radical cation and dication) during cyclic voltammetry. The scheme represents the transparent (neutral), green (radical cation) and possibly purple (dication) states of the film. There may be other irreversible chemical reactions that altered the chemical structure of the purple form. In addition, it is possible that the polymer coupled through the 3 position, but 4, 7 coupling is shown for simplicity.

While the complete chemical structure of PDMICA has not been elucidated, XPS of the films indicated that the monomer unit remained intact during electrochemical

polymerization. Since films that are made with tetrabutylammonium perchlorate (TBAP) counter-ion could have produced nitrogen peaks from both the tetrabutylammonium and the PDMICA, films made with lithium perchlorate ($LiClO_4$) counter-ion were also investigated. The survery spectrum (Figure 4.3a) demonstrated that all of the expected elements were present – carbon, oxygen and nitrogen from PDMICA and chlorine from the perchlorate counter-ion. The C 1s characterstic region (Figure 4.3b) and the N 1s characteristic region (Figure 4.3c) provided more detailed information about the bonding of these elements. In the C 1s spectra were peaks or shoulders present around 285, 286.5 and 289 eV, which correspond to C-C/C-H, C-O/C-N and C=O bonding, respectively.[21] These peaks were also confirmed in the monomer C 1s spectrum (Appendix C) and occurred in relatively the same ratio. These results indicated that the methoxy and carboxylic acid functional groups were present in the polymer and that the carbon frame was not disrupted. PDMICA films made with TBAP had a more prominent C-C/C-H peak, most likely due to the presence of tetrabutylammonium cation. Although the cation should not have been incorporated into the film as a dopant, it could have been trapped in the film during polymerization or present as residual material that was not removed during washing. The N 1s spectra also support the conclusion that tetrabutylammonium was present in PDMICA TBAP films. A second nitrogen peak around 402 eV was present in the PDMICA TBAP spectrum and was absent in the PDMICA $LiClO_4$ spectrum. This peak also varied in intensity based on the amount of TBAP present in the film. The presence of one nitrogen peak in PDMICA $LiClO_4$ films indicated that the nitrogen only had one bonding configuration in the polymer. This information, along with the supporting evidence that the nitrogen peak occurred at almost the same binding

energy in the monomer N 1s spectrum as the polymer N 1s spectra (around 400.7 eV), indicated that the amine functional group remained intact in PDMICA. However, the C-C bonding structure between polymer repeat units was still unclear. The repeat units could have been be connected through the non-functionalized carbons at positions 3, 4 or 7.

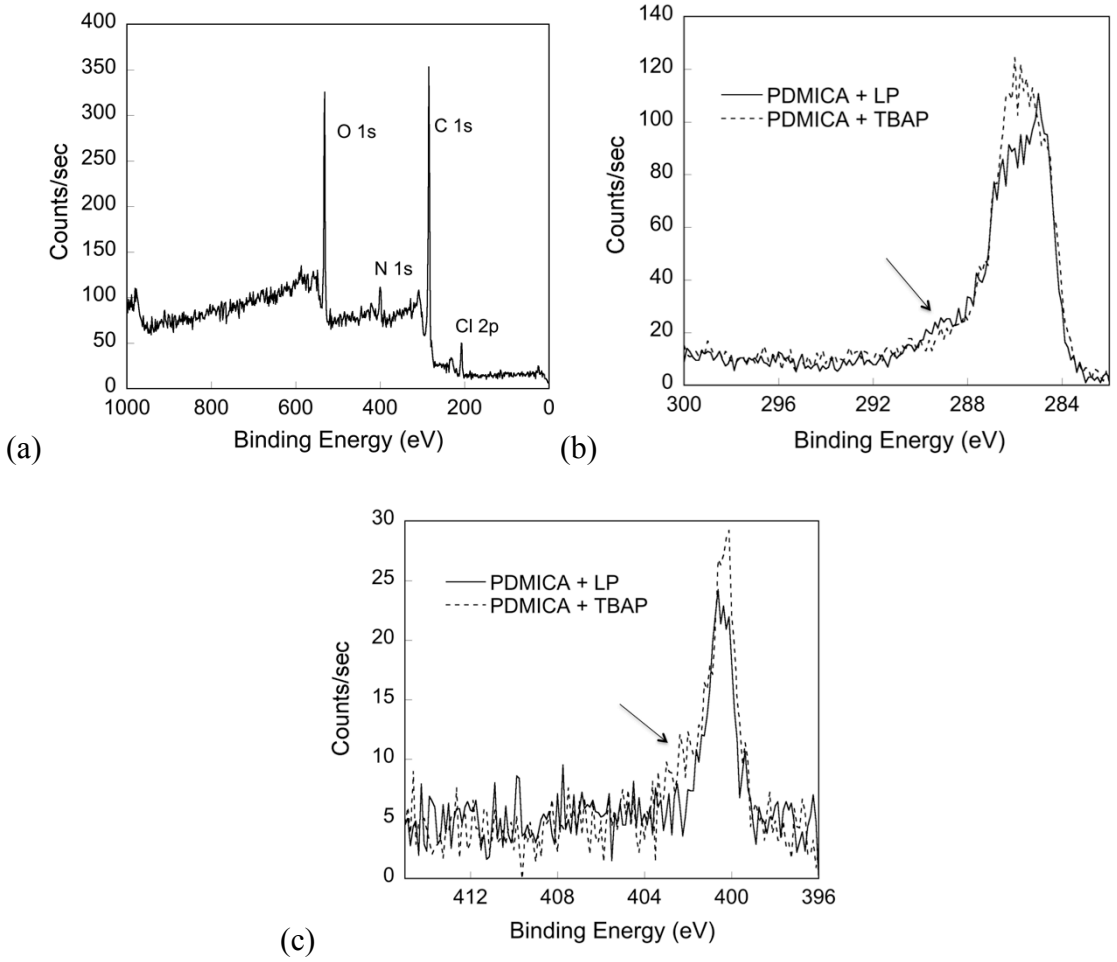

Figure 4.3 XPS spectra of PDMICA films: (a) survey spectrum demonstrating the presence of carbon, oxygen, nitrogen and chlorine; (b) C 1s spectra of PDMICA with lithium perchlorate (LP) and tetrabutylammonium (TBAP) counter-ions. The arrow highlights the small peak for C=O, indicating the presence of the COOH functional group. (c) N 1s spectra of PDMICA with LP and TBAP counter-ions. The arrow highlights the nitrogen peak for tetrabutylammonium, which varied in intensity based on the amount of residual or trapped TBAP in the film.

The chemical structure of PDMICA was also examined using ATR FTIR (Figure 4.4). The polymer spectrum had an amine bending peak at 1606 cm^{-1} and a carbonyl stretching peak at 1782 cm^{-1}, which agreed with the XPS evidence that the structure of the monomer was still intact. Interestingly, the carboxylic acid peak was shifted to a higher wavenumber for the polymer compared to the monomer spectrum. This may be because polymerization disrupted the dimerization of carboxylic acids between monomers. Additionally, there was broad absorption across the entire region from 4000-2000 cm^{-1}, which is seen for conjugated polymers that are in an oxidized state.

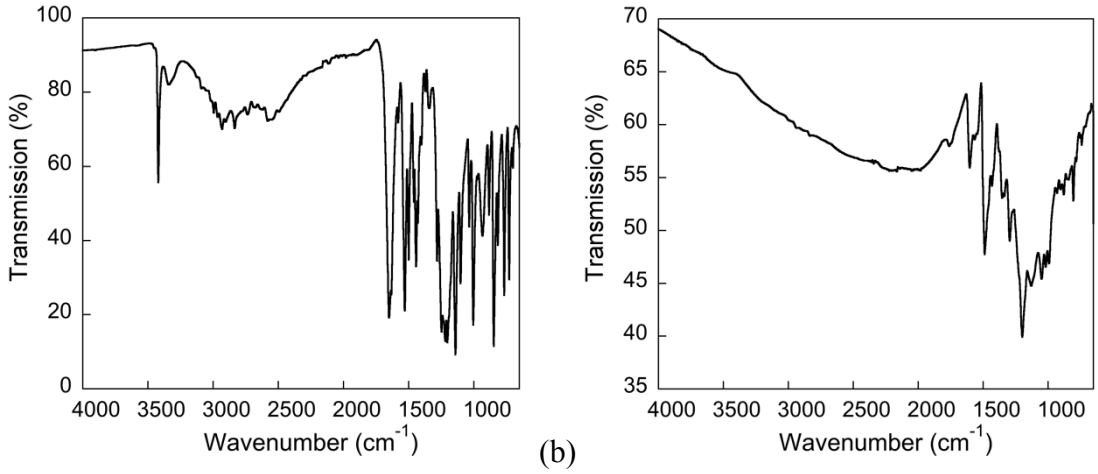

Figure 4.4 FTIR spectra of (a) DMICA monomer and (b) PDMICA polymer film. The PDMICA spectrum demonstrates broad absorption at high wavenumber, indicating the formation of an oxidized conjugated polymer. Additionally, the polymer retains peaks for the amine (1606 cm^{-1}) and carboxylic acid (1782 cm^{-1}) functional groups.

X-ray diffraction patterns of the PDMICA films revealed a surprising amount of structural order. Figure 4.5 presents the 2D diffraction patterns and azimuthally averaged data for the transparent, green and purple films. The 2θ peaks at 21.40°, 30.45°, 35.25°, 36.20° and 37.40° were from diffraction off the ITO electrode. The 6.35°, 27.50° and 31.70° peaks, which correspond to d-spacings of 1.39 nm, 0.32 nm and 0.28 nm, were diffraction peaks from the PDMICA films. Initial estimates of the solid-state packing of

the melanin derivatives using molecular modeling indicated that the 1.39 nm spacing corresponds to the distance between PDMICA chains edge-to-edge, whereas the spacings near 0.32 and 0.28 nm may correspond to the packing of PDMICA face-to-face. The 0.32 nm spacing was similar to, but somewhat smaller than, the interlayer spacing in graphite (0.335 nm).[22] Further study is needed to determine the exact packing structure of the molecules within the unit cell. These may include more experimental studies such as diffraction and transmission electron microscopy, along with crystal structure modeling.

The scattering intensity from the transparent films (Figure 4.5a) was weaker than the scattering from the green (Figure 4.5b) and purple (Figure 4.5c) films. The transparent films should have contained neutral PDMICA. Since the initially prepared PDMICA conjugated polymer backbone was positively charged, there were negative counter-ions, such as perchlorate ions, coordinated to the backbone of the polymer. The switch from positive to neutral backbone would have caused these counter-ions to be released from the film, which may have disrupted the structure of the polymer, thus weakening the scattering intensity.

The relatively sharp diffraction peaks from PDMICA are unique compared to synthetic and natural melanin polymers. Structural studies in literature demonstrate that previous melanin-like synthetic polymers and natural eumelanins were largely disordered but contained nano-size aggregates consisting of stacked parallel sheets of indole oligomers.[23-27] Interestingly, X-ray diffraction patterns of these materials had extremely broad peaks with d-spacings near 0.3 – 0.4 nm[27] and transmission electron microscopy has demonstrated π-π stacking of melanin layers with spacings between 0.37 – 0.40 nm.[28] Although they are slightly larger, these results are similar to the 0.32 nm spacing seen in

the X-ray diffraction patterns of PDMICA. However, PDMICA also appears to have well-defined edge-to-edge packing (at ~1.4 nm), which has not been seen in synthetic or natural eumelanins.

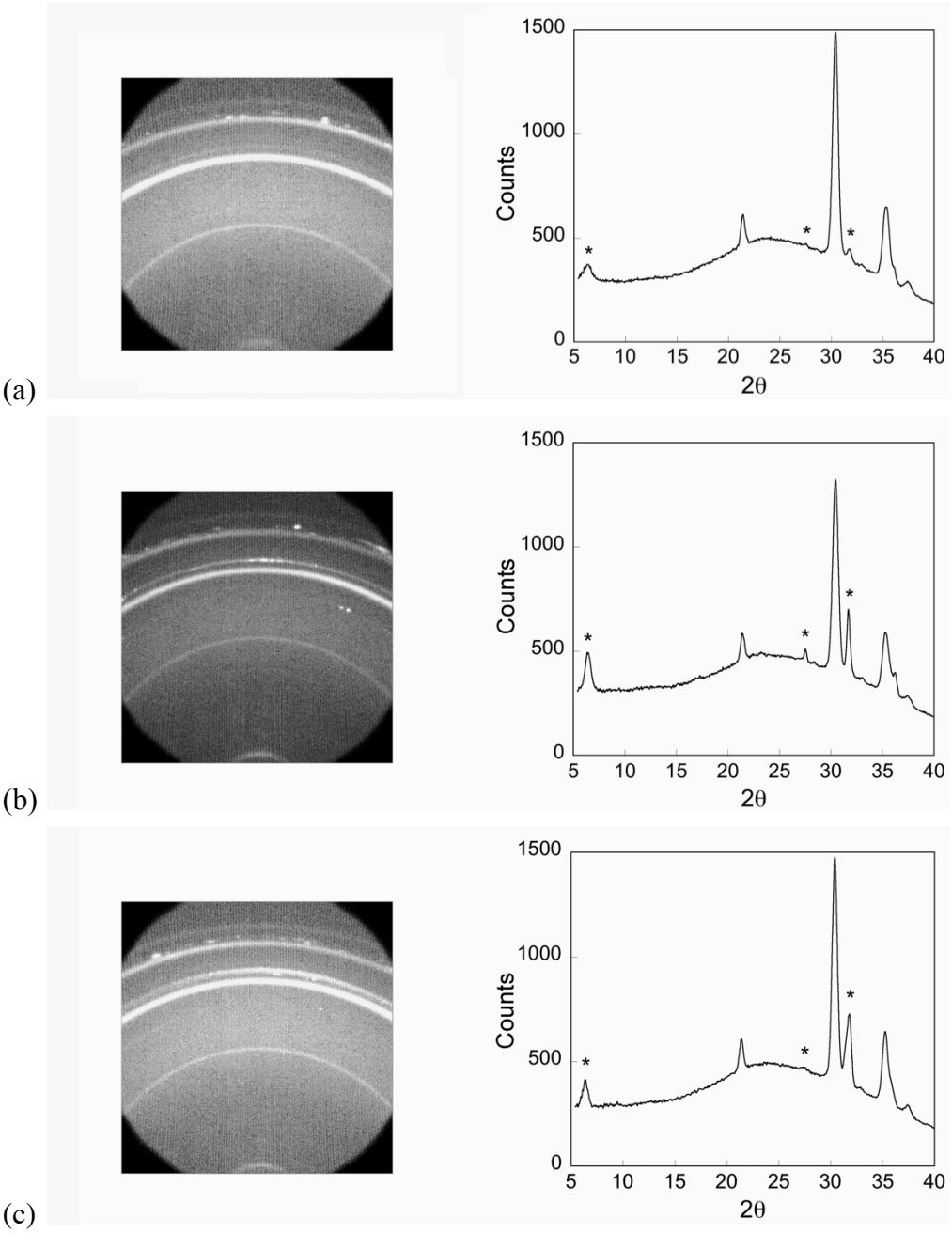

Figure 4.5 X-ray diffraction data for (a) transparent (b) green and (c) purple PDMICA. Left: 2D scans of scattering intensity from a thin film of PDMICA, 0 degrees 2θ at the bottom middle of the figure. Right: Azimuthally averaged scans of intensity as a function of 2θ. The marked peaks represent scattering from PDMICA and all other peaks are produced by the ITO substrate.

The scanning electron micrographs of PDMICA films, shown in Figure 4.6, also support the conclusion that PDMICA was semi-crystalline. The micrographs demonstrate that the films were extremely porous and contained short nano-rods of PDMICA. Figure 4.6c shows that these rods were approximately 30 nm in diameter and were bundled together to form the porous structure. Although fibers or rods were formed, they did not appear to have any preferred orientation, either in the SEM images or when examined for birefringence in optical microscopy.

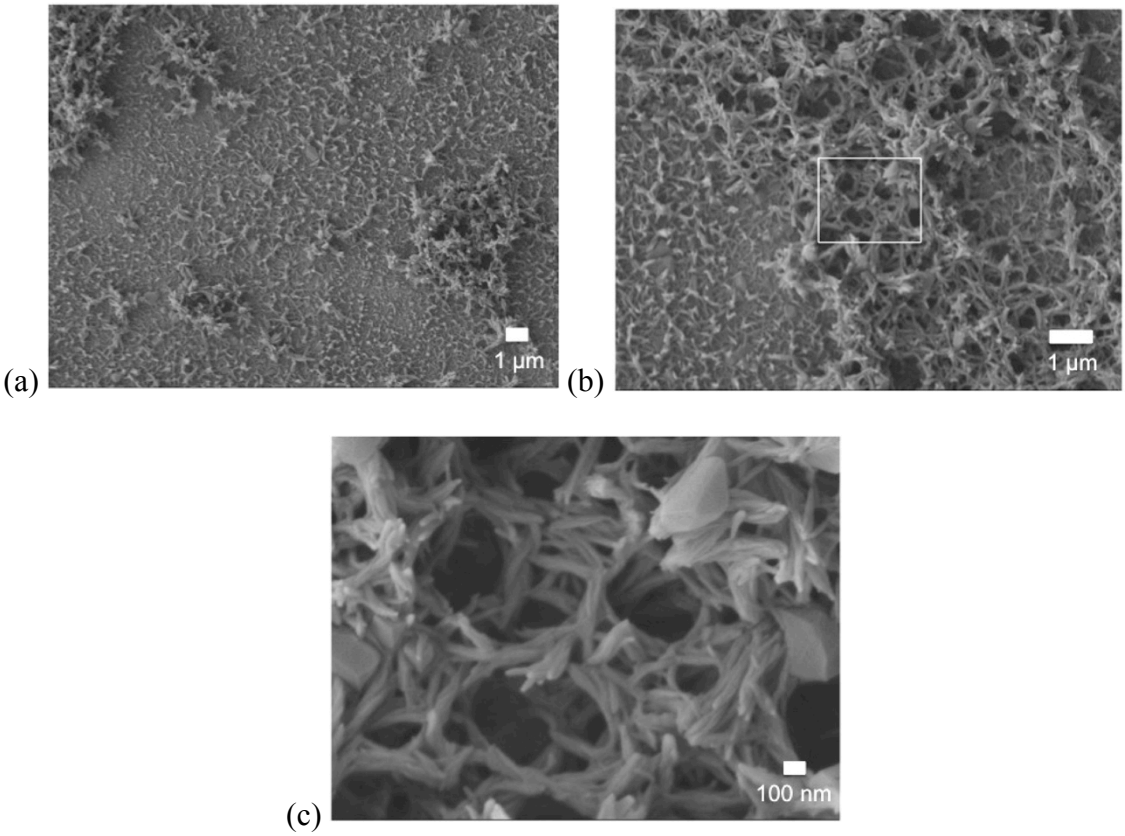

Figure 4.6 Scanning electron micrographs of PDMICA at (a) lower magnification to show the clustering of polymer in certain regions, (b) medium magnification to demonstrate the porous nature of the films and (c) high magnification of the inset in (b) to show the nanofibrous structure of the polymer.

4.4 Summary and Future Outlook

We have electrochemically polymerized PDMICA, a green melanin-like polymer that changed color when subjected to cyclic voltammetry. The polymer changed from transparent, to green and then to purple as the voltage was scanned from -1 V to +1 V. The optical properties of the polymer were different from those of L-DOPA melanin, which has broad-band UV-vis absorption. In addition, the polymer films had more structural order than synthetic and natural melanins, as shown by sharp X-ray diffraction peaks and a nano-rod structure in SEM images. The exact unit cell of PDMICA is unknown and future work should be aimed at analyzing the unit cell using transmission electron microscopy and electron diffraction. This information may help us understand why PDMICA forms nano-rods and nano-fibers, how the structure can be manipulated and if it relates at all to the structures of natural melanins, which remain somewhat elusive.

4.5 References

(1) Wakamatsu, K.; Ito, S. *Pigment Cell Research* **2002**, *15*, 174-183.

(2) Fedorow, H.; Tribl, F.; Halliday, G.; Gerlach, M.; Riederer, P.; Double, K.L. *Progress in Neurobiology* **2005**, *75*, 109-124.

(3) Zucca, F.A.; Giaveri, G.; Gallorini, M.; Albertini, A.; Toscani, M.; Pezzoli, G.; Lucius, R.; Wilms, H.; Sulzer, D.; Ito, S.; Wakamatsu, K.; Zecca, L. *Pigment Cell Research* **2004**, *17*, 610-617.

(4) Tachibana, M. *Pigment Cell Research* **1999**, *12*, 344-354.

(5) Subianto, S.; Will, G.; Meredith, P. *Polymer* **2005**, *46*, 11505-11509.

(6) da Silva, M.I.N.; Deziderio, S.N.; Gonzalez, J.C.; Graeff, C.F.O.; Cotta, M.A. *Journal of Applied Physics* **2004**, *96*, 5803-5807.

(7) Rivas, G.A.; Rubianes, M.D. *Analytica Chimica Acta* **2001**, *440*, 99-108.

(8) Robinson, G.M.; Iwuoha, E.I.; Smyth, M.R. *Electrochimica Acta* **1998**, *43*, 3489-3496.

(9) Riesz, J.; Gilmore, J.; Meredith, P. *Biophysical Journal* **2006**, *90*, 4137-4144.

(10) Seagle, B.L.L.; Rezai, K.A.; Kobori, Y.; Gasyna, E.M.; Rezaei, K.A.; Norris, J.R. *Proc. Natl. Acad. Sci. U.S.A.* **2005**, *102*, 8978-8983.

(11) Meredith, P.; Riesz, J. *Photochemistry and Photobiology* **2004**, *79*, 211-216.

(12) Littrell, K.C.; Gallas, J.M.; Zajac, G.W.; Thiyagarajan, P. *Photochemistry and Photobiology* **2003**, *77*, 115-120.

(13) Meredith, P.; Powell, B.J.; Riesz, J.; Nighswander-Rempel, S.P.; Pederson, M.R.; Moore E.G. *Soft Matter* **2006**, *2*, 37-44.

(14) d'Ischia, M.; Napolitano, A.; Pezzella, A.; Meredith, P.; Sarna, T. *Angewandte Chemie-International Edition* **2009**, *48*, 3914-3921.

(15) Argun, A.A.; Aubert, P-H.; Thompson, B.C.; Schwendeman, I.; Gaup, C.L.; Hwang, J.; Pinto, N.J.; Tanner, D.B.; MacDiarmid, A.G.; Reynolds, J.R. *Chemistry of Materials* **2004**, 16, 4401-4412.

(16) Roncali, J. *Chemical Reviews* **1997**, *97*, 173-205.

(17) DeLongchamp, D.M.; Kastantin, M.; Hammond, P.T. *Chemistry of Materials* **2003**, *15*, 1575-1586.

(18) Cho, S.I.; Kwon, W.J.; Choi, S.J.; Kim, P.; Park, S.A.; Kim, J.; Son, S.J.; Xiao, R.; Kim, S.H.; Lee, S.B. *Advanced Materials* **2005**, *17*, 171-175.

(19) Udum, Y.A.; Dudukcu, M.; Koleli, F. *Reactive & Functional Polymers* **2008**, *68*, 861-867.

(20) Billaud, D.; Maaroouf, E.B.; Hannecart, E. *Polymer* **1994**, *35*, 2010-2011.

(21) Moulder, J. F.; Stickle, W. F.; Sobol, P. E.; Bomben, K. D. *Handbook of X-ray Photoelectron Spectroscopy: A Reference Book of Standard Spectra for Identification and Interpretation of XPS Data.* Physical Electronics: Eden Prairie, MN, 1992.

(22) Tuinstra, F.; Koenig, J.L. *Journal of Chemical Physics* **1970**, *53*, 1126-1130.

(23) Cheng, J.; Moss, S.C.; Eisner, M. *Pigment Cell Research* **1994**, *7*, 263 – 273.

(24) Cheng, J.; Moss, S.C.; Eisner, M. *Pigment Cell Research* **1994**, *7*, 255 – 262.

(25) Clancy, C.M.R.; Simon, J.D. *Biochemistry* **2001**, *40*, 13353 – 13360.

(26) Liu, Y.; Simon, J.D. *Pigment Cell Research* **2003**, *16*, 606 – 618.

(27) Capozzi, V.; Perna, G.; Carmone, P.; Gallone, A.; Lastella, M.; Mezzenga, E.; Quartucci, G.; Ambrico, M.; Augelli, V.; Biagi, P.F.; Ligonzo, T.; Minafra, A.; Schiavulli, L.; Pallara, M.; Cicero, R. *Thin Solid Films* **2006**, *511*, 362-366.

(28) Watt, A.A.R.; Bothma, J.P.; Meredith, P. *Soft Matter* **2009,** *5*, 3754-3760.

CHAPTER 5

Synthetic Melanins as Bio-electrode Coatings

5.1 Introduction

Melanins are dark pigments made up of conjugated macromolecules (oligomers or polymers) and are found in many different human tissues, including the skin, hair, eye, ear and brain. These pigments consist primarily of two subclasses of melanin – eumelanin and pheomelanin – that are both derived from the molecule tyrosine (Scheme 5.1) and are contained within cells called melanocytes.[1] The function of melanin largely depends on its location in the body. Melanin in the skin has been most widely studied and it has been shown to have a role in photoprotection because its conjugated structure allows it to absorb a broad spectrum of visible and UV light.[2,3] Melanin in the brain, ear and parts of the eye are not subjected to direct light exposure, but are still believed to provide protection to the surrounding tissue. Ocular melanin is found in both anterior and posterior melanocytes in the eye.[4] Although anterior melanin adsorbs most of the UV and visible light that hits the eye, some light reaches posterior melanin, such as the melanin in retinal pigment epithelial cells (Figure 5.1). These cells protect the retina from scattered visible light and may also protect the area from oxidative damage by binding to free radicals with the catechol portion of eumelanin. Cochlear melanin may play a similar protective role against oxidation and it is possible that it helps maintain the endocochlear potential that makes hearing possible.[5] For many years it was thought that melanin in the

brain, or neuromelanin, was mainly a waste product. More recently there is evidence that neuromelanin binds to and regulates potentially harmful metal cations, especially iron, and that it reduces oxidative stress in neurons through the sequestration of free radicals.[6,7] More research needs to be conducted to fully understand the function and complete structure of melanin in all of these tissues.

Since melanin is a natural, potentially conductive material, there is interest in exploring the use of melanin in the place of synthetic conjugated polymers for biological applications. Melanin could be especially useful for applications that require an electrical connection between electrically active cells, such as neural cells, and electrodes on prosthetic devices (neural probes, prosthetic limbs, pace makers, etc). Few studies have been performed to investigate the use of melanin as a biomaterial. Bettinger *et al*. demonstrated that synthetic eumelanin purchased from Sigma could be made into thin films through spin coating and used as a substrate for primary rat Schwann cells and PC-12 cells.[8] Schwann cells grew faster on melanin than uncoated glass and collagen-coated glass (Figure 5.2). Also, PC-12 cells grew longer neurites on melanin than the control substrates when treated with nerve growth factor (NGF). The same type of melanin films fell apart due to mechanically disruption when implanted on top of rat sciatic nerves. The melanin fragments did not seem to damage the adjacent nerve and, interestingly, the fragments appeared to be consumed by macrophages or giant cells within 8 weeks of implantation. Although this study does demonstrate that chemically synthesized commercially available eumelanin is a potentially useful biomaterial, only one variation of melanin was studied. Thus more biocompatibility tests are necessary to study other forms of synthetic and natural melanin.

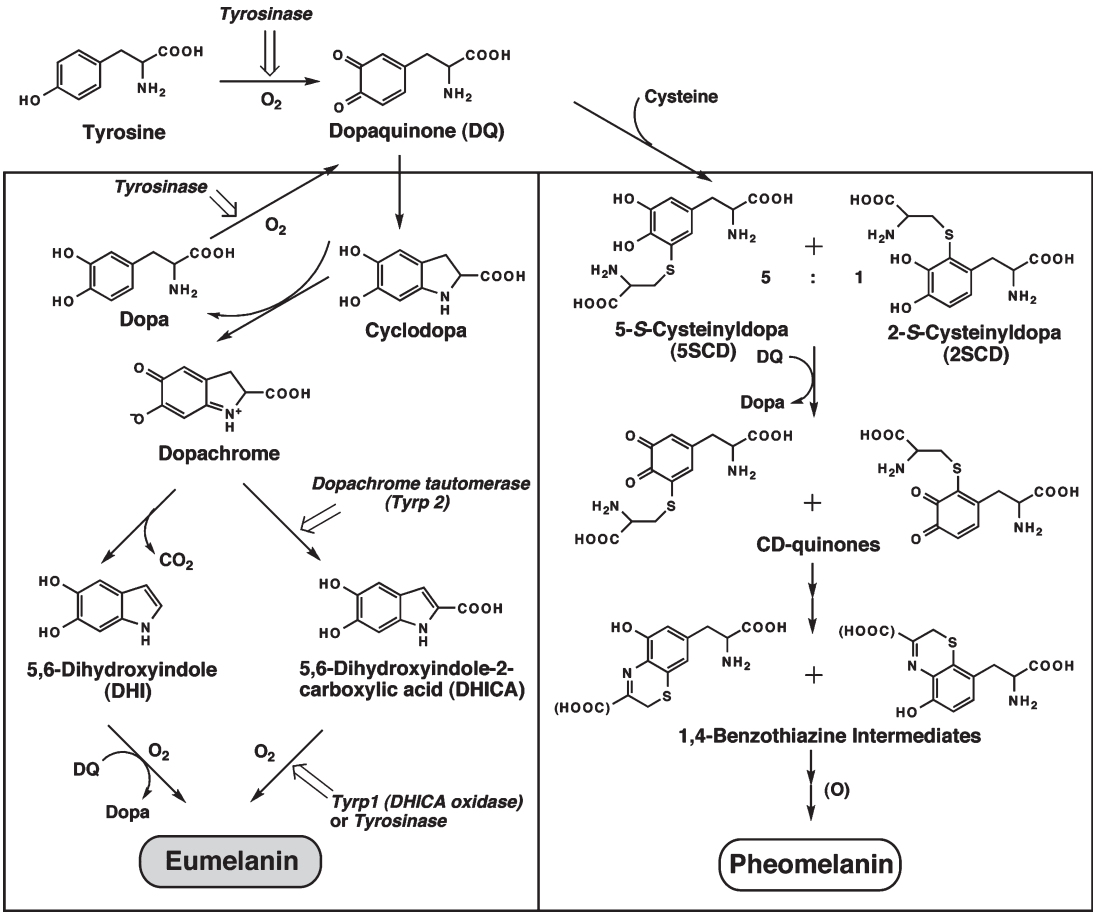

Scheme 5.1 Enzymatic pathways for eumelanin and pheomelanin, both derived from tyrosine.[1] Reprinted from *Photochemistry and Photobiology*, 84, Ito, S. and Wakamatsu, K., "Chemistry of mixed melanogenesis--pivotal roles of dopaquinone", 582-92, Copyright (2008), with permission from Wiley.

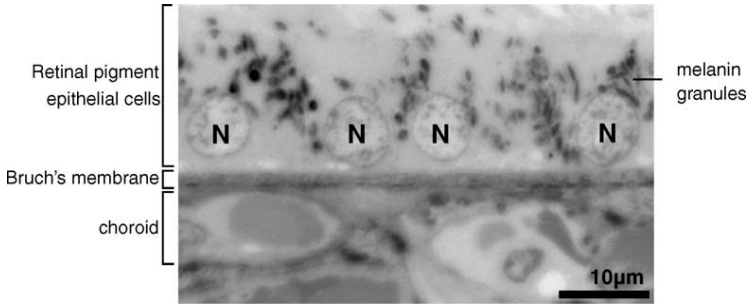

Figure 5.1 Melanin granules around the nuclei (N) of retinal pigment epithelial cells.[7] Reprinted from *Progress in Neurobiology*, 75, Fedorow, H.; Tribl, F.; Halliday, G.; Gerlach, M.; Riederer, P. and Double, K.L., "Neuromelanin in human dopamine neurons: comparison with peripheral melanins and relevance to Parkinson's disease", 109-24, Copyright (2005), with permission from Elsevier.

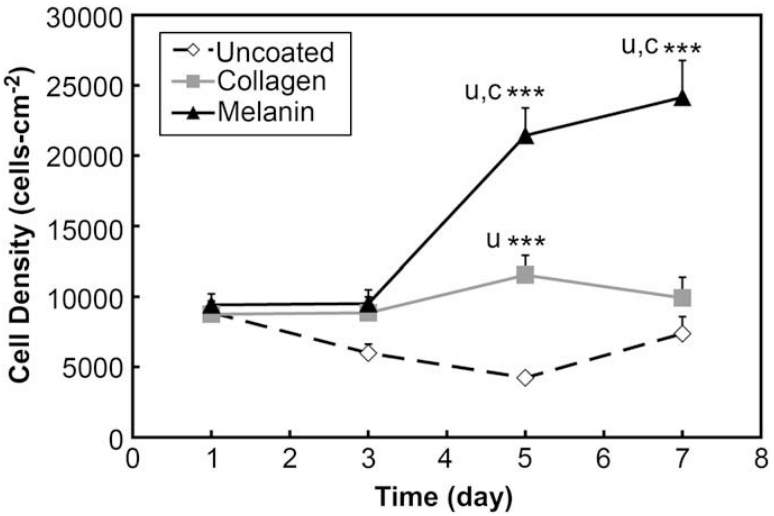

Figure 5.2 Growth dynamics of Schwann cells on uncoated, collagen coated and melanin coated substrates. SCs cultured on melanin substrates grew more rapidly compared to SCs cultured on collagen (***$p < 0.001$) or uncoated substrates (***$p < 0.001$).[8] Reprinted from *Biomaterials*, 30, Bettinger, C.J.; Bruggeman, J.P.; Misra, A.; Borenstein, J.T. and Langer, R., "Biocompatibility of biodegradable semiconducting melanin films for nerve tissue engineering", 3050-7, Copyright (2009), with permission from Elsevier.

We are interested in developing eumelanin-like conjugated polymers that can be used as electrode coatings for interfacing prosthetic devices with neural tissue (referred to as bio-electrodes). Since this type of polymer electrode is typically coated on top of metal electrodes, the most useful synthesis technique is electrochemical polymerization. During this process, polymer is formed in solution and precipitates out onto the working electrode, which can be any type of conductive material. In this chapter we have investigated the ability of four different monomers – L-3,4-dihydroxyphenylalanine (L-DOPA), 5,6-dihydroxyindole (DHI), 5,6-dihydroxyindole-2-carboxylic acid (DHICA) and 5,6-dimethoxyindole-2-carboxylic acid (DMICA) – to form eumelanin-like conjugated polymer films through electrochemical polymerization (Figure 5.3). The practicality of using these monomers was compared with conventional conjugated polymers such as poly(3,4-ethylenedioxythiophene) (PEDOT) and polypyrrole (PPy) and

in vitro cell experiments were performed. The results demonstrated that DMICA has the most potential for making bio-electrode coatings and that some of the other monomers are not suitable for electrochemical polymerization. For these monomers, other types of polymerization or processing may be more practical and are discussed at the end of the chapter.

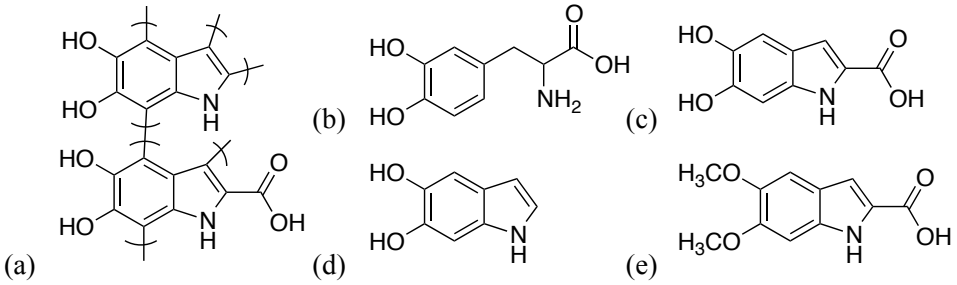

Figure 5.3 (a) Approximate structure of eumelanin, demonstrating possible cross-linking positions and synthetic melanin monomers (b) L-DOPA, (c) DHICA, (d) DHI and (e) DMICA

5.2 Experimental Procedures

5.2.1 Synthesis of DHI and DHICA

5,6-dihydroxyindole (DHI) was synthesized from 5,6-diacetoxyindole (DAI, TCI America), as previously reported (Scheme 5.2).[9] First, potassium carbonate (Acros, 41 mg , 0.3 mmol) and DAI (28 mg , 0.12 mmol) were placed in a 50 ml round bottom flask that was then degassed and flushed with argon gas. After adding anhydrous methanol (Aldrich, 3 ml) the solution immediately turned purple and was allowed to stir for 15 minutes. Next, degassed phosphate buffered saline (PBS, 9 ml) was added as an electrochemical polymerization electrolyte and 2 ml of the solution was transferred to a degassed electrochemical cell for polymerization. Characterization of the monomer was not performed since it was unstable under normal atmospheric conditions.

5,6-dihydroxyindole-2-carboxylic acid (DHICA) was synthesized from 5,6-dimethoxyindole-2-carboxylic acid (DMICA, Alfa Aesar) as previously reported (Scheme 5.2).[10] DMICA (221 mg, 1 mmol) was dissolved in dichloromethane (Acros, 10 ml) and cooled to -40 °C using an acetonitrile and dry ice bath. Under an argon atmosphere 1.0 M boron tribromide solution in dichloromethane (Aldrich, BBr_3, 8 ml, 8 mmol) was added and the solution was stirred for 4 hours. Deionized water was slowly added to the quench the reaction and the mixture was allowed to warm to room temperature. The aqueous layer was filtered out using phase separating paper (Whatman) and the organic layer was removed under vacuum. Conversion of the methoxy groups to hydroxyl groups was confirmed with ^1H nuclear magnetic resonance spectroscopy (NMR, Bruker AV400-ICON) and Fourier transform infrared spectroscopy (FTIR, Perkin Elmer Spectrum 100) and polymerization of the product was tested without further purification (7:3 mixture of DHICA:DMICA).

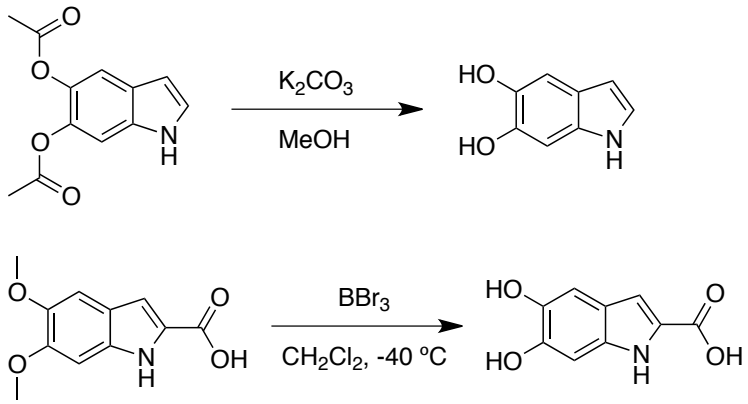

Scheme 5.2 One step synthesis routes for DHI (top) and DHICA (bottom)

5.2.2 Electrochemical Polymerization and Cyclic Voltammetry

L-3,4-dihydroxyphenylalanine (L-DOPA, Aldrich), DMICA, DHICA and DHI were electrochemically polymerized onto ITO-coated glass (Delta Technologies, Ltd) in

a 2-electrode cell using an Autolab PGstat12 Potentiostat/Galvanostat (EcoChemie) with a platinum wire or foil counter electrode. L-DOPA films were polymerized between 3-6 hours at concentrations of 0.02 M in water using 0.05 M sodium tetraborate (Aldrich) as the counter-ion. DHI films were electrochemically polymerized *in-situ* using an air-free polymerization cell. A solution of DHI, potassium carbonate, methanol and PBS was carefully transferred via syringe to a sealed polymerization cell. This cell contained an alligator clip that held the working electrode and was soldered onto a wire that pierced through the sealed cap. Electrochemical polymerization of DHICA was attempted using various solvents and counter-ions including propylene carbonate (Acros) with lithium perchlorate (Acros, $LiClO_4$), acetonitrile (Acros) with tetrabutylammonium perchlorate (Acros) and deionized water with sodium carbonate (Fisher) and $LiClO_4$. DMICA was polymerized for 10 minutes with poly(acrylic acid) (PAA, 1800 g/mol, Aldrich) in the polymerization solution to increase the mechanical stability of the films compared to regular PDMICA for cell culture. These films were made from 0.02 M – 0.05 M DMICA monomer dissolved in propylene carbonate with 0.05 M $LiClO_4$ and 0.5 wt% PAA. Additionally, 2.5 vol% water was added to provide better solubility for the PAA. All films were polymerized with current densities around 0.1 – 0.2 mA/cm^2.

PDMICA films were subjected to cyclic voltammetry (CV) using the same Autolab potentiostat/galvanostat with a platinum counter electrode, a saturated calomel reference electrode and phosphate buffered saline electrolyte (PBS, Hyclone Media). Cycling was performed between -0.6 V and +0.9 V with a scan rate of 0.12 V/s.

5.2.4 Chemical and Structural Characterization

Chemical analysis was performed on DHI melanin films using a PHI 5600 X-ray photoelectron spectrometer with a monochromatic aluminum X-ray source (Al Kα = 1486.6 eV) and a hemispherical electron energy analyzer. The pass energy for the survey spectra and characteristic region spectra were 187.85 eV and 58.7 eV, respectively. A take-off angle of 45° was used and the base chamber pressure was < 2 $x10^{-9}$ Torr. All spectra were referenced to the C-C/C-H peak at 285.0 eV. FTIR was performed on DHICA melanin and PDMICA films using a Perkin Elmer Spectrum 100 FTIR Spectrometer in attenuated total reflectance (ATR) mode. UV-Vis spectrometry was performed on L-DOPA and DHI melanin films between 300 to 800 nm using either a Cary 50 UV-Vis spectrophotometer (Agilent) or UV-3600 UV-Vis-NIR spectrophotometer (Shimadzu). Morphological studies of L-DOPA melanin and PDMICA were conducted using a JEOL JSM-7400F field emission scanning electron microscope at 3kV operating voltage. Films were sputter-coated with gold-palladium for 40 seconds in order to provide a more conductive surface.

5.2.5 In Vitro Cell Experiments

Cytotoxicity experiments were performed on L-DOPA melanin films using C2C12 mouse myoblasts and SH-SY5Y human neuroblastoma cells. The cells were seeded in Dulbecco's Modified Eagles Medium (DMEM, Cellgro) with 10% fetal bovine serum (FBS, Cellgro) for 5 days and then fixed with 4% formaldehyde. After washing with PBS, the cells were stained with rhodamine-phalloidin (Invitrogen) overnight and with Hoechst (Invitrogen) for 10 minutes before imaging. After washing with PBS, the

samples were mounted with anti-fade mounting media and imaged with an Olympus BX-51 fluorescence microscope.

Cytotoxicity experiments were performed on PDMICA films using NG108 neuroblastoma-glioma hybrid cells. At passage 3 10,000 cells/cm^2 were seeded in DMEM with 1% or 10% FBS on PDMICA/PAA films or on ITO as a control. After 3 days, the cells were fixed with formaldehyde, stained with rhodamine-phalloidine and mounted with ProLong Gold Anti-Fade mounting media with DAPI (Invitrogen). The cells were then imaged using a Nikon Eclipse Ti inverted fluorescence microscope and NIS-Elements Imaging Software.

5.3 Results and Discussion

5.3.1 L-DOPA Melanin

Initial attempts at making synthetic melanin biomaterials involved the use of L-DOPA as the monomer. L-DOPA was previously electrochemically polymerized on electrodes by other groups[11,12] but interactions between this type of melanin and cells had not been thoroughly investigated. L-DOPA was electrochemically polymerized with sodium tetraborate and water, conditions that were previously shown to work well.[11] The films produced were dark brown and had broad-band UV-Vis absorption (Figure 5.4), which is typical for natural and synthetic eumelanins.[13] This broad absorption indicated that the films were chemically disordered with different types of repeat units and a continuous spectrum of varying conjugation lengths.[14] The morphologies of the L-DOPA films were imaged with SEM, as shown in Figure 5.5. As was also seen with optical microscopy, there were a significant amount of large cracks in the films. Besides cracks that were close to 10 μm long, there were also extremely small nanometer scale cracks

(Figure 5.5d). In addition, there appeared to formation of ridges (possibly from buckling) that were about 100 nm wide. While buckling indicated there might be some ductility in the films, they also appeared to fracture easily as indicated by the number of cracks seen. Other than the buckling and cracking, the surface of the films looked relatively smooth.

The polymerization of L-DOPA films took much longer than the polymerization times of most conjugated polymer films. A uniform, relatively thick (μm) film of PEDOT or PPy typically takes around 10 minutes to polymerize, whereas L-DOPA required 3-6 hours under similar current densities to form films that were less than or around 1 μm thick. Subianto *et al.* found that free-standing L-DOPA melanin films took 6-10 days to form using the similar conditions.[11] Part of the reason for the slow polymerization is that L-DOPA first had to cyclize into dopachrome (Scheme 5.1) before polymerization could proceed. As this occurred the monomer solution turned orange and then as polymerization continued the solution turned brown. The small molecular weight oligomers or polymers that turned the solution brown in color did not immediately precipitate onto the electrode surface, resulting in long polymerization times.

(a) 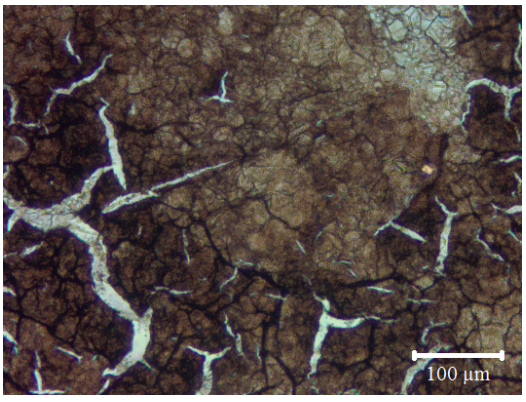

(b) 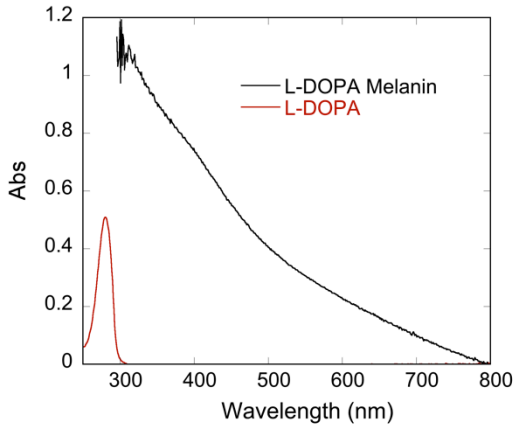

Figure 5.4 (a) Optical micrograph of electrochemically polymerized L-DOPA melanin with sodium borate counter-ion and (b) UV-Vis spectra demonstrating broad-band absorption for the film.

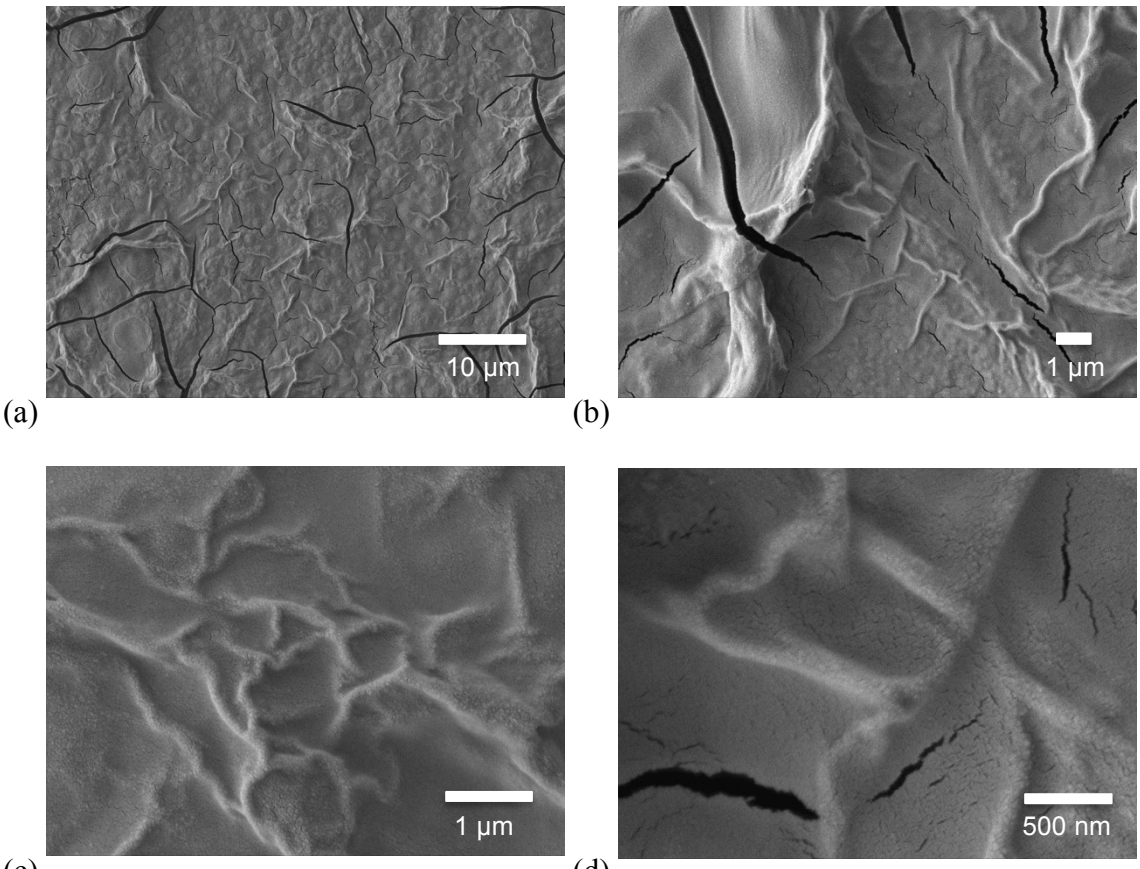

(a) (b)

(c) (d)

Figure 5.5 SEM micrographs of L-DOPA melanin demonstrating significant buckling and cracking at multiple scale lengths.

In order to investigate to use of L-DOPA melanin as a biomaterial, the cytotoxicity was investigated. C2C12 myoblasts and SH-SY5Y neuroblastoma cells were seeded on substrates for 5 days and compared with cells on uncoated ITO. As shown in Figure 5.6, C2C12 cells did not adhere well to L-DOPA melanin but grew to 100% confluency on ITO. Similar results were also seen with SH-SY5Y cells (not shown). In addition, the uncoated ITO portions of the L-DOPA electrodes also had cells attached. These results indicate that even immortal cell lines like C2C12 and SH-SY5Y did not want to attach to L-DOPA melanin. One possible explanation for this was the presence of the tetraborate counter-ion, which may have been toxic to the cells. Also, it is possible

that the charge state of the melanin films caused proteins from the serum to denature, which inhibited cell attachment. After this result, L-DOPA films were polymerized with sodium carbonate counter-ion rather than sodium tetraborate. However, the films made with carbonate were patchy on the electrode surface and did not seem suitable as coatings. Therefore, due to the length of time for polymerizations and the potential toxicity of the films, electrochemically polymerized L-DOPA melanins were not pursued further as a biomaterial.

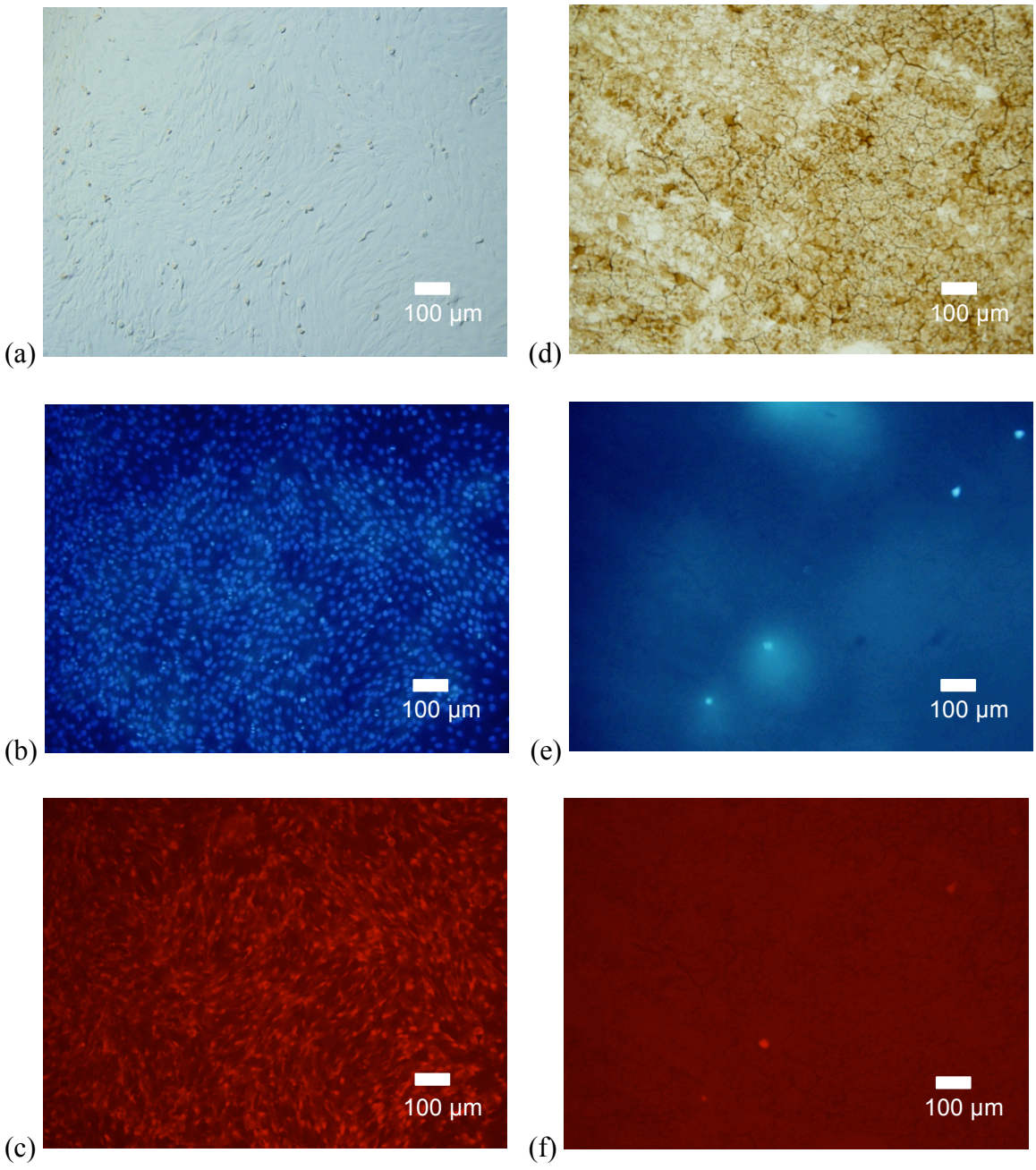

Figure 5.6 Optical and fluorescent images of C2C12 myoblasts on ITO (a-c) and L-DOPA melanin (d-f). Cells were stained with Hoescht to highlight the nuclei (blue) and phalloidin (red) to highlight the actin cytoskeleton. Very few cells adhered to the L-DOPA melanin surface.

5.3.2 DHI Melanin

DHI melanin was made by hydrolyzing DAI and directly electrochemically polymerizing the monomer in an argon atmosphere polymerization cell. DHI monomer

was very unstable and when isolation of the monomer was attempted polymerization occurred in air. Electrochemical polymerization was possible when taking specific precautions. However, besides polymerizing on the electrode surface, polymer also formed in solution and precipitated onto the glass cell and the glass side of the ITO electrode. The polymer that formed was dark brown, similar to L-DOPA melanin, and had broad absorption, although the absorption did not cover the entire spectrum (Figure 5.7). The chemical composition of DHI melanin was analyzed using XPS. Figure 5.8 demonstrates that carbon, nitrogen and oxygen were all still present after polymerization, indicating that the monomer structure stayed intact. While polymerization of DHI does produce melanin-like films, the necessity for an air-free environment and the lack of control over the polymerization process makes this method impractical for bio-electrode coatings.

(a) 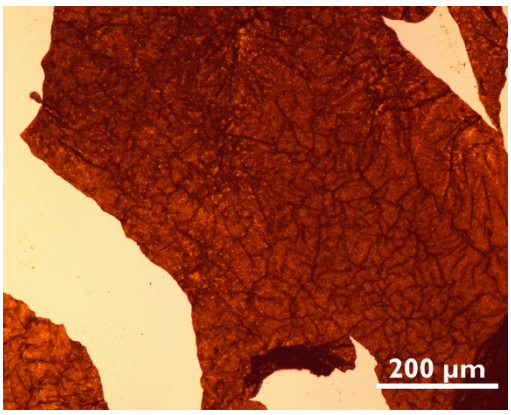

(b) 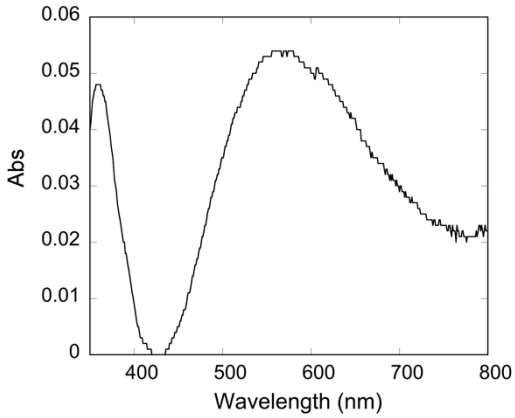

Figure 5.7 (a) Optical micrograph of DHI melanin film along with (b) the UV-Vis spectrum. The film had broad absorption and was dark brown in color, similar to L-DOPA melanin. Absorption at 350 nm may be DHI dimers or oligomers (DAI absorption is at 280 nm). DHI absorption is not shown since the molecule is not stable in air.

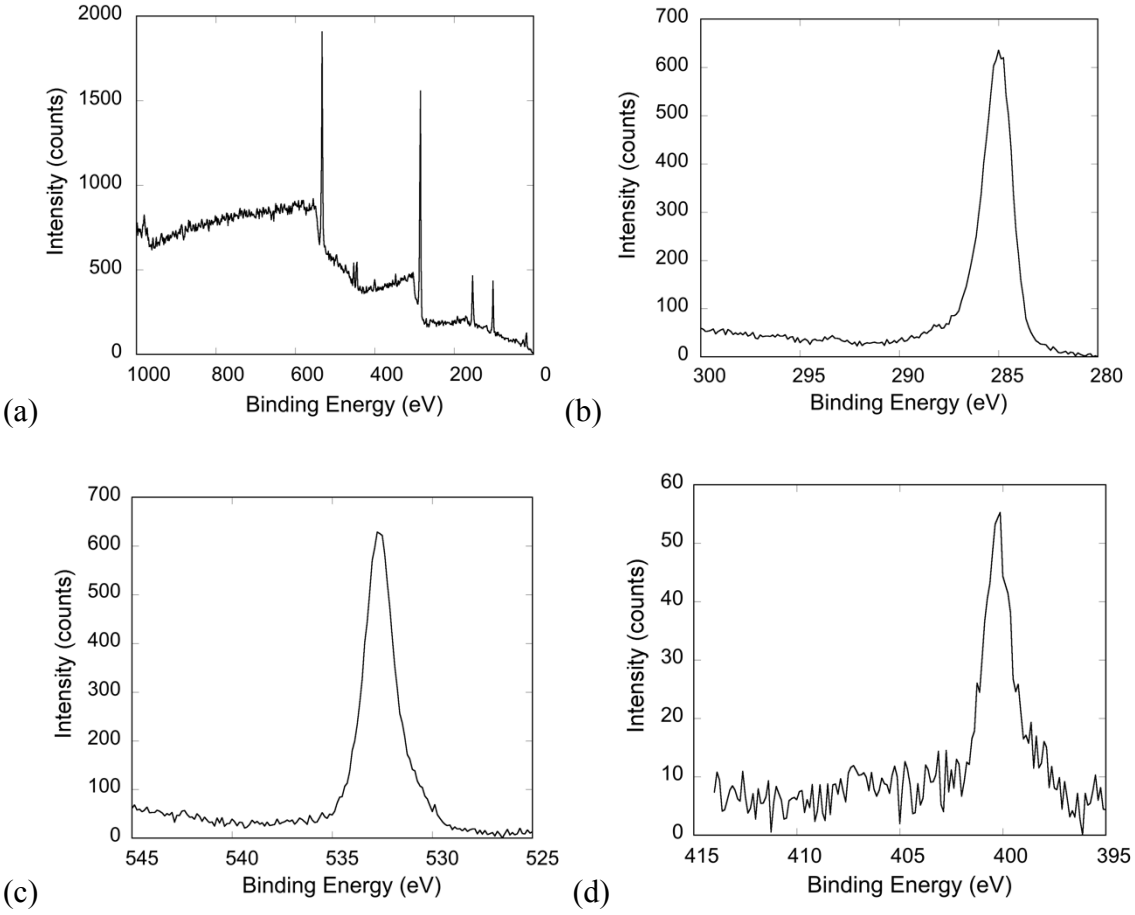

Figure 5.8 (a) Survey spectrum and high resolution (b) C1, (c) O 1s and (d) N 1s spectra for DHI melanin

5.3.3 DHICA Melanin

DHICA melanin was investigated by first synthesizing the DHICA monomer. NMR of the product demonstrated a drastically reduced peak at 3.8 ppm, which represented the methoxy C-H on DMICA (Figure 5.9a). The ratio of this peak to the other C-H hydrogens was 6:3 for DMICA and was reduced to 2:3 for the product. Therefore, about 67% of the product was DHICA and 33% was unreacted DMICA. Additionally, FTIR of the product demonstrates reduced peaks at 1440 cm^{-1} (C-H bending) and 1005 cm^{-1} (C-O-C stretching), which are derived from the methoxy groups on DMICA (Figure 5.9b). Since it had already been confirmed that DMICA can

electrochemically polymerize, the mixture of DHICA and DMICA was used to test the potential of DHICA to electrochemically polymerize. When current was applied to DHICA solutions (in water, acetonitrile and propylene carbonate) polymer formed in solution as indicated by a dark brown appearance. However, very little polymer precipitated onto the electrode after 60 minutes in any of the attempted conditions and it seemed that the polymer chains that formed were too soluble. When analysis of any material that precipitated onto the electrodes was attempted, the material typically fell apart. Also, when FTIR was attempted with minimal washing, the spectral signals were mostly from the solvents or counter-ions used in the polymerization. Interestingly, even though DMICA was present in the polymerization solution, PDMICA did not form on the electrode surface. It may be possible to make DHICA melanin films with polymerization times longer than an hour, like L-DOPA, but then production of the films becomes impractical compared to conventional conjugated polymer films. Therefore, polymerization and characterization of DHICA melanin was not pursued further.

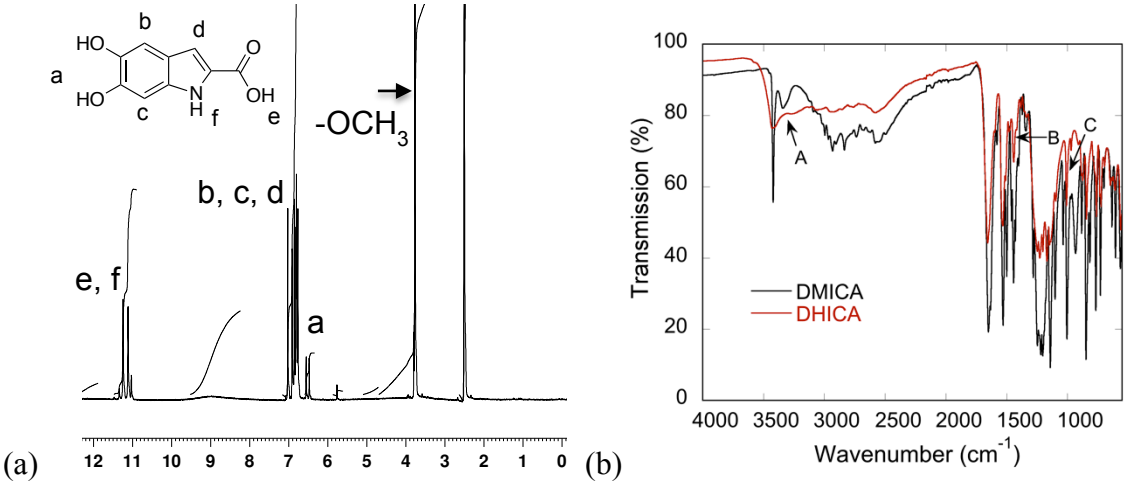

Figure 5.9 (a) NMR spectra for crude DHICA with decreased methoxy hydrogens labeled with the arrow and hydroxy hydrogens labeled a. (b) FTIR spectra for DMICA and crude DHICA monomers. The broad peak starting at 3500 cm^{-1} (A) indicated the presence of hydroxyl functional groups and shortened peaks at 1440 cm^{-1} (B) and 1005 cm^{-1} (C) indicated the reduction of methoxy groups.

5.3.4 PDMICA Melanin

As explained in Chapter 4, DMICA was electrochemically polymerized to form PDMICA films that were electrochromic and semi-crystalline with a nano-rod structure. While these films were unusual compared to synthetic melanins, they had a tendency to fall apart when cells were seeded on them. To address this problem, poly(acrylic acid) (PAA) was added to the polymerization solution, resulting in films of approximately 1 μm thickness (based on the current density and time of polymerization), although the thickness appeared to vary significantly throughout the films. PAA was successfully incorporated into PDMICA, as indicated by the FTIR spectra in Figure 5.10. The carbonyl stretching peak for PAA was present in the PDMICA PAA spectra and was not seen in the spectra for normal PDMICA films. Cyclic voltammetry (Figure 5.11) also indicated that the films were still electrically active and retained a high charge capacity (6.5 mC/cm^2 compared to 0.007 mC/cm^2 for bare ITO) even after cycling 50 times and losing their electrochromic activity. Importantly, PDMICA PAA films had increased mechanical stability compared to PDMICA. This was demonstrated simply by soaking both films in water overnight. The PDMICA films completely fell apart whereas the PDMICA PAA films remained intact.

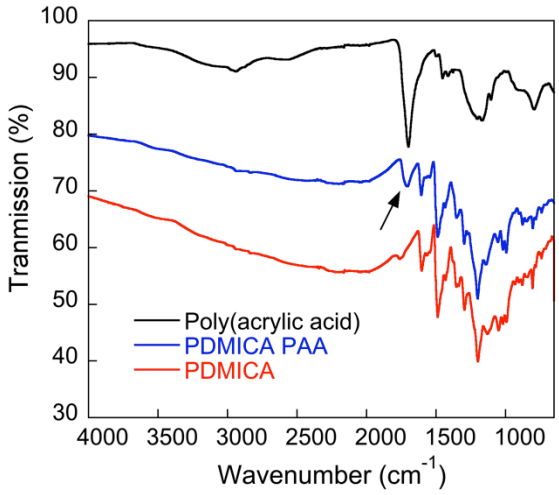

Figure 5.10 FTIR spectra demonstrating the presence of poly(acrylic acid) (PAA) in PDMICA films polymerized with PAA. Peak highlighted at 1711 cm^{-1} indicates PAA carboxylic acid.

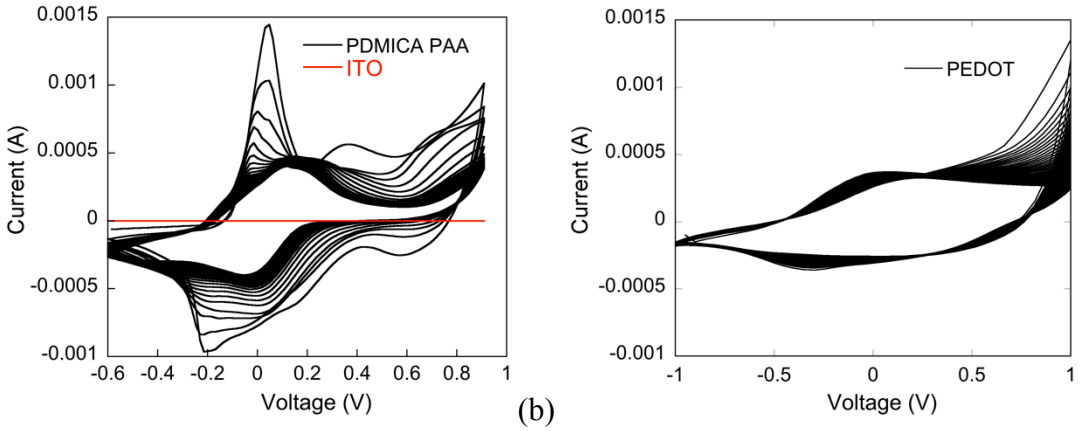

Figure 5.11 (a) Cyclic voltammetry of PDMICA with PAA demonstrating stability after loss of electrochromic activity over 50 cycles. CV of ITO and (b) PEDOT $LiClO_4$ are also shown under the same conditions, current scale and film area for comparison.

Previously published literature has shown that PEDOT can be polymerized with PAA and $LiClO_4$ and that PAA produced a fibrous, high surface area morphology in the resulting film.[15] Therefore, the morphology of PDMICA PAA was analyzed to reveal if PAA produces a similar effect. SEM images of the PDMICA PAA films demonstrated that the polymer still retained a defined nanostructure (Figure 5.12 a-d). However, the structures were more mesh-like than the previous PDMICA films and rather than nano-

rods, the films were composed of longer fibers that were hundreds of nanometers to micrometers in length with diameters around 30 nm (the same diameter as PDMICA in Chapter 4). A similar micro- and nano-structure was seen for films polymerized without PAA but in propylene carbonate with $LiClO_4$ and water (Figure 5.12 e-f). Therefore, it did not seem that the PAA drastically changed the visible structure of the PDMICA, even though it did provide increased mechanical stability.

Preliminary cell experiments demonstrated that PDMICA PAA films are not inherently cytotoxic to NG108 neuroblastoma-glioma cells. As shown in Figure 5.13, cells were able to adhere to the films and remained intact over 3 days in 1% serum. The round morphology of the cells indicated that most of the cells were not differentiated into neurons. The cells also seemed to prefer to adhere to each other rather than the surface, as shown by their preference to clump; however, this was also seen in the samples with bare ITO as the substrate. One of the PDMICA samples had a few cells that formed long neurites (Figure 5.14), but this was not a consistent observation. In 10% serum the polymer films fell apart over 3 days. This may have occurred because the cells attached more strongly to the films due to the greater quantity of cell adhesion proteins present on the surface. Currently, we are optimizing the cell system to preferentially produce a neuronal phenotype through either serum starvation, DMSO or biochemical cues such as N^6,$O^{2'}$-dibutyryl adenosine 3':5'-cyclic monophosphate (dibutyryl cyclic AMP) and are optimizing the conditions and time periods for these types of cells and samples.[16,17] However, the initial results demonstrate that the PDMICA PAA films have potential as electrically active bio-electrode coatings.

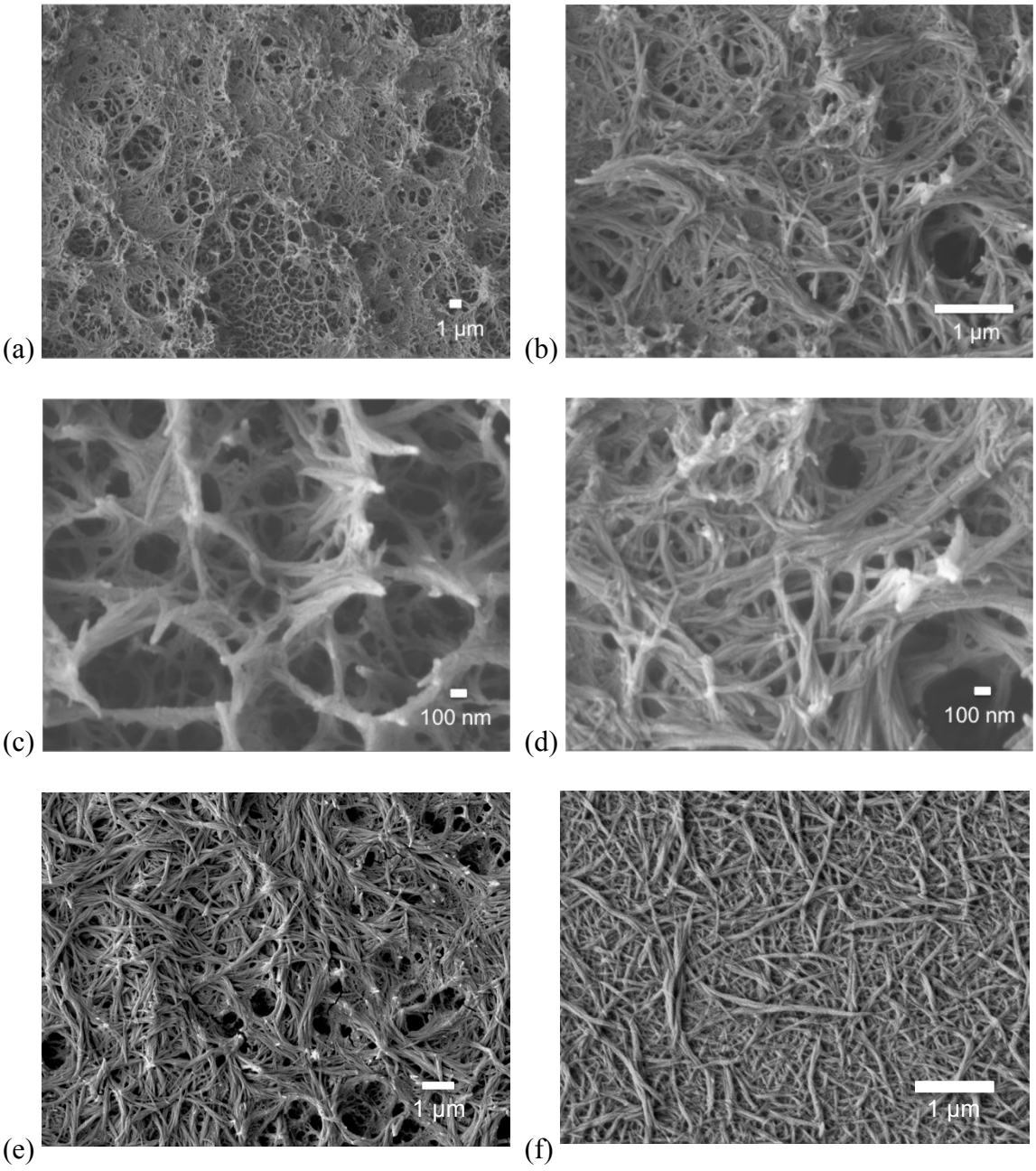

Figure 5.12 SEM images of PDMICA with PAA (a-d) and PDMICA without PAA (e-f) using the same conditions. Both samples had a fibrillar and mesh-like structure.

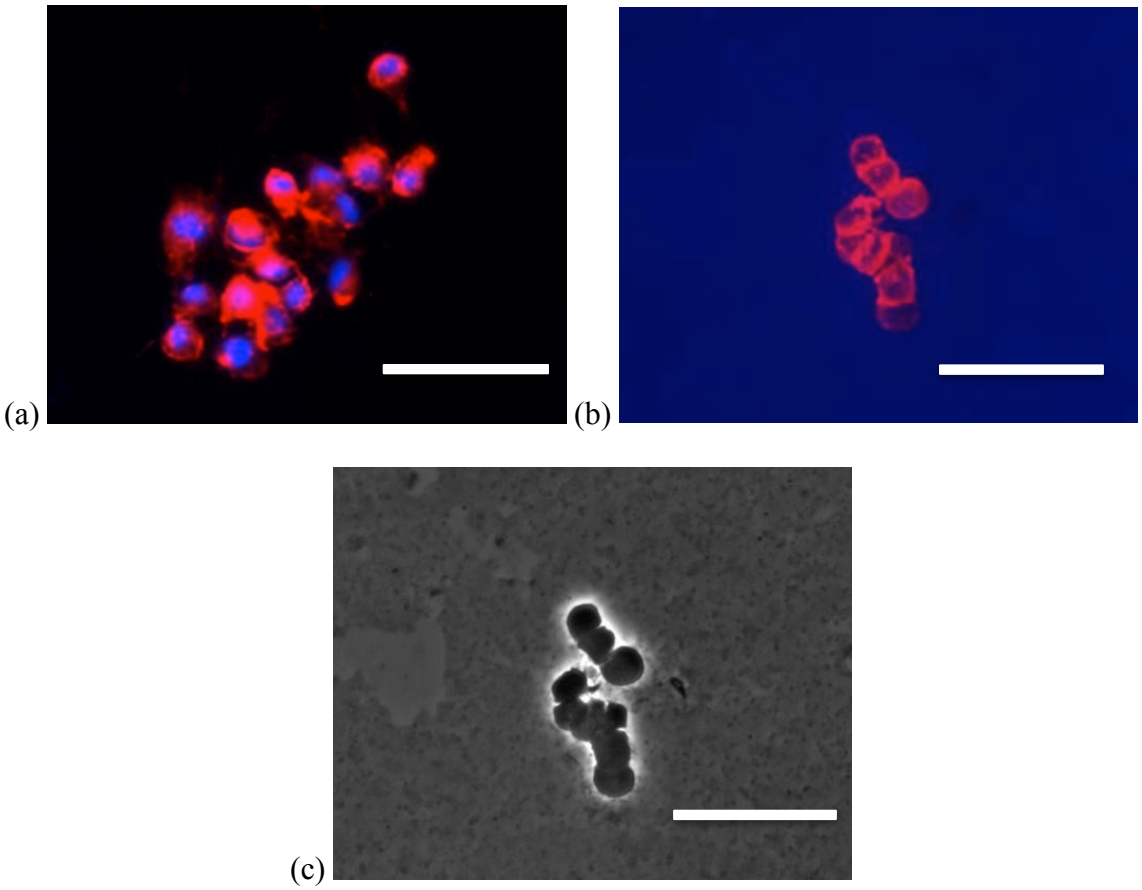

Figure 5.13 NG108 cells in 1 % serum on (a) ITO and (b) PDMICA PAA films for 3 days and stained with rhodamine phalloidin and DAPI. The PDMICA PAA sample had background blue fluorescence where film was present, indicating that the film may have bound to DAPI in a manner that allowed it to fluoresce. The brightfield image for PDMICA PAA is also shown (c) to highlight the presence of the underlying film. Scale bars represent 100 µm.

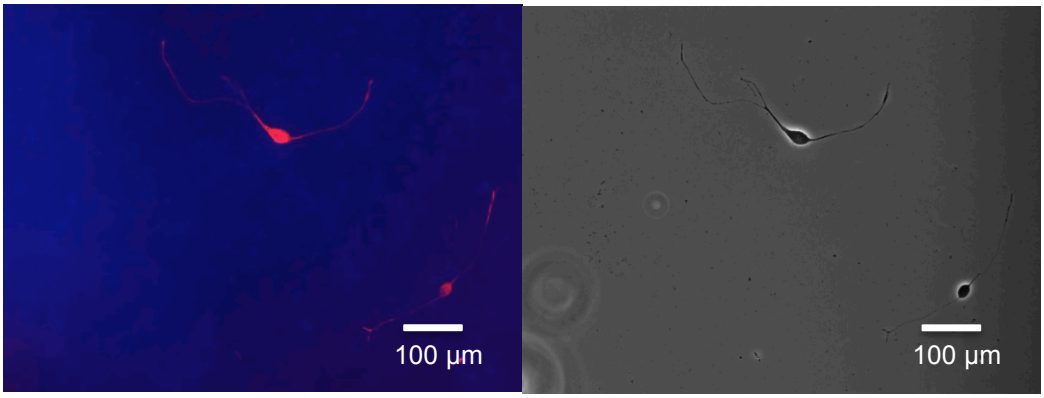

Figure 5.14 Fluorescence and bright field images of NG108 cells on PDMICA PAA that had differentiated into a neuronal phenotype.

5.4 Summary and Future Outlook

Electrochemical polymerization attempts for L-DOPA, DHI and DHICA have demonstrated that these materials may not be suitable for forming bio-electrode coatings. L-DOPA films appeared to be cytotoxic and polymerization times were long, DHI was too unstable in monomer form and the polymerization could not be controlled, and DHICA did not easily precipitate onto the electrode surface. The catechol functionality on DHICA and L-DOPA appears to make the oligomers and polymers that form too soluble to form polymer electrodes quickly, especially in aqueous environments. While these monomers may not be easily electrochemically polymerized, they could be used for chemical polymerization of melanins through simple methods such as oxidative polymerization. We have seen that L-DOPA will polymerize in solution simply by stirring in high pH water. Additionally, natural melanins such as sepia melanin (derived from the cuttlefish species *Sepia officinalis*) should be studied as possible biomaterials. These melanins may be easier to process than electrochemically polymerized films and could be used for different biomaterial applications. Interestingly, we have seen that commercially available sepia melanin forms relatively uniform nanoparticles (unpublished data) that could used to investigate the interactions between cells and melanin particles that are smaller than the typical cell size.

Since DMICA has methoxy functional groups instead of hydroxy, it did not have the same solubility and stability issues as the other monomers tested. When PDMICA was synthesized with PAA in solution, mechanically robust films were produced that had a nano-fibrous structure. These films have potential to be used as biomaterials, as shown by experiments with NG108 cells. Additional *in vitro* experiments should be performed

using both transformed cells such as NG108s or SH-SY5Y neuroblastomas and also primary neural cells such as primary rat motor neurons or dorsal root ganglia. If it is shown that PDMICA films stay electrically active and are non-toxic to primary cells, then *in vivo* experiments should be performed in rats or similar animals. These experiments will help compare PDMICA with natural melanins and synthetic conjugated polymers to reveal if it is a suitable electrically active biomaterial.

5.5 References

(1) Ito, S.; Wakamatsu, K. *Photochemistry and Photobiology* **2008**, *84*, 582-92.

(2) Kollias, N.; Sayre, R. M.; Zeise, L.; Chedekel, M. R. *Journal of Photochemistry and Photobiology B, Biology* **1991**, *9*, 135-160.

(3) Kadekaro, A. L.; Kavanagh, R. J.; Wakamatsu, K.; Ito, S.; Pipitone, M. A.; Abdel-Malek, Z. A. *Pigment Cell Research* **2003**, *16*, 434-47.

(4) Hu, D.-N.; Simon, J. D.; Sarna, T. *Photochemistry and Photobiology* **2008**, *84*, 639-44.

(5) Ohlemiller, K. K.; Rice, M. E. R.; Lett, J. M.; Gagnon, P. M. *Hearing Research* **2009**, *249*, 1-14.

(6) Double, K. L.; Dedov, V. N.; Fedorow, H.; Kettle, E.; Halliday, G. M.; Garner, B.; Brunk, U. T. *Cellular and Molecular Life Sciences* **2008**, *65*, 1669-82.

(7) Fedorow, H.; Tribl, F.; Halliday, G.; Gerlach, M.; Riederer, P.; Double, K. L. *Progress in Neurobiology* **2005**, *75*, 109-24.

(8) Bettinger, C. J.; Bruggeman, J. P.; Misra, A.; Borenstein, J. T.; Langer, R. *Biomaterials* **2009**, *30*, 3050-7.

(9) Hatcher, L. Q.; Simon, J. D. *Photochemistry and Photobiology* **2008**, *84*, 608-12.

(10) Sechi, M.; Rizzi, G.; Bacchi, A.; Carcelli, M.; Rogolino, D.; Pala, N.; Sanchez, T. W.; Taheri, L.; Dayam, R.; Neamati, N. *Bioorganic & Medicinal Chemistry* **2009**, *17*, 2925-35.

(11) Subianto, S.; Will, G.; Meredith, P. *Polymer* **2005**, *46*, 11505-11509.

(12) Rubianes, M. D.; Rivas, G. A. *Analytica Chimica Acta* **2001**, *440*, 99-108.

(13) Capozzi, V.; Perna, G.; Carmone, P.; Gallone, A.; Lastella, M.; Mezzenga, E.; Quartucci, G.; Ambrico, M.; Augelli, V.; Biagi, P. *Thin Solid Films* **2006**, *511-512*, 362-366.

(14) Tran, M. L.; Powell, B. J.; Meredith, P. *Biophysical Journal* **2006**, *90*, 743-52.

(15) Yang, J.; Lipkin, K.; Martin, D. C. *Journal of Biomaterials Science Polymer Edition* **2007**, *18*, 1075-89.

(16) Seidman, K. J.; Barsuk, J. H.; Johnson, R. F.; Weyhenmeyer, J. A. *Journal of Neurochemistry* **1996**, *66*, 1011-8.

(17) Nelson, P.; Christian, C.; Nirenberg, M. *Proceedings of the National Academy of Sciences of the United States of America* **1976**, *73*, 123-7.

CHAPTER 6

Conclusions and Future Work

6.1 Conclusions

In this thesis we presented the synthesis and characterization of peptide-functionalized PEDOT-PEDOTacid and melanin-like conjugated polymers for interfacing electrodes with biological tissue. The carboxylic acid functionalized monomer EDOTacid was synthesized using a 7-step procedure and electrochemically copolymerized with EDOT to produce PEDOT-PEDOTacid conjugated polymer films that retained a relatively high charge capacity, between 6.5 – 9.6 mC/cm^2. The carboxylic acids on these films were reacted with GGGGRGDS peptide to create PEDOT-PEDOTacid films with a high density (60 – 600 pmol/cm^2) of covalently attached RGD. This peptide increased adhesion of primary rat motor neurons by 3 to 9 times compared to unfunctionalized controls, which demonstrated that biomolecules can remain active after being chemically attached to PEDOT-PEDOTacid. This peptide-coupling scheme could be used to tailor the surface of PEDOT-PEDOTacid with any peptide in order to control the behavior of cells in a specific manner.

In our attempts to electrochemically polymerize melanin-like conjugated polymer films for biological applications we discovered that poly(5,6-dimethoxyindole-2-carboxylic acid) (PDMICA) has the most potential as a bio-electrode coating. This conjugated polymer produced green films that were electrochromic – changing from

transparent, to green and then to purple as the voltage applied was scanned from -1 V to +1 V – and had well-defined nano-rods or nano-fibers. In addition, NG108 neuroblastoma-glioma cells were able to attach to PDMICA with poly(acrylic acid) (PAA) and survived for 3 days before being fixed. Besides being non-toxic, these films were also electrically active, with charge capacities of 6.5 mC/cm^2 after 50 voltage cycles. Electrochemical polymerization attempts for L-3,4-dihydroxyphenylalanine (L-DOPA), 5,6-dihydroxyindole (DHI) and 5,6-dihydroxindole-2-carboxylic acid (DHICA) demonstrated that these materials may not be suitable for forming bio-electrode coatings, although they may be synthesized and processed with other methods. While there have been some challenges in the formation of melanin-like films, it is still a promising area of research, especially with PDMICA, solution polymerized melanin and natural melanin.

6.2 Future Work

As state previously, the PEDOT-PEDOTacid platform could in principle be extended to any peptide or biomolecule that reacts with carboxylic acids and could eventually be used to attract neurons to an electrode surface through the use of IKVAV or L1. These peptide or protein modified surfaces need to be investigated *in vitro* using a mixture of neuronal and non-neuronal primary cells to ensure that neurons are preferentially attracted to the surface. *In vivo* experiments could then be performed to investigate whether neural-selective PEDOT-PEDOTacid-peptide can attract enough neurons to maintain electrical connection, even with possible glial scar formation.

It is unlikely that PEDOT-PEDOTacid-peptide films alone can completely overcome the formation of a glial scar because there are many possible factors involved in the initiation of gliosis.[1,2] Cells may respond to mechanical forces created by the initial

implantation and forces caused by stiffness mismatches between soft brain tissue and a hard implant. There may also be cellular responses to the presence of foreign chemical substances. In addition, implantation of a foreign material could cause changes in the structures of biological molecules and disruptions in biological signaling between cells. To address multiple factors, PEDOT-PEDOTacid-peptide films should be combined with other approaches that aim to mitigate the loss of neural signaling associated with glial scar formation. To address mechanical issues, PEDOT-PEDOTacid-peptide coatings can be placed on probes that are made from polymeric materials such as parylene.[3] These films could also be grown through hydrogels that coat the entire probe, thus greatly reducing the hardness of the implant.[4-6] In addition, PEDOT-PEDOTacid-peptide films could be electrochemically polymerized with drugs that can be released on command.[7] With this method neurons could be attracted to peptides on the surface of the implant while the film releases anti-inflammatory drugs to reduce gliosis at the same time. A final approach would be growing PEDOT-PEDOTacid-peptide directly in the brain tissue, or *in-situ*.[8,9] This method could be used to grow conjugated polymer through a glial scar, thus eliminating the need to reduce scar formation. By combining PEDOT-PEDOTacid-peptide with these other methods, we have a greater chance of improving the outcome of neural probe implantations and chronic recordings.

As discussed earlier in this chapter, the polymer PDMICA seems to have the most promise as a melanin-like biomaterial, due to its ease of synthesis, high charge capacity and low cytotoxicity. The research presented in this thesis represents initial attempts at studying and using melanins as biomaterials. Therefore, there is still a vast amount of research that should be conducted on both synthetic and natural melanins.

From a materials viewpoint, it is necessary to develop methods for polymerizing and processing melanins so that they can be used as films, free-standing structures or incorporated into devices. Also, the interactions between cells and chemically or biologically synthesized melanins should be studied in depth and compared with studies of electrochemically polymerized films. In terms of biological research, it is important to continue exploring the structures and functions of natural melanins so that these structures can be replicated and the complete utility of melanin –like polymers can be understood. Besides simply acting as electrically conductive polymers, it seems that both synthetic and natural melanins could have anti-oxidant, metal-chelating and possibly ion transporting properties. If the complete structure/function relationship is understood, not only will the possible outcomes of implanting melanin biomaterials be better understood, but it may also be possible to develop new devices that utilize the innate functionality of melanins. For example, melanin films incorporated into cochlear implant electrodes may be able to help restore lost endonuclear potentials. Also, melanin films implanted on deep-brain stimulating (DBS) electrodes could help with Parkinson's treatment if it is found that the loss of melanin during the development of the disease increases damage to the brain.

Finally, the materials and ideas developed in this thesis could be combined to develop new synthetic/bio hybrid systems. For instance, EDOT can be electrochemically co-polymerized with DMICA to produce conjugated polymer films that have biomimetic and completely synthetic components. It should also be possible to copolymerize EDOT or EDOTacid with L-DOPA and other melanin precursors through chemical polymerization. In addition, the peptide-coupling schemes presented for PEDOT-

PEDOTacid could be applied to PDMICA, L-DOPA melanin and DHICA melanin since these polymers all contain carboxylic acids. It may also be possible to bind peptides to natural melanin to create purely biological hybrid materials. The research projects and new materials that could be built of off topics in this thesis are numerous and it will be exciting to see the new developments that arise in the field of conjugated polymer biomaterials in the next decade.

6.3 References

(1) Biran, R.; Martin, D. C.; Tresco, P. A. *Experimental Neurology* **2005**, *195*, 115-26.

(2) Kotov, N. A.; Winter, J. O.; Clements, I. P.; Jan, E.; Timko, B. P.; Campidelli, S.; Pathak, S.; Mazzatenta, A.; Lieber, C. M.; Prato, M.; Bellamkonda, R. V.; Silva, G. A.; Kam, N. W. S.; Patolsky, F.; Ballerini, L. *Advanced Materials* **2009**, *21*, 3970-4004.

(3) Takeuchi, S.; Ziegler, D.; Yoshida, Y.; Mabuchi, K.; Suzuki, T. *Lab on a Chip* **2005**, *5*, 519-23.

(4) Kim, D.-H.; Abidian, M.; Martin, D. C. *Journal of Biomedical Materials Research. Part A* **2004**, *71*, 577-85.

(5) Kim, D.-H.; Wiler, J. A.; Anderson, D. J.; Kipke, D. R.; Martin, D. C. *Acta Biomaterialia* **2010**, *6*, 57-62.

(6) Abidian, M. R.; Martin, D. C. *Advanced Functional Materials* **2009**, *19*, 573-585.

(7) Abidian, M. R.; Kim, D.-H.; Martin, D. C. *Advanced Materials* **2006**, *18*, 405-409.

(8) Richardson-Burns, S. M.; Hendricks, J. L.; Foster, B.; Povlich, L. K.; Kim, D.-H.; Martin, D. C. *Biomaterials* **2007**, *28*, 1539-52.

(9) Richardson-Burns, S. M.; Hendricks, J. L.; Martin, D. C. *Journal of Neural Engineering* **2007**, *4*, L6-L13.

Appendices

Appendix A. EDOTacid Characterization

EDOTacid NMR

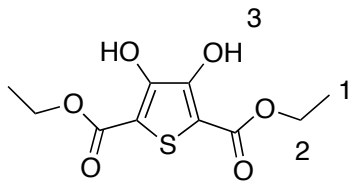

compound (4)

(400 MHz, d_6-DMSO) δ ppm (*J* Hz): 1.214 (t, 6 H, $J_{1,2}$ 7.2 Hz, H^1), 4.205 (q, 4 H, $J_{2,1}$ 7.2 Hz, H^2), 10.305 (br s, 2 H, H^3)

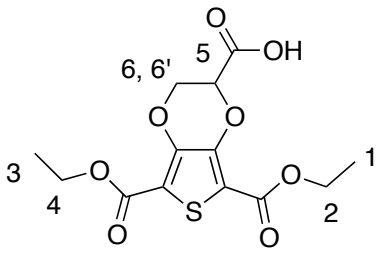

compound (6)

(400 MHz, d_6-DMSO) δ ppm (*J* Hz): 1.203 (t, 3 H, $J_{1,2}$ 7.2 Hz, H^1), 1.215(t, 3 H, $J_{3,4}$ 7.2 Hz, H^3), 4.158-4.278 (m, 4 H, H^2, H^4), 5.281 (t, 1 H, $J_{5,6}$ 2.8 Hz, H^5), 4.599 (dd, 1 H, $J_{6,5}$ 2.8 Hz, $J_{6,6'}$ 12.0 Hz, H^6), 4.382 (dd, 1 H, $J_{6',5}$ 2.8 Hz, $J_{6',6}$ 12.0 Hz, $H^{6'}$)

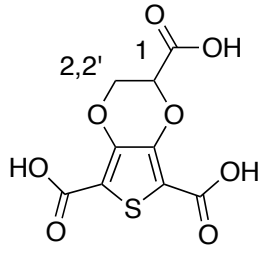

compound (7)

(400 MHz, d_6-DMSO) δ ppm (*J* Hz): 4.942 (t, 1 H, $J_{1,2}$ 2.8 Hz, H^1), 4.428 (dd, 1 H, $J_{2,1}$ 2.8 Hz, $J_{2,2'}$ 11.8 Hz, H^2), 4.319 (dd, 1 H, $J_{2',1}$ 2.8 Hz, $J_{2',2}$ 11.8 Hz, $H^{2'}$)

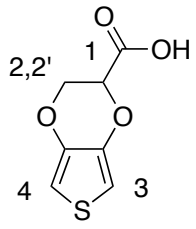

compound (8)

(300 MHz, d_6-DMSO) δ ppm (*J* Hz): 4.972 (t, 1 H, $J_{1,2}$ 3.0 Hz, H^1), 4.367 (dd, 1 H, $J_{2,1}$ 3.0 Hz, $J_{2,2'}$ 12.0 Hz, H^2), 4.220 (dd, 1 H, $J_{2',1}$ 3.0 Hz, $J_{2',2}$ 12.0 Hz, $H^{2'}$), 6.581 (d, 1 H, $J_{3,4}$ 3.6 Hz, H^3), 6.627 (d, 1 H, $J_{4,3}$ 3.6 Hz, H^4)

EDOTacid Mass Spectroscopy

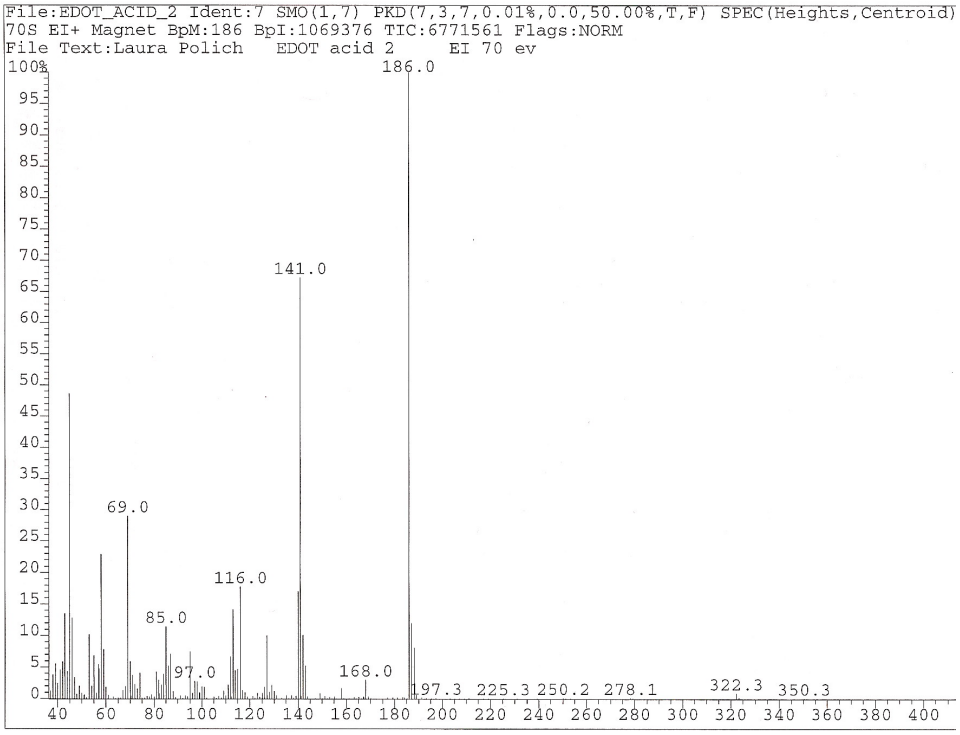

Figure A-1 EDOTacid electron ionization mass spectroscopy demonstrating the predicting molecular weight of 186 g/mol and a fragmented species at 141 g/mol.

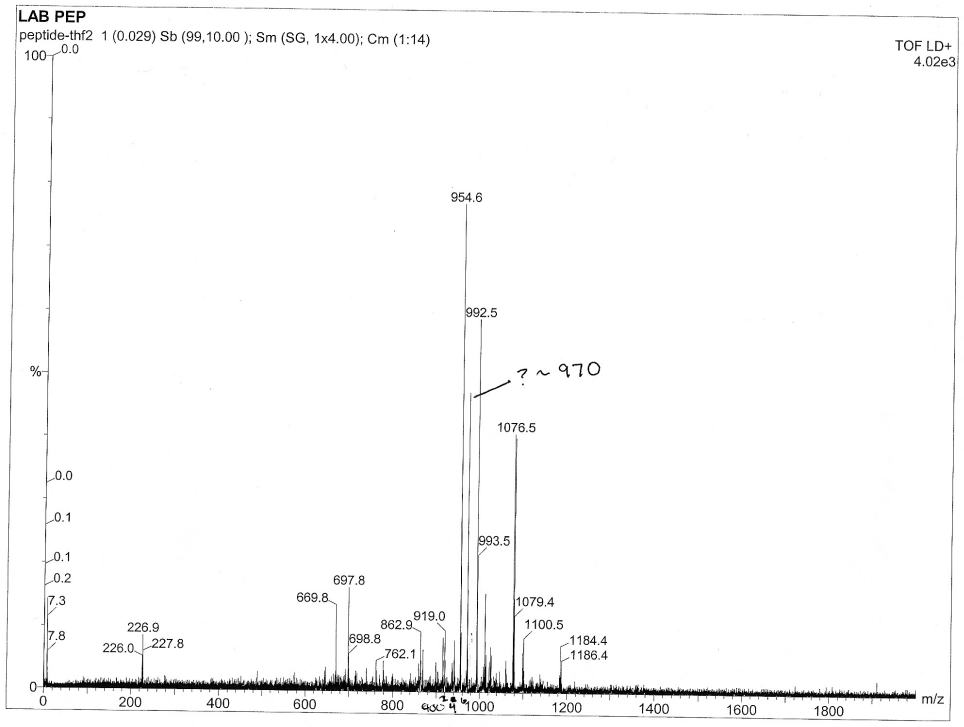

Figure A-2 MALDI mass spectroscopy for unmodified GRGDS peptide.

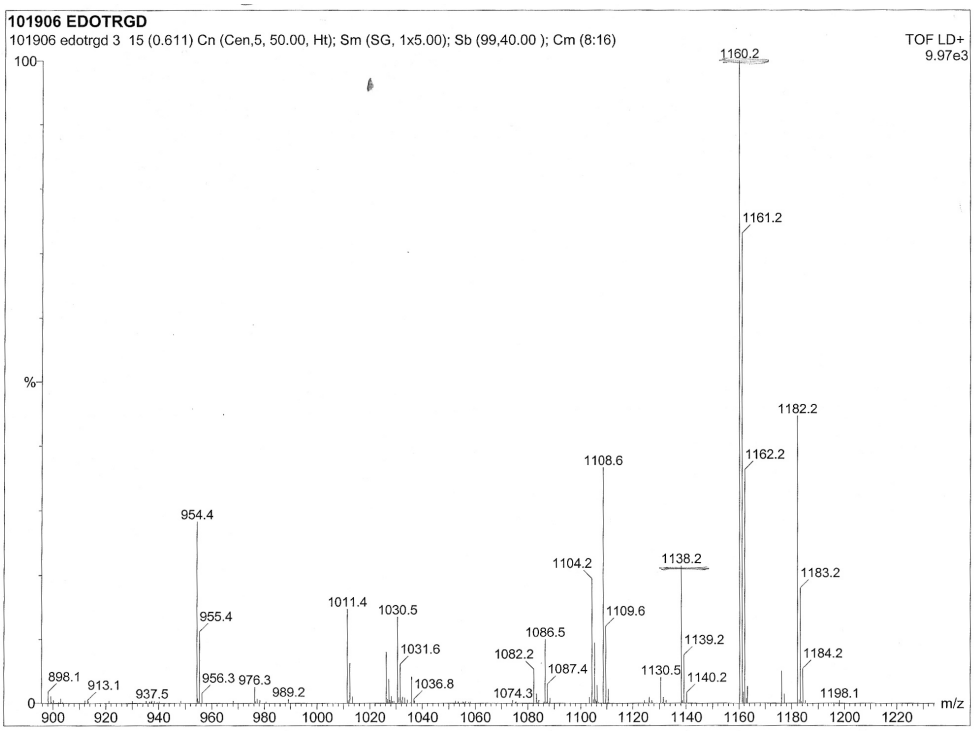

Figure A-3 MALDI mass spectroscopy for EDOTacid bound to GRGDS peptide, demonstrating increased molecular weight compared to unmodified GRGDS.

Appendix B. Rat Dissection Protocol

E15 Rat Dissection Protocol

Week Before

Fax in rat order form by the Monday before the desired week. Have rat delivered on Monday as E12.

Clean coverslips in piranha etch

Plasma etch fibers for DRG

Night Before

Apply PLGA moats to substrates

Dilute 1mg collage in 10ml sterile acetic acid. Rock for at least 4hr

Flame glass coverslips for DRG explants

Preparation

Check that the rat is pregnant

Apply substrate coatings

Thaw 3mls each of trypsin and FBS

Firepolish 3 pastuer pipettes

Warm up bottle of L15

Euthanization

1st injection: 0.75ml of 3:1 Ketamine to xylezene (IP)

Wait 15 minutes - check to make sure the animal displays no reflexes

2nd injection: 0.3ml FatalPlus (IC)

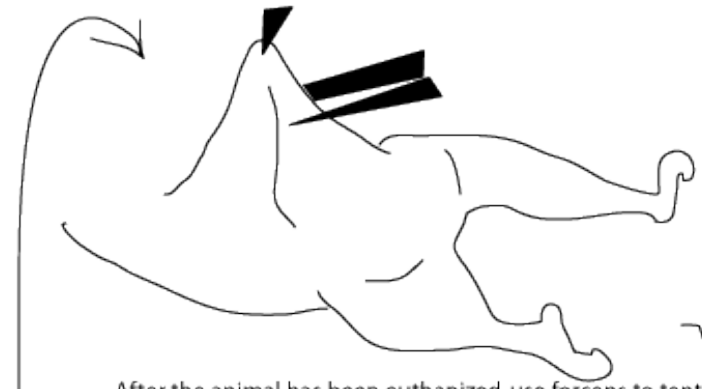

After the animal has been euthanized, use forceps to tent the skin of the abdomen. Then use scissors to cut through both the skin and muscle layers, exposing the abdominal cavity.

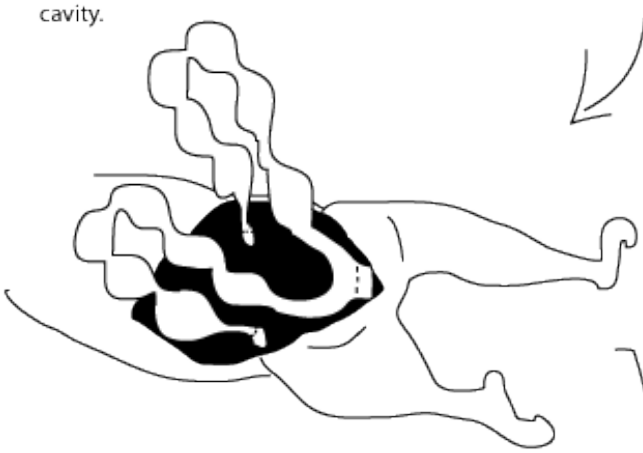

The rat uterus is U-shaped. The embryos appear as beads on a string. Detach the uterus at the cervix and just in front of each ovary.

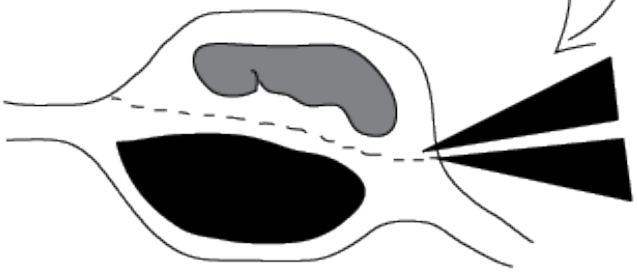

Free the embryos from the amniotic sac by cutting along the side of the uterus. Do not try to cut on the muscle side (darker).

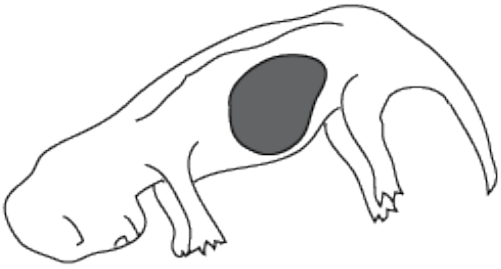

Place the embryo on its side. You will be able to see the line of the spinal cord and dark organs in the abdomen.

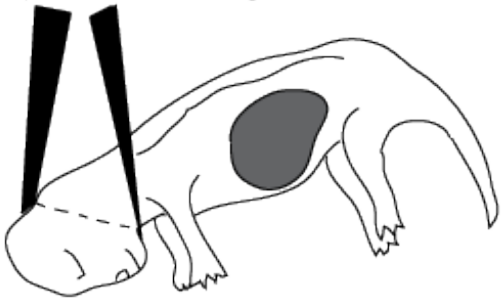

Decapitate the embryo by placing your forceps under the chin and against the notch on the back of the head.

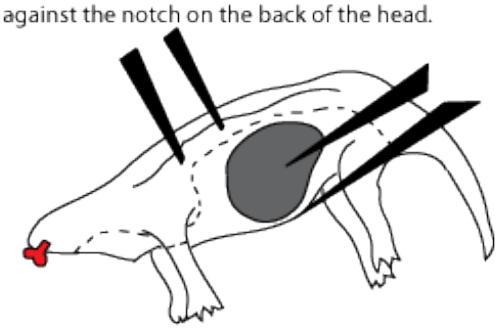

You will be able to see the beginning of the spinal cord exposed at the neck (it is white but highlighted here in red). Insert your left forceps into the side of the embryo to protect the spinal cord. Use your right forceps to strip away the limbs and organs. You may want to leave the stump of the left forelimb as something to hold onto during the next steps.

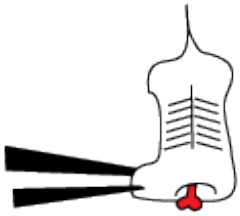

Turn the embryo on its back and orient it with its tail pointing up. Hold onto the limb stump with your left forceps. If you see horizontal lines, you have left the ribs. Peel them away carefully.

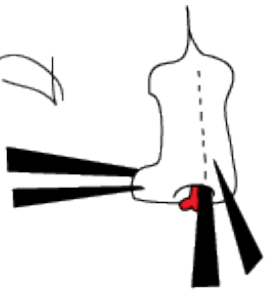

Still holding the embryo in place, insert your right forceps into the space above the spinal cord at the neck. Holding your right forceps parallel to the ~~place~~ of the spinal cord, **snip** the tissue above the cord along the length of the embryo, thus exposing the whole cord.

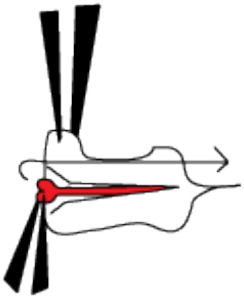

Turn the embryo to the side, still holding on to the limb stump. Gently grab the end of the spinal cord and pull it over itself towards the tail. The cord should come free with the DRG attached.

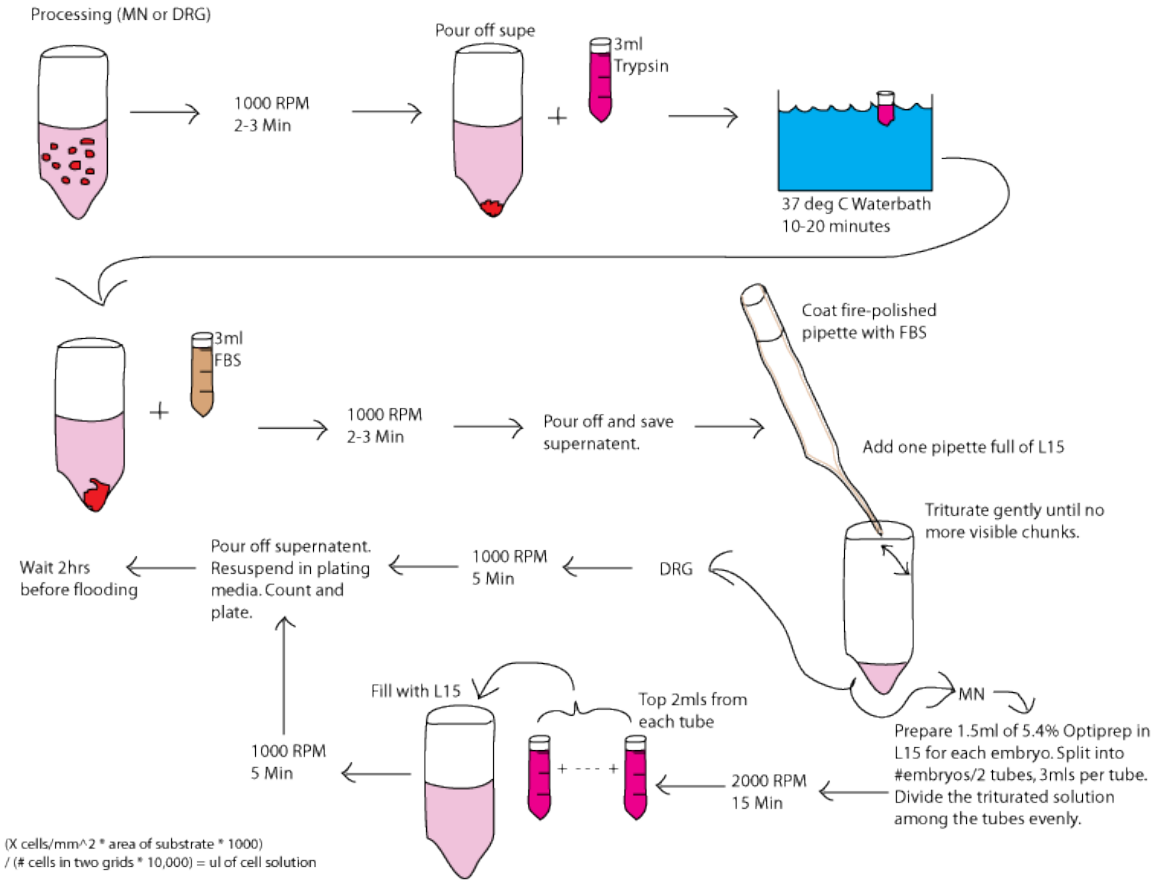
Processing (MN or DRG)
1000 RPM
2-3 Min
Pour off supe
3ml
Trypsin
37 deg C Waterbath
10-20 minutes
3ml
FBS
1000 RPM
2-3 Min
Pour off and save
supernatent.
Coat fire-polished
pipette with FBS
Add one pipette full of L15
Triturate gently until no
more visible chunks.
DRG
1000 RPM
5 Min
Pour off supernatent.
Resuspend in plating
media. Count and
plate.
Wait 2hrs
before flooding
MN
Prepare 1.5ml of 5.4% Optiprep in
L15 for each embryo. Split into
#embryos/2 tubes, 3mls per tube.
Divide the triturated solution
among the tubes evenly.
2000 RPM
15 Min
Top 2mls from
each tube
Fill with L15
1000 RPM
5 Min
(X cells/mm^2 * area of substrate * 1000)
/ (# cells in two grids * 10,000) = ul of cell solution

Appendix C. DMICA XPS

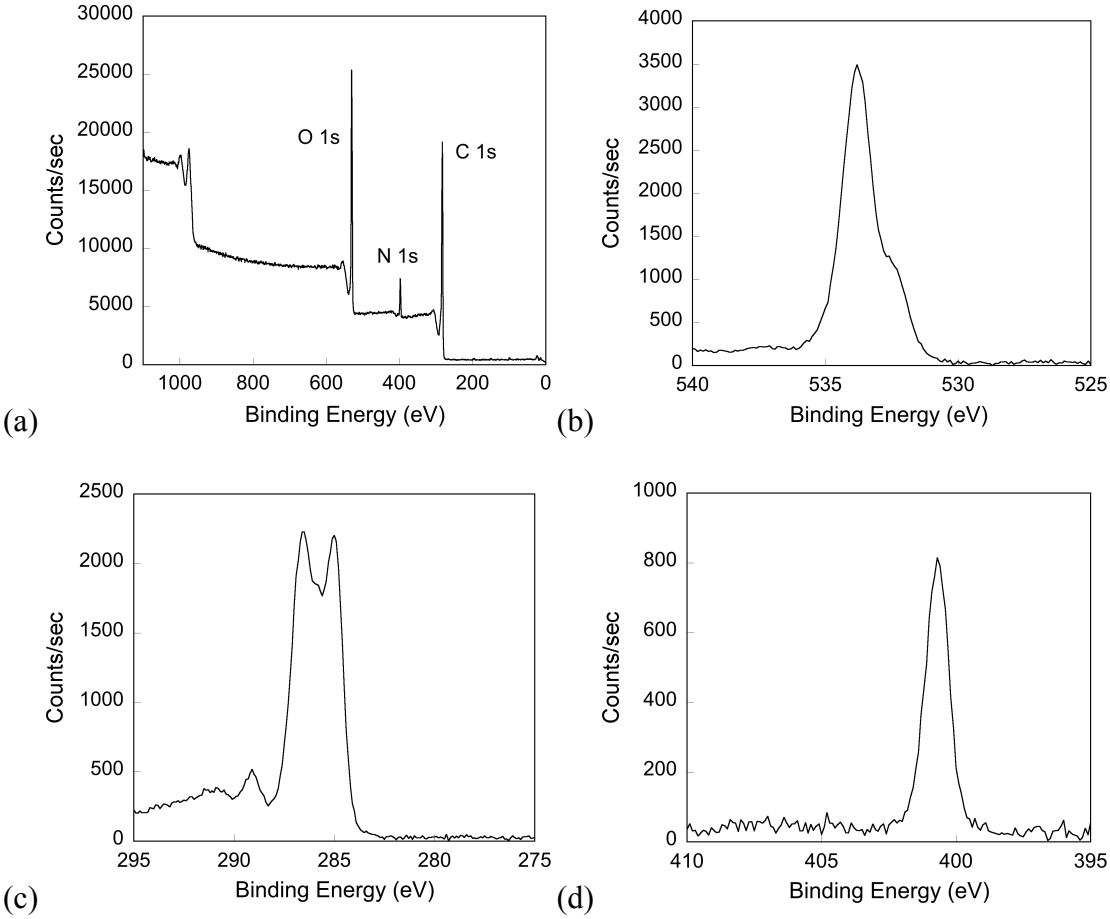

Figure C-1 (a) Survey and (b) O 1s, (c) C 1s and (d) N 1s XPS spectra for 5,6-dimethoxyindole-2-carboxylic acid.